JÜLICH
FORSCHUNGSZENTRUM

Neutron scintillation detectors

30. June 2016 | ZEA-2 | Ralf Engels

Science Campus Jülich

4,470 staff
(1,500 scientists)
+ 600 international
visiting scientists

Budget: € 435 mio
incl. € 110 mio
from third-party funds

42 institutes in 9 departments

Education
> 625 ongoing PhDs
> 350 trainees

**Research for
key technologies
of the next generation**

Detector Systems at ZEA-2

- In 1969 the group was established
- Early 70s developments with ^{3}BF, later ^{3}He Detectors began
- End 70s early 80s we started with scintillation detectors for the SNQ
- Mid 80s we improved our developments for the renewed FRJ-2
- Beginning 90s we started developments for the ESS
- Since end 90s we focused on the FRM-2 & SNS
- Since 2004 we service instruments @FRM-2 from JCNS
- Beginning 2009 we started developments for the He-3 replacement with Wavelength-Shifting-Fibers
- In 2015 we start working on a high rate scintillation Detector for ESS

Content

1. Introduction
2. Photomultiplier
3. Scintillation Process and Materials
4. „General Scintillation Detector System
5. Scintillation Detectors based on Anger Camera
6. Scintillation Detectors based on WLS fiber principle
7. Semiconductor, SiPM,
8. Other Neutron Scintillation Detectors

Neutron sources / facilities

source: veqter.co.uk

Neutron scattering - JCNS

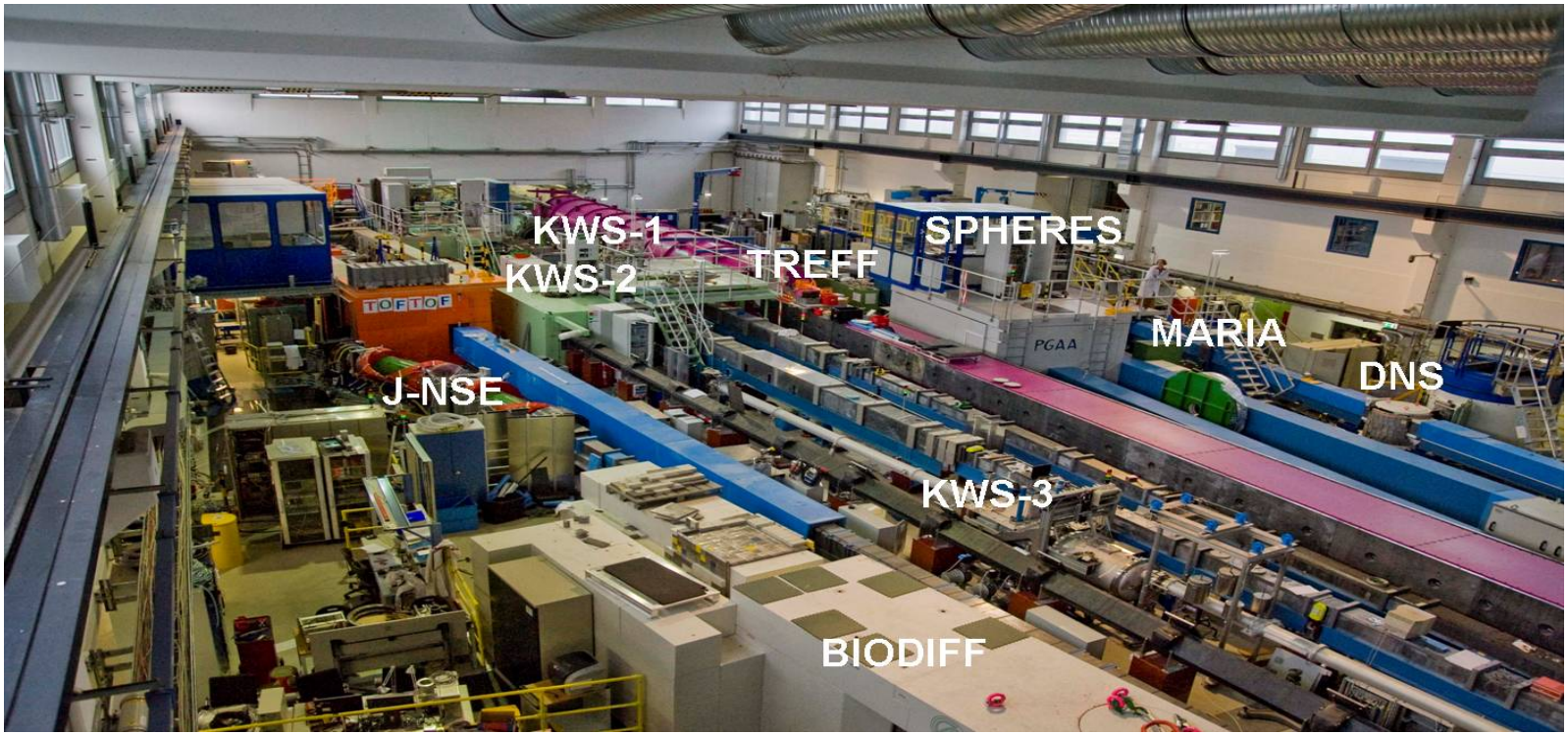

- Challenge: Installation of JCNS-Satellite at FRM-2 in Garching after shutdown FRJ-2 @ Jülich in 2004
  - Transfer of instruments FRJ-2 → FRM-II and new instruments
  - New controll- and DAQ-Systems for all Instruments
  - Detector systems for KWS-1/2, KWS-3 and Maria
  - Biggest satellite of JCNS (>30 employees)

Scintillation Detectors

Phenomenon:

- Some material emits light when struck by radiation
  - first discovered by Röntgen in 1900 with $BaPt(CN)_4$
  - today large variety of different scintillator material available

Components of scintillation detectors:

- Scintillating material
  - available as inorganic crystals, fluids, organic materials
- Photodetector
  - gas-, solid-state- & vacuum tubed based photodetectors

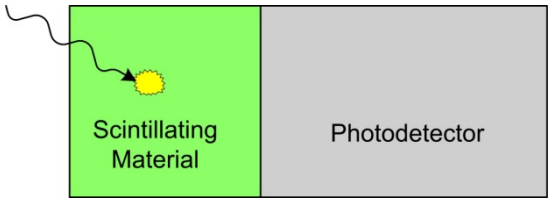

Grains of BaPt(CN)4 on a photographic plate

Advantages of scintillation detectors:

- Simple & rugged technology
- Fast signals
  - good time resolution
- High density detector material
  - high detection efficiency, good energy resolution

Concentrate on: inorganic scintillators and vacuum tube & solid-state photodetectors

Basic Processes in Inorganic Scintillators

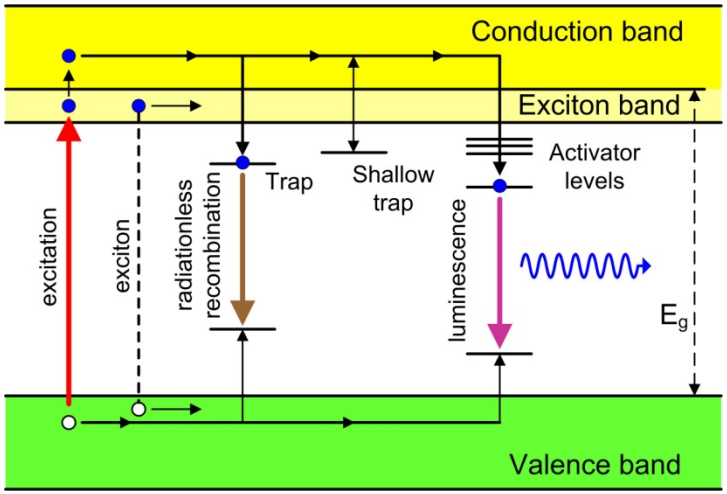

- Photon yield described by:

$$N_{Photon} = \frac{E_\gamma}{E_{eh}} \cdot S \cdot Q$$

- Conversion losses introduced by:
  - S - energy transfer to activator
  - Q - quantum efficiency of activator

- Addition of impurities (activators)
  - energy levels of activators within the bandgap of the crystal
  - transition between activator excited and ground state in visible range
- Excitation of material by energy deposition of incident particle
  - electron elevated to conduction band
  - hole in valence band ionize activator
- De-excitation by scintillation process
  - electron can drop into ionized activator excited state
  - fast de-excitation by emission of visible photon (luminescence)
- Competing processes (conversion losses)
  - forbidden transitions of activator states (phosphorescence)
  - radiationless transition

Common Inorganic Scintillators

Material	λ_{max} (nm)	τ_f (ns)	ρ (g/cm^3)	Photons per MeV
NaI(Tl) (20°C)	415	230	3.67	38,000
pure NaI (-196°C)	303	60	3.67	76,000
$Bi_4Ge_3O_{12}$ (20°C)	480	300	7.13	8,200
$Bi_4Ge_3O_{12}$ (-100°C)	480	2000	7.13	24,000
CsI(Na)	420	630	4.51	39,000
CsI(Tl)	540	800	4.51	60,000
CsI (pure)	315	16	4.51	2,300
CsF	390	2	4.64	2,500
BaF_2 (slow)	310	630	4.9	10,000
BaF_2 (fast)	220	0.8	4.9	1,800
Gd_2SiO_5(Ce)	440	60	6.71	10,000
$CdWO_4$	530	15000	7.9	7,000
$CaWO_4$	430	6000	6.1	6,000
CeF_3	340	27	6.16	4,400
$PbWO_4$	460	2, 10, 38	8.2	500
Lu_2SiO_5(Ce)	420	40	7.4	30,000
$YAlO_3$(Ce)	390	31	5.35	19,700
Y_2SiO_5(Ce)	420	70	2.70	45,000

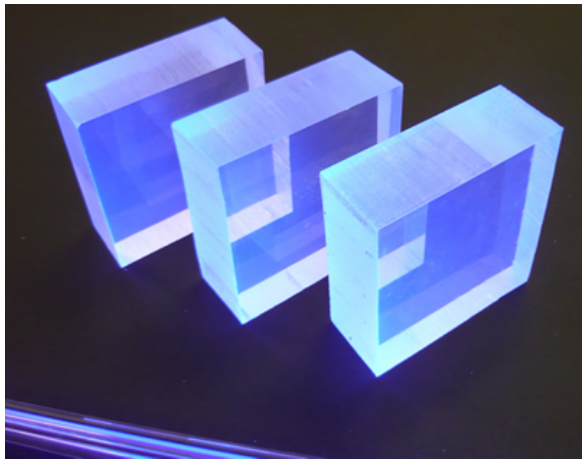

- Common activator dopants:
  - Tl^+, Ce^{3+}, Eu^{2+}
- Decay time of scintillator typically follow exponential decay:

$$N(t) = N_0 \cdot e^{-t/\tau}$$

- Fast decay times deliver good time resolution
- Number of photons important for energy and position resolution

Photomultiplier Tube (PMT)

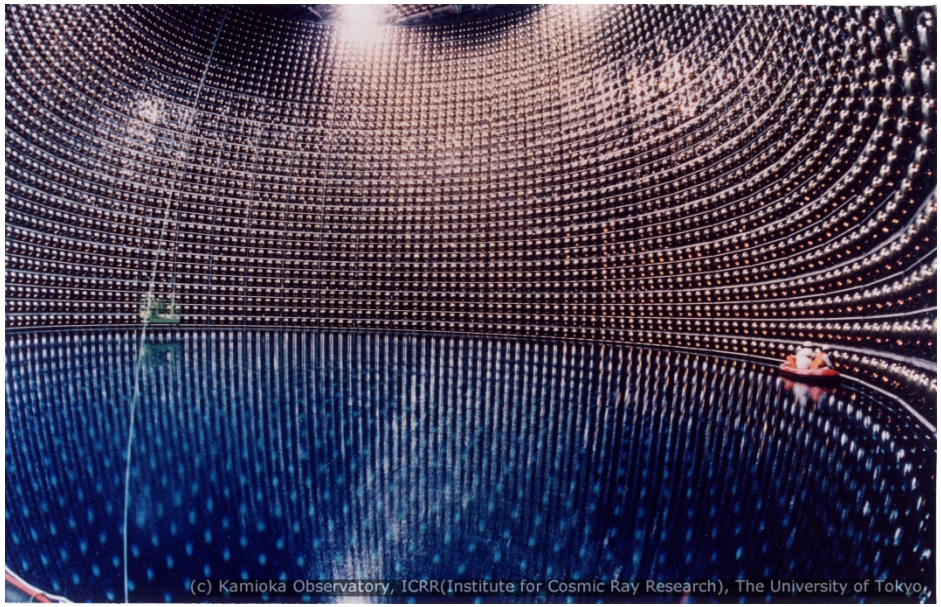

PMT – Convert light into curent

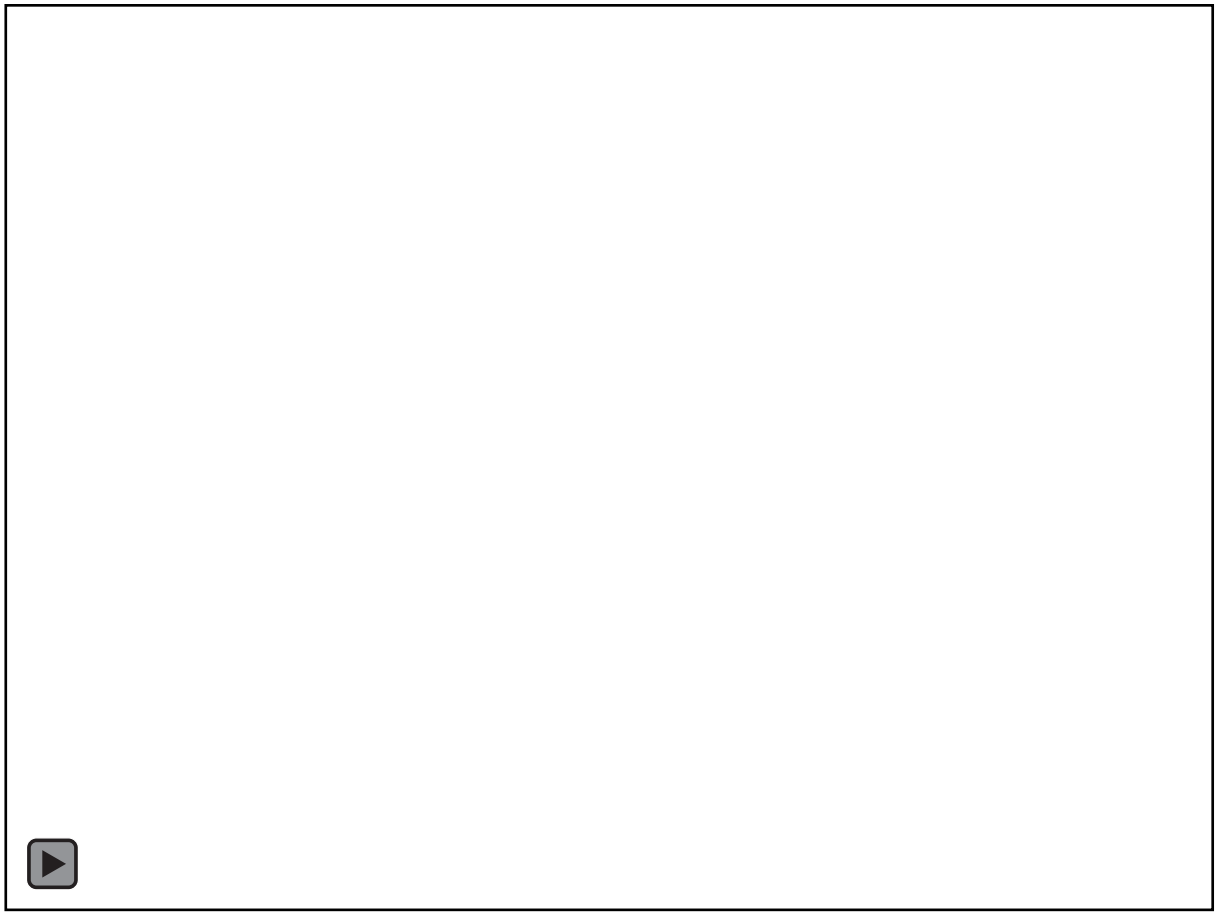

Structure of a linear focus PMT

The light is collected on the front face of a photomultiplier tube (PMT), where the light photons are absorbed on a photocathode and free electrons are emitted. The electrons are accelerated by the high voltage on the internal structure of the PMT and the number of electrons is increased forming a current signal at the final stage of the PMT.

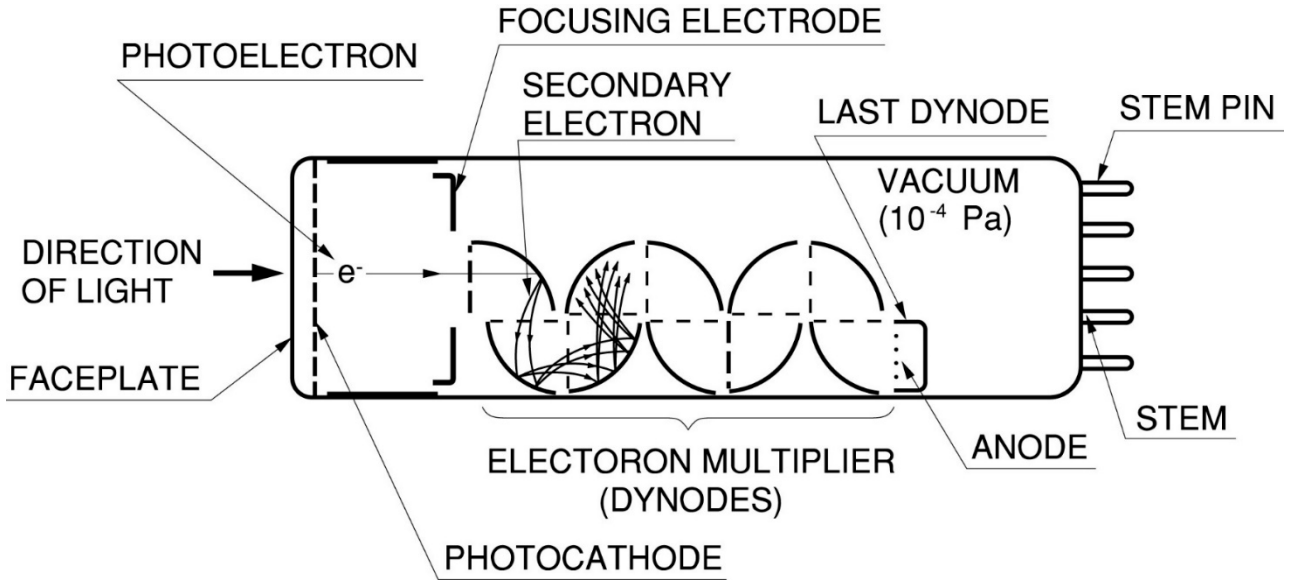

Source : Hamamatsu Photonics K.K.

Why do we use still PMTs instead of semiconductor detectors

- Low noise – photon counting
- Fast speed
- Larger area for covering

HOWEVER

- Poor quantum efficiency
- Bulky
- expensive

Aim of the Photon Detector

- Record all the quantities of photons as precise as possible:
  - number of photons
  - arrival time of photons
  - position of photons
- Define a photon detector as a device that detects photons of an arbitrary energy.
- Define a photodetector as a device that detects in the eV few keV range (IR to X-ray). These photons may be detected directly or may be produced by some other type of photon detectors

Quantum Efficiency

$$QE = \frac{\#Emmitted\ Photoelectrons\ by\ cathode}{\#\ of\ incident\ photons}$$

$$\mathrm{QE} = \frac{N_{PHE}}{N_{Phot}}$$

Quantum efficiency symbolized by QE and generally expressed as a percent. Incident photons transfer energy to electrons in the valence band of photocathode, however not all these electrons are emitted photoelectrons. As a result, the maximum quantum efficiency occurs at a wavelength slightly shorter the wavelength of the peak radiant sensitivity.

source: Hamamatsu

Quantum Efficiency

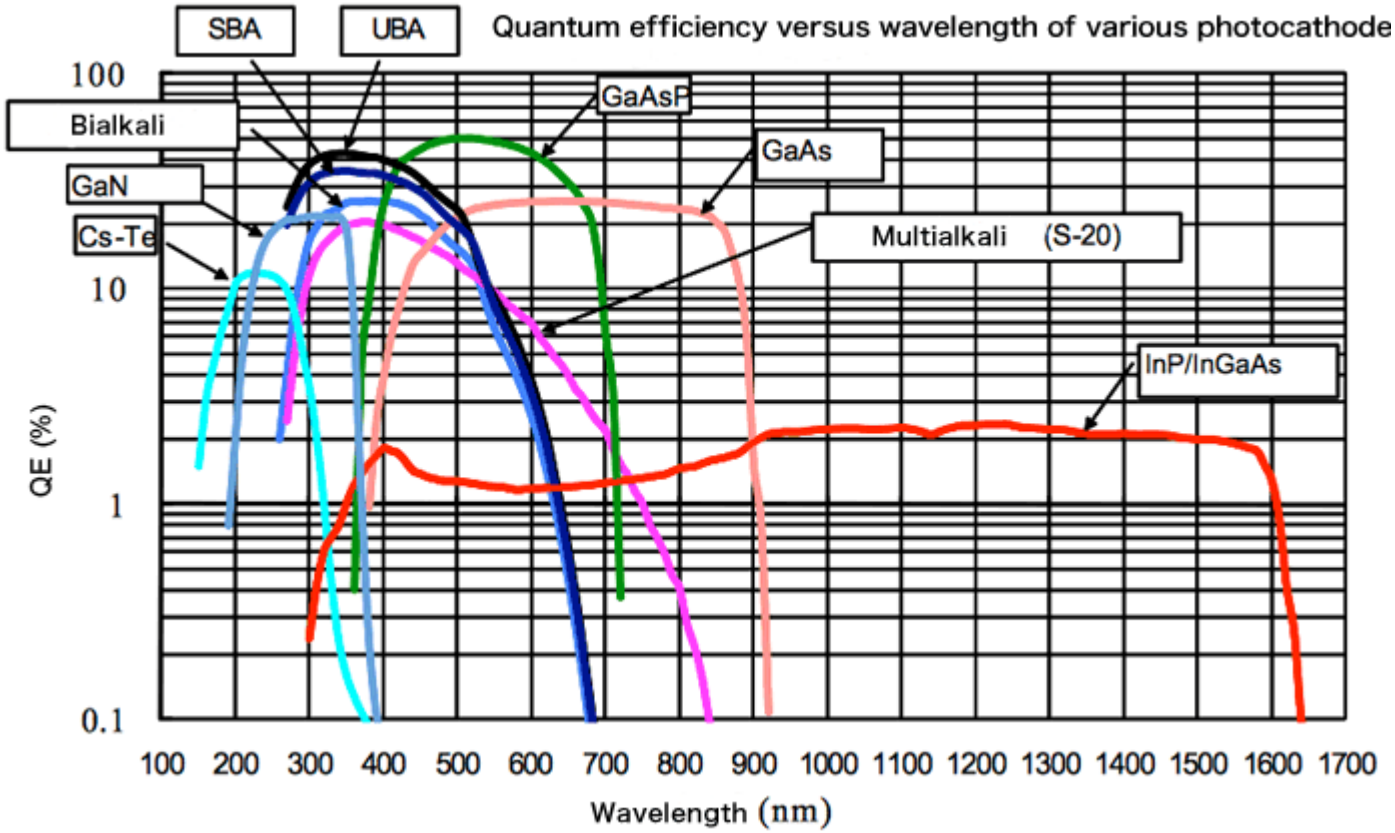

Quantum efficiency versus wavelength of various photocathodes Quantum efficiency (abbreviated "QE") is the number of photoelectrons emitted from the photocathode divided by the number of incident photons, and is usually expressed as a percent.

source: Hamamatsu

Quantum Efficiency

Hamamatsu Photonics succeeded in significantly enhancing the quantum efficiency of an alkali photocathode by improving photocathode activation process. In this photocathode, an average QE of 43% at 350nm was achieved at peak wavelength and is named the “ultra bialkali” or UBA for short. Besides this “ultra bialkali”, they also developed another photocathode with moderately high sensitivity called the “super bialkali” or SBA for short and which delivers an average quantum efficiency of 35% at 350 nm. The Figure shows typical spectral response characteristics of these UBA and SBA along with those of an ordinary bialkali photocathode.

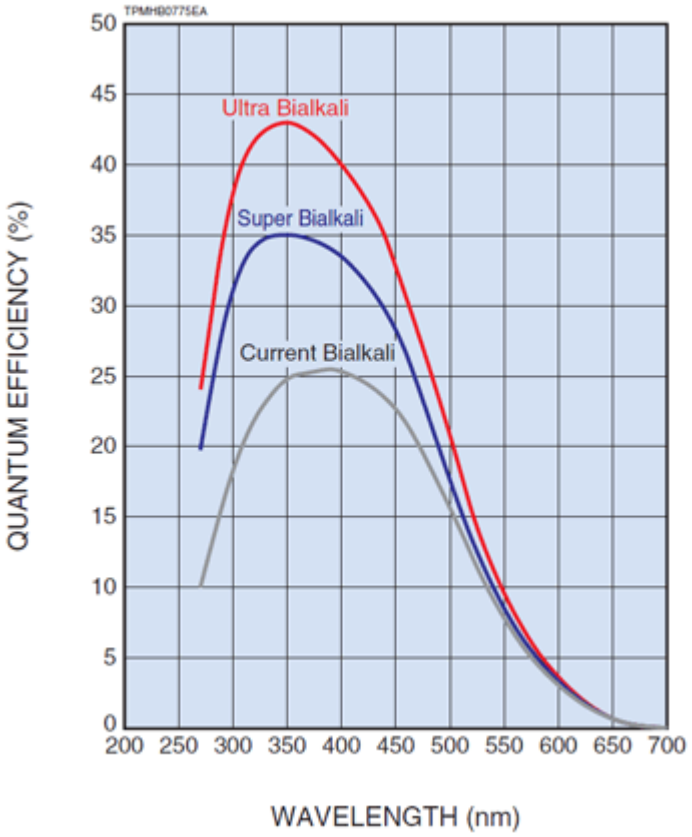

source: Hamamatsu

Quantum Efficiency

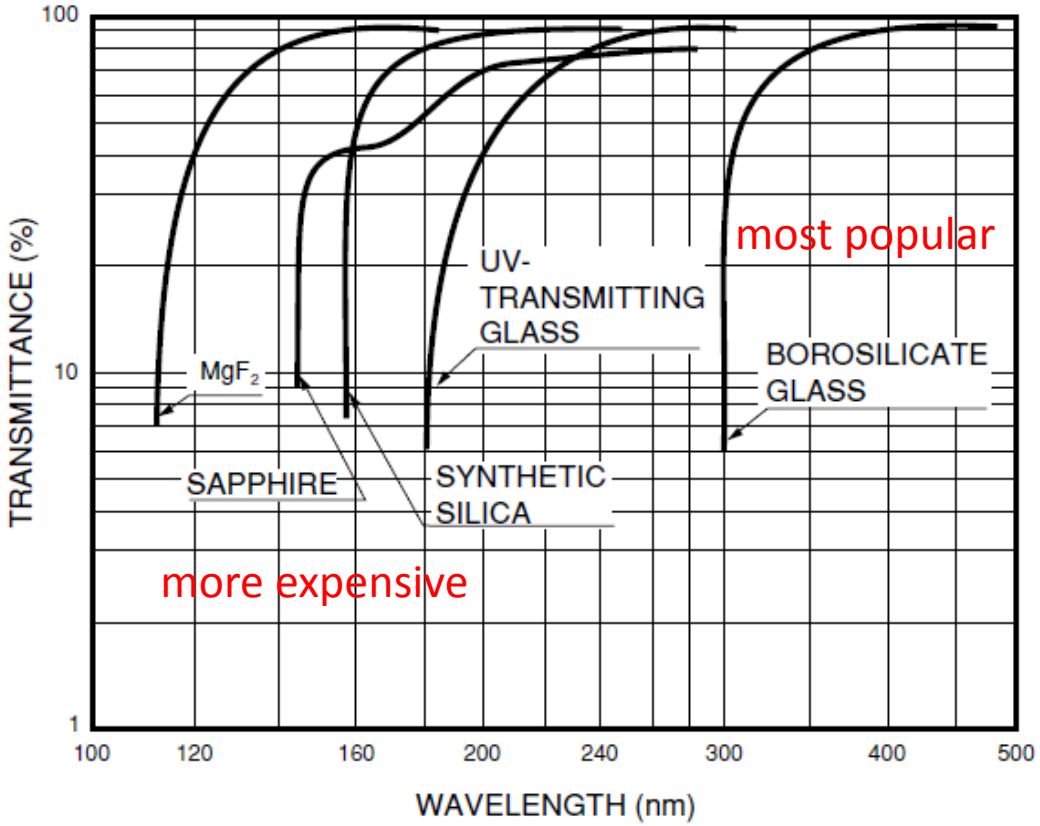

Spectral transmittance characteristics of various window materials

source: Hamamatsu

Quantum Efficiency

The QE is limited due too:

- The Absorption of the photon at the photocathode, based on e.g. wavelength
- The emitted photoelectrons at the photocathode
- Isotropic emission of photoelectrons (dark current, thermal)

source: Hamamatsu

Quantum Efficiency

The QE can be measured with a reference system:

- Connect the anode with all dynodes and add 100V more for 100% efficiency
- Measure the cathode current and compare this with the reference system where the QE is known.

$$QE_{new\ device} = \frac{I_{C_{new\ device}}}{I_{C_{known\ device}}} \cdot QE_{known\ device}$$

source: Hamamatsu

Detection Quantum Efficiency

The DQE can be measured with a reference system:

- Use a pulsed source (e.g. blue LED) to measure the single PE peak with more pulses in the pedestal than in SEP
- Measure the SPE and compare this with the reference system where the DQE is known.

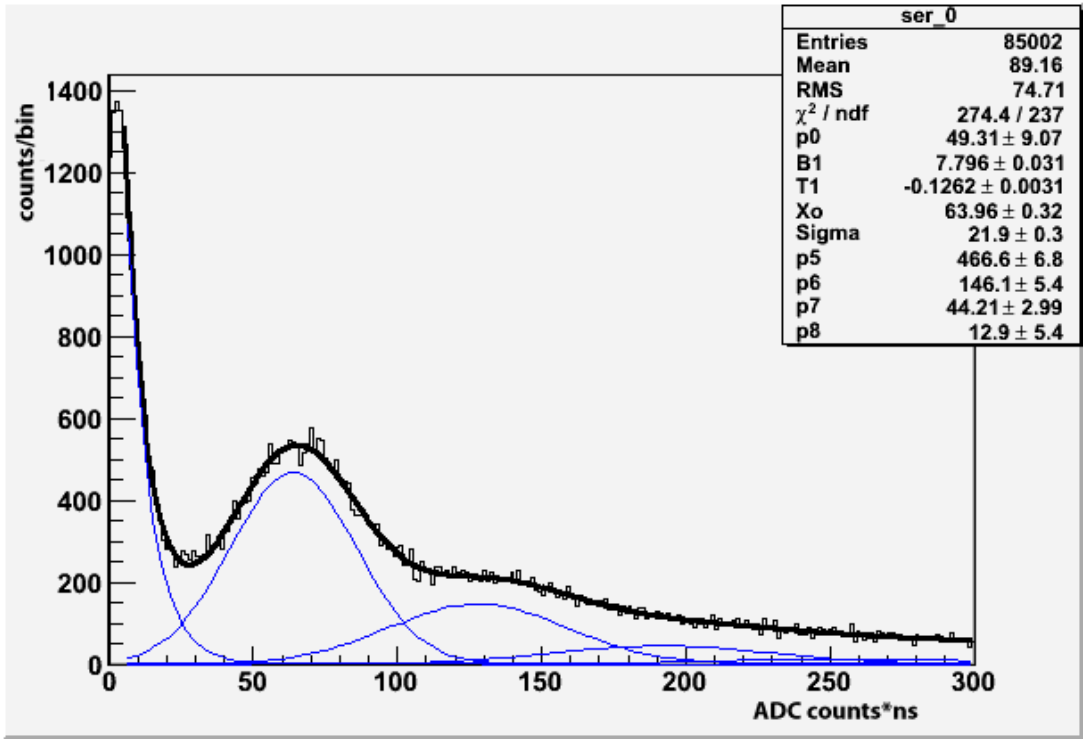

The fit superimposed is obtained by the sum of an exponentially falling function (dark count distribution) and three Gaussian functions for the single photo-electron and multiple photo-electron distributions.

Measuring a single Electron

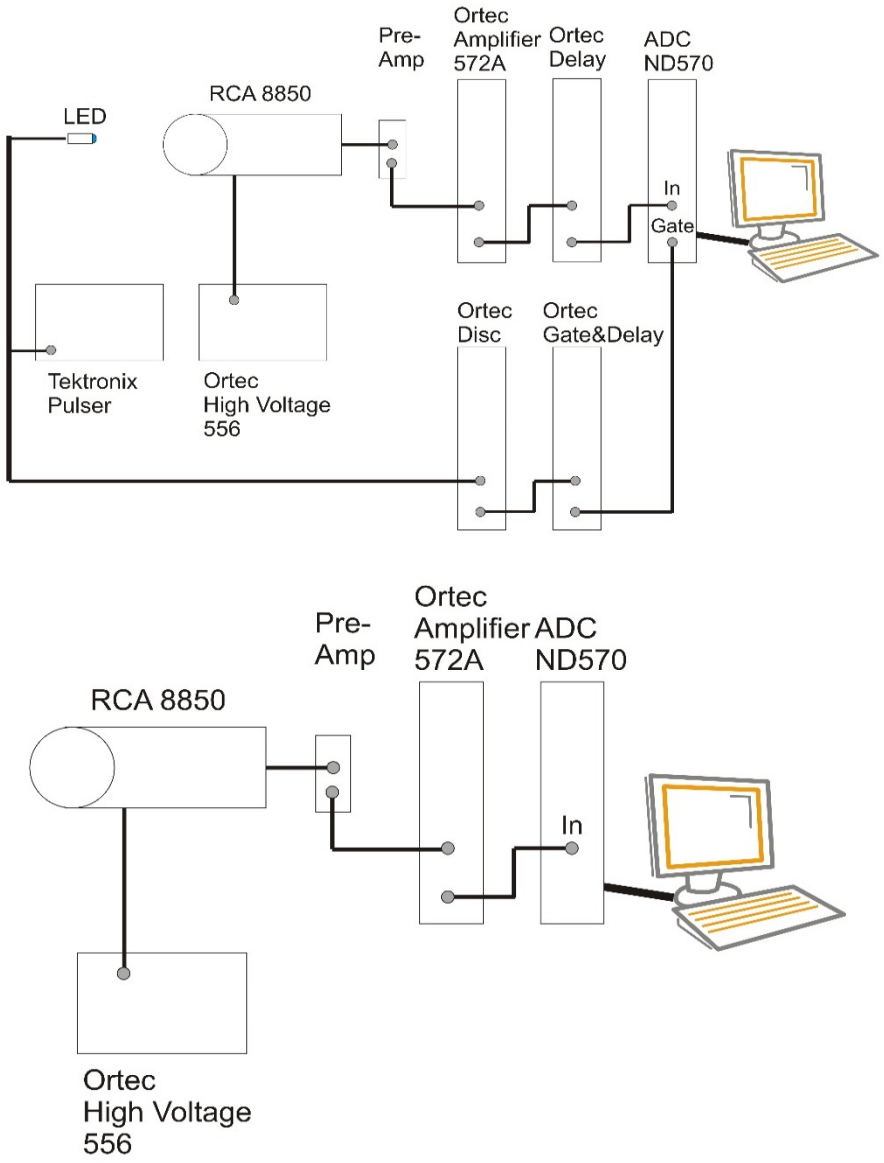

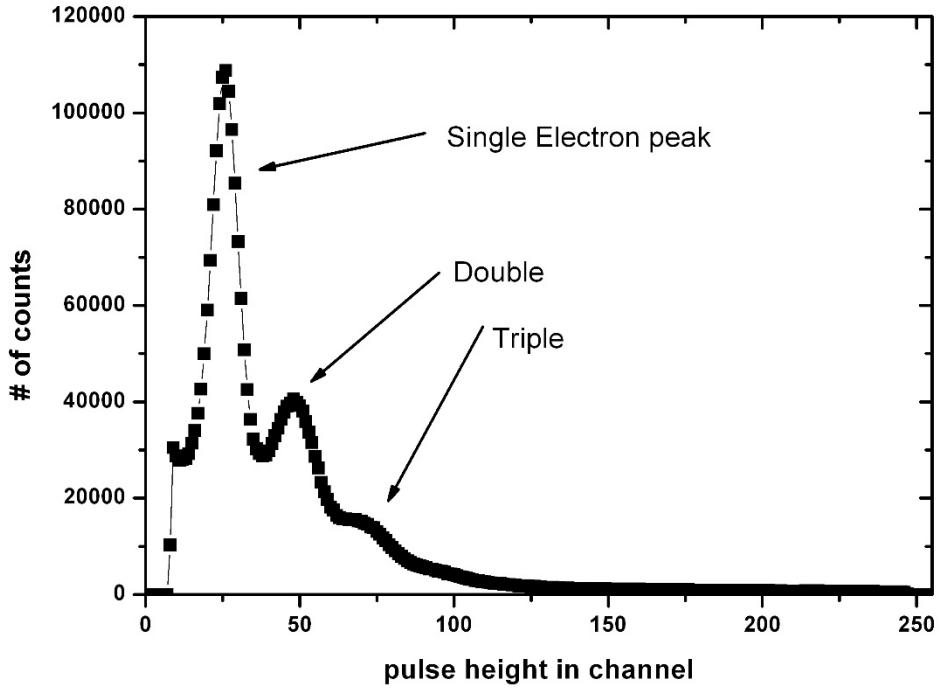

Scintillator Parameter

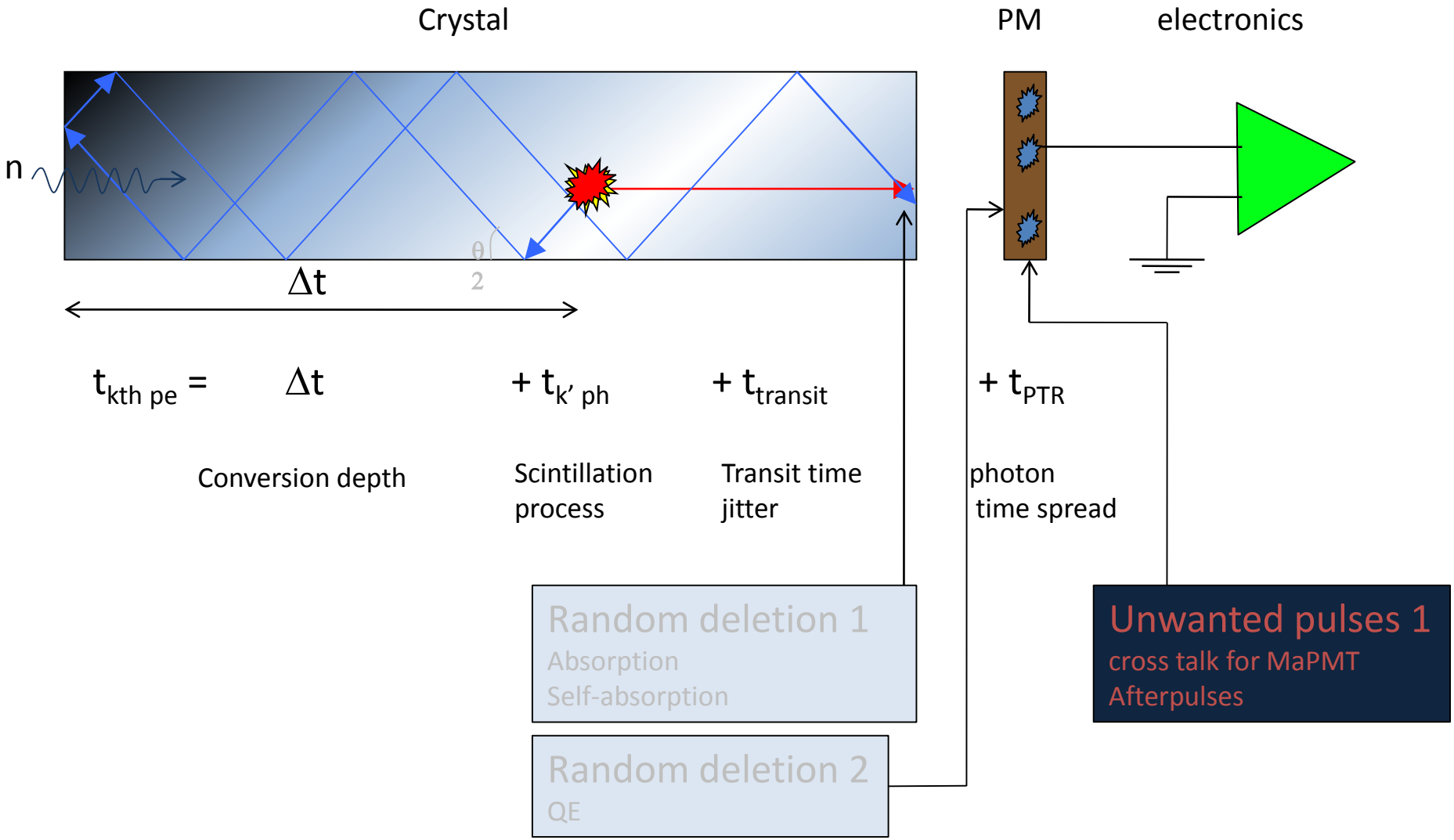

Scintillator Parameter

P. Lecoq et al, IEEE Trans. Nucl. Sci. 57 (2010) 2411-2416

Besides all factors related to photodetection and readout electronics the scintillator contributes to the time resolution through:

1. The scintillation mechanism
   - Light yield,
   - Rise time,
   - Decay time

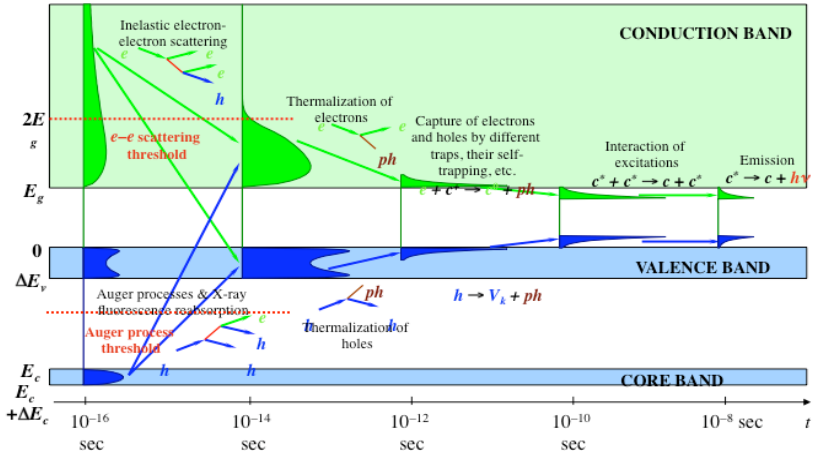

A. Vasil'ev, SCINT2001 proceedings, NIMA 486 (2002) 367

2. The light transport in the crystal
   - Time spread related to different light propagation modes
3. The light extraction efficiency
   - Impact on photostatistics
   - Weights the distribution of light propagation modes

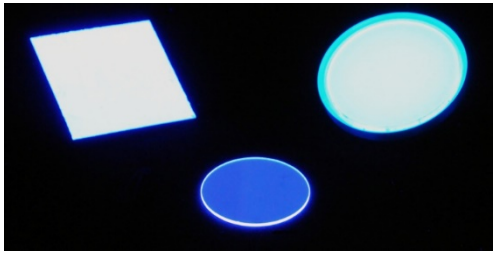

Scintillator Parameter

The intensity of light signal of a scintillating crystal can be described by the Shao Formula

$$I(t) = \frac{N_{phe}(\tau_r + \tau_d)}{\tau_d^2}(1 - e^{-t/\tau_r})e^{-t/\tau_d}$$

The number of photo-electrons firing the photo-detector N(t) between 0 and t after simplifications is given by :

$$N(t) = \int_0^t I(t) = \frac{N_{phe}}{\tau_d} * \frac{t^2}{2\tau_r}$$

Mean arrival time of first photon ≈ time jitter if Poisson statistics:

$$t_{1st} = \sqrt{2 * \tau_d \frac{\tau_r}{Nphe}}$$

e.g.: τ_r < 100ps, τ_d = 70-90 ns, Nphe = 6,000

source: P, Lecoq

Interactions of Slow Neutrons

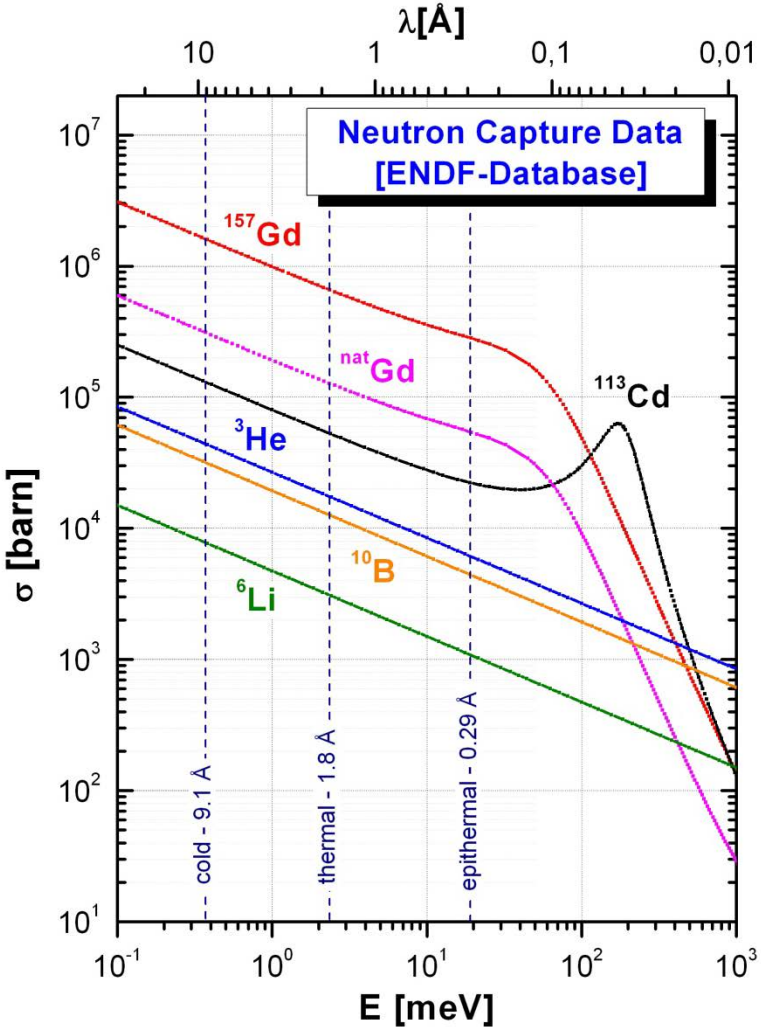

- Slow neutron are indirectly detected by nuclear capture reactions
- Major reactions used for neutron detection:

$n + {}^{3}He$		$\rightarrow {}^{3}H + p + 764\ keV$
$n + {}^{10}B$	(6.4%)	$\rightarrow {}^{7}Li + \alpha + 2.78\ MeV$
	(93.6%)	$\rightarrow {}^{7}Li + \alpha + \gamma + 2.31\ MeV$
$n + {}^{6}Li$		$\rightarrow {}^{3}H + \alpha + 4.78\ MeV$

- Others:

  $n + {}^{157}Gd \rightarrow {}^{158}Gd + \gamma's + e's$

- Ionization & excitation of detector material by reaction products

Photodetectors

- **Purpose**: convert light into detectable electrical signal
  - use photoelectric effect to convert photons (γ) to photoelectrons (pe)
- **Standard requirement:** high quantum efficiency, expressed as:

$$QE(\%) = \frac{N_{pe}}{N_{\gamma}} \quad \text{or} \quad QE(\%) \approx 124 \cdot \frac{S(mA/W)}{\lambda(nm)}$$

S: radiant sensitivity

- **Photosensitive materials**:

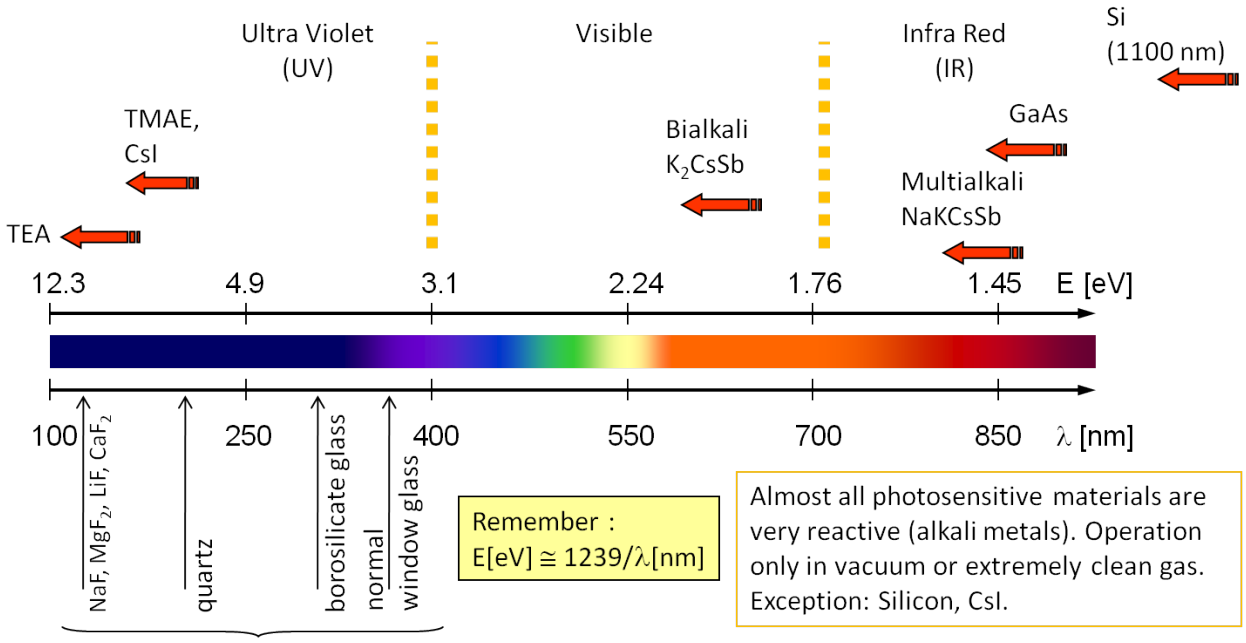

Remember :
E[eV] ≅ 1239/λ[nm]

Almost all photosensitive materials are very reactive (alkali metals). Operation only in vacuum or extremely clean gas. Exception: Silicon, CsI.

Photomultiplier Tubes (PMT)

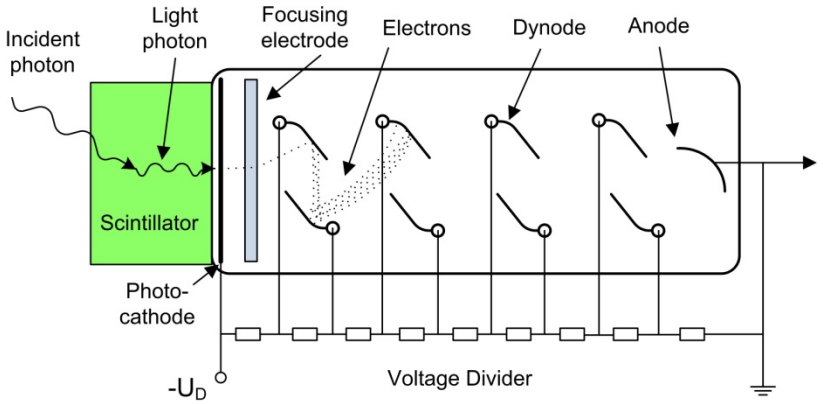

- Transit time: time between the arrival of the photon and the electrical signal at the anode (≈15 ns)
- Time spread: transit time variation between different events (< 100 ps)
- Dark count rate:
  - depends on the cathode type, the cathode area, and the temperature.
  - few kHz (threshold = 1 pe)
  - is highest for cathodes with high sensitivity at long wavelengths.

Principle of operation:

- Vacuum tube with photocathode/dynode structure
- Photoemission from photocathode
- Secondary emission from N dynodes:
  - dynode gain: g≈3-50 (function of incoming electron energy E)

Total gain: $M = \prod_{i=1}^{N} g_i$

- Example:
  - 10 dynodes with g=4,
  - $M = 4^{10} \approx 10^6$
- With high gain (>10^6):
  - ability to measure single photons
  - gain fluctuations mainly dominated by first dynode
- But: Photomultiplier are sensitive to magnetic fields!

Photocathode and Dynode Types

Photocathodes:

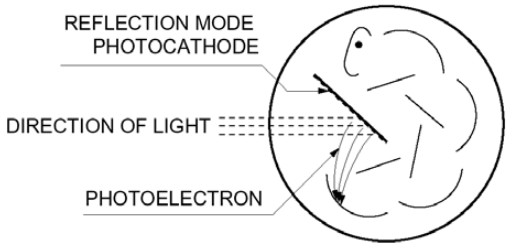

Reflection mode photocathode

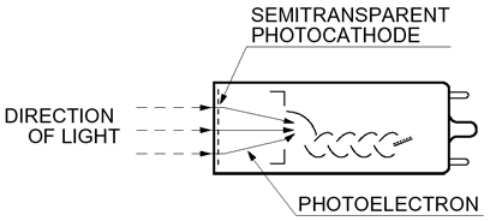

Semitransparent photocathode

Dynode structures:

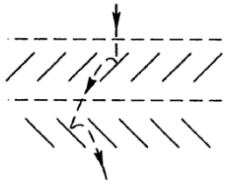

Venetian Blind

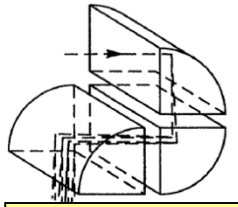

Box and Grid

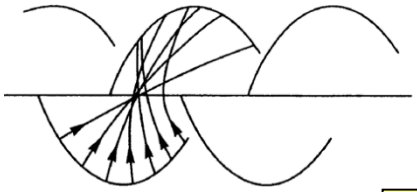

Linear focusing

Circular cage

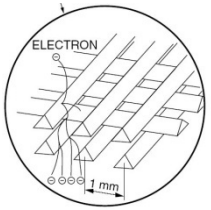

Mesh dynodes

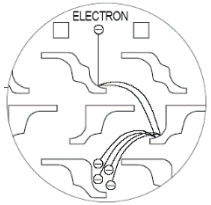

Metal channel

Photocathode and Dynode Types

METAL CHANNEL

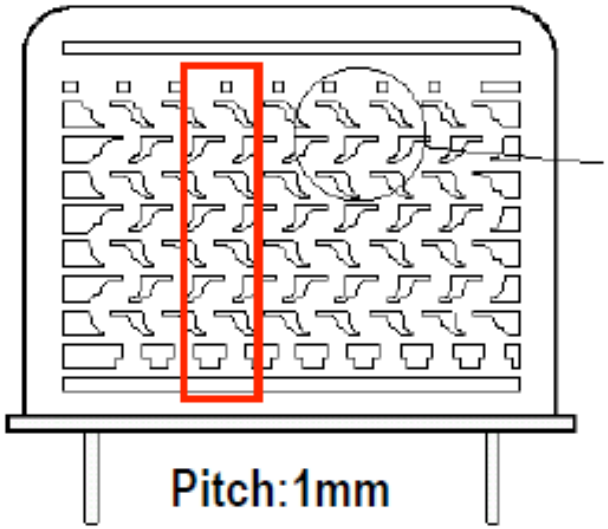

Compact
Fast time response
Position sensitive

PMT with Metal Channel Dynode

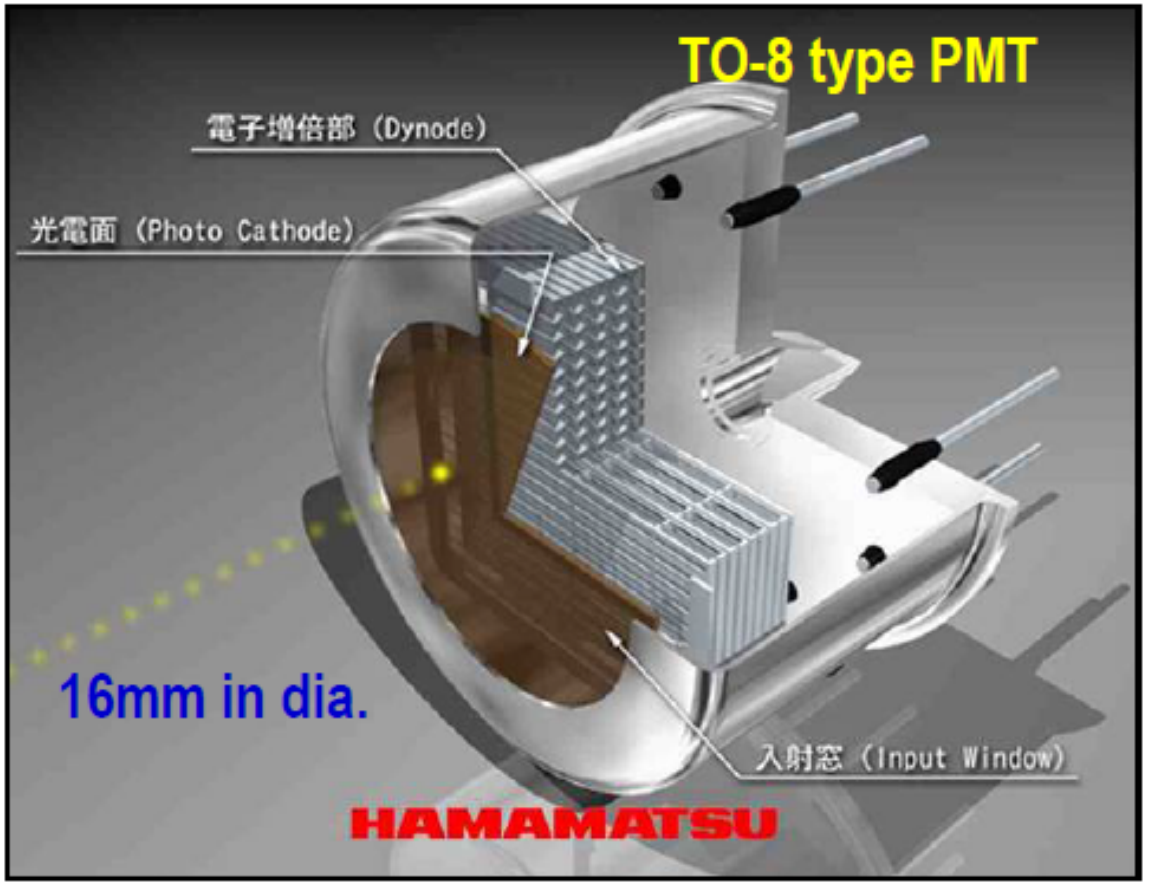

Katsushi Ariska

Photomultiplier

Single anode photomultipliers

Multi anode photomultipliers

H7546 (Hamamatsu)

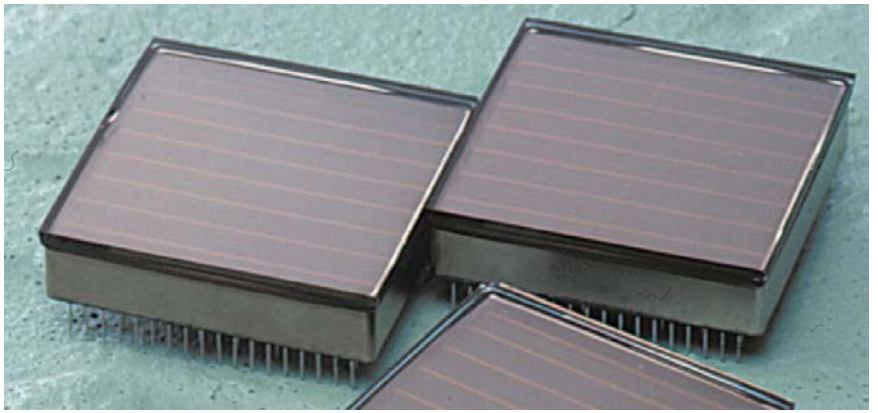

H8500 (Hamamatsu)

Final Remarks

- PMTs are still used in many applications for good reasons:
  - Intrinsic high gain
  - Extremely low noise – photon counting
  - Fast speed < 1ns possible
  - Large area >> 130 mm

- However PMTs are not perfect. There are many issues to be concerned:
  - Anode and Cathode uniformity
  - Non linearity
  - Effect of magnetic field
  - Long-term stability

^{6}Li based scintillation Detector examples

Options of Scintillation Detector Designs which will described here in more detailed

- **1. Option**
  - Detectors based on Anger camera principle
  - Key issues: large area, optical imaging components, light detection devices, low γ-sensitivity, position reconstruction, count rate capability

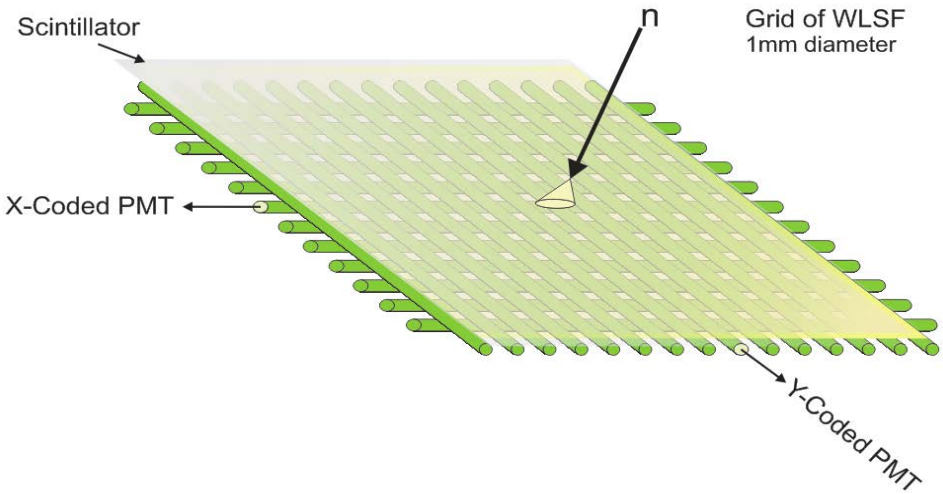

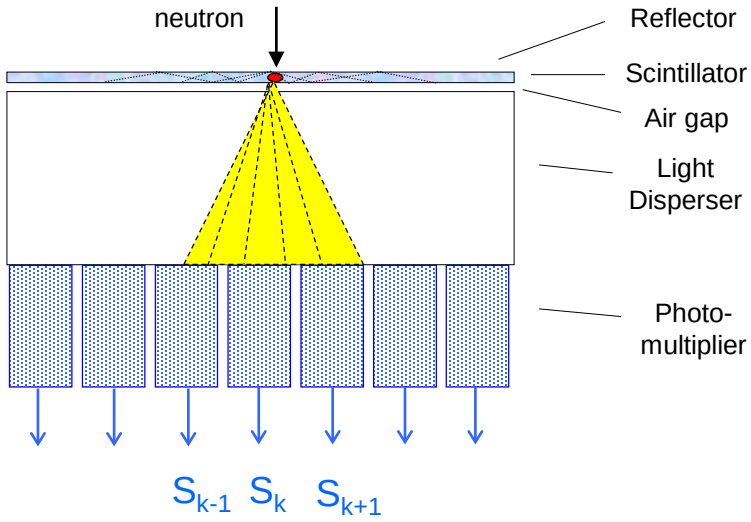

- **2. Option**
  - Detectors with wavelength-shifting-fiber light readout
  - Key issues: large area with minimum dead space, fiber layout, low γ-sensitivity, position resolution, detection efficiency

One dimensional Anger-Detector

- 1 mm ^{6}Li-Glas Scintillator with light disperser to spread the light to minimum three Photomultiplier
- Detection Efficiency for thermal Neutrons (2Å): ~85%
- γ- Sensitivity (with pulse height discrimination): ~10^{-4}

Sensitivity Area

200 x 20 mm^2

680 x 25 mm^2

940 x 75 mm^2

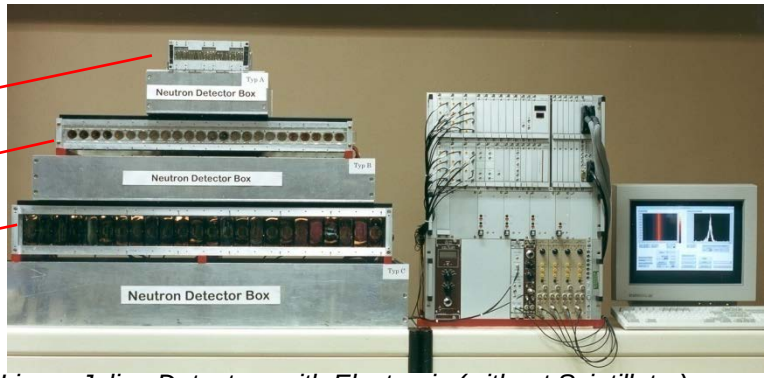

Linear Julios-Detectors with Electronic (without Scintillator)

- 24 Photomultiplier in linear a arrangement, Position identification with three side by side Photomultiplier
- Spatial resolution depends on the PMT size: 1.2/2.3/3.3mm
- In operation at FRJ-2 (in future FRM2), ISIS, HMI
  - New development for a TOF powder diffractometer

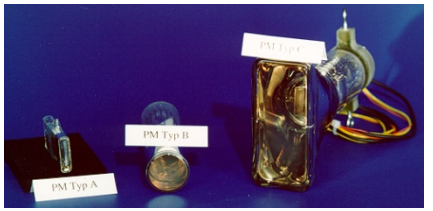

Neutron Scintillation Detectors

Anger Camera Detector:

- Simple method to form large detectors
  - invented by H.O. Anger
  - ^{6}Li-glass scintillator
  - disperser for light distribution
  - array of photomultipliers
- Detection of thermal neutrons
  - capture of neutron in scintillator
  - light spread over several photomultipliers
  - computation of event position by signals of light detection devices
- Detector performance
  - resolution dependent on light yield and size of photomultipliers
  - with Li-glass ~ 0.1 $\cdot d_{PMT}$
- Method also used for gamma-cameras in medical applications

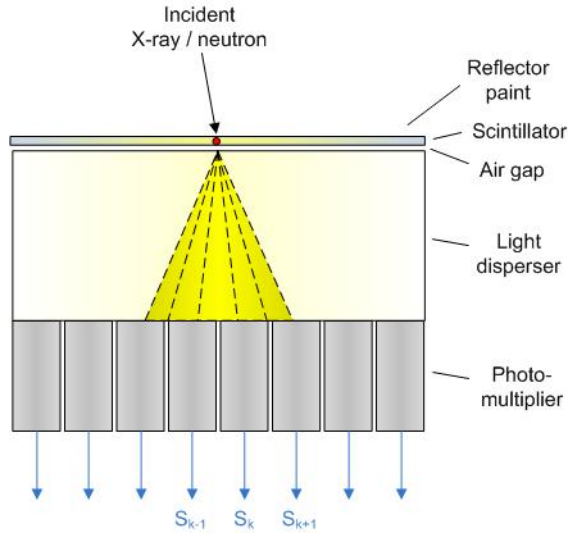

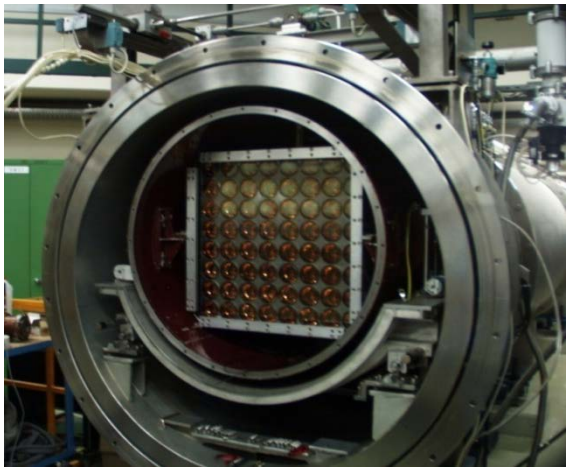

Standard Neutron Scintillator: GS20-^{6}Li-glass

- Neutron capture reaction:

$$n + {}^6\mathrm{Li} \rightarrow {}^4\mathrm{He} + {}^3\mathrm{H} + 4.79\,\mathrm{MeV}$$

- 6.6 weight% Li, 95% ^{6}Li-enriched
- Emission peak at ~390 nm (Ce doped)
- Light yield ~ 6000 photons/n (corresponds ~1.5 MeV gamma)

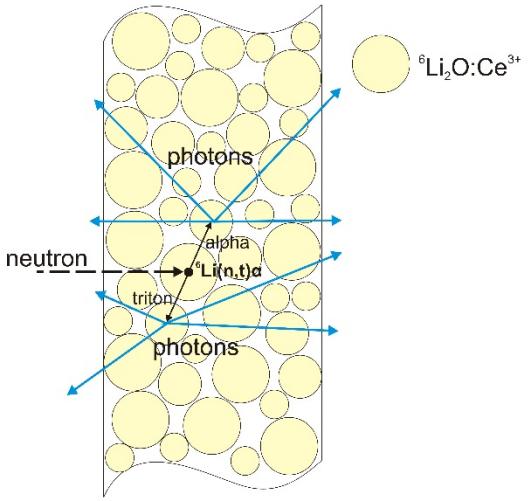

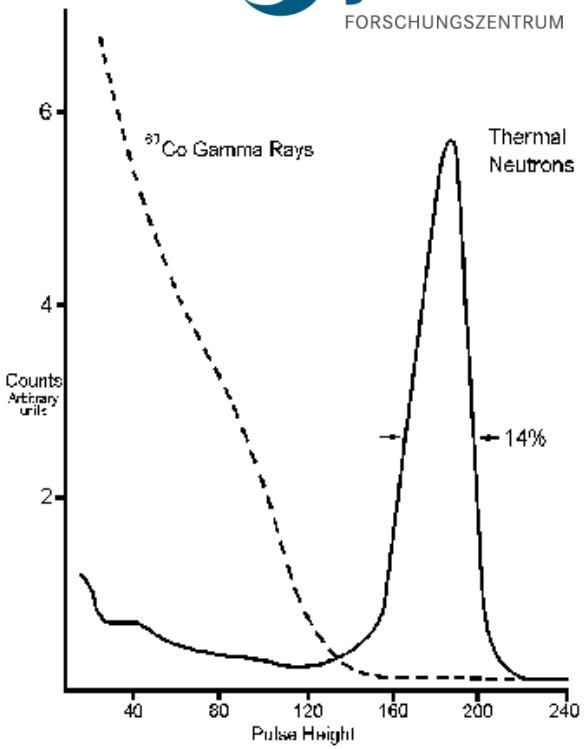

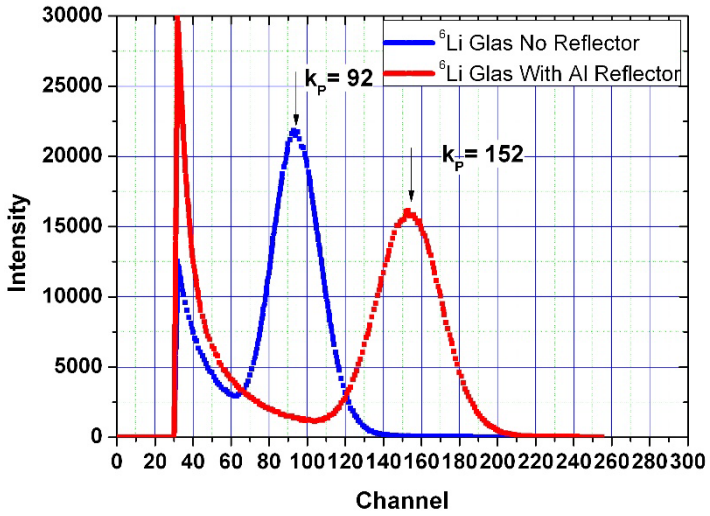

APPLIED SCINTILLATION TECHNOLOGIES
is now...
scintacor
THE CENTRE OF SCINTILLATION

www.scintacor.com

Test setup with a source (n)

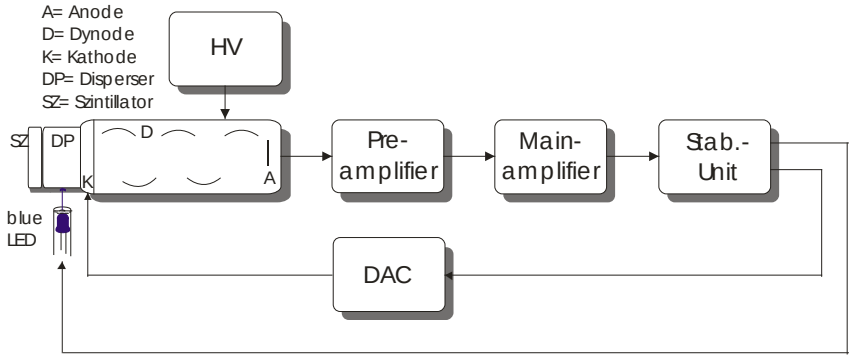

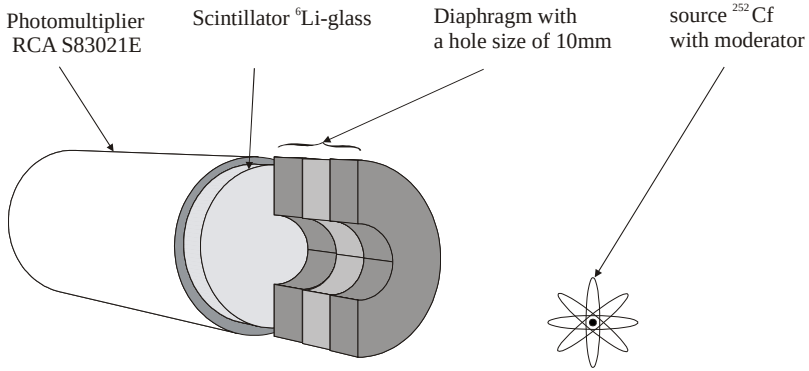

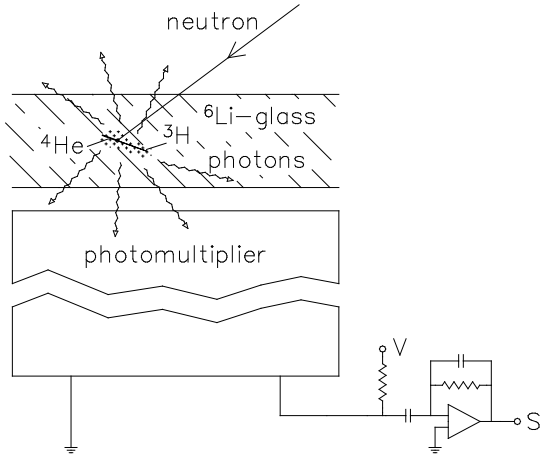

$$n + {}^{6}Li \rightarrow {}^{4}He + {}^{3}H + 4.79MeV$$

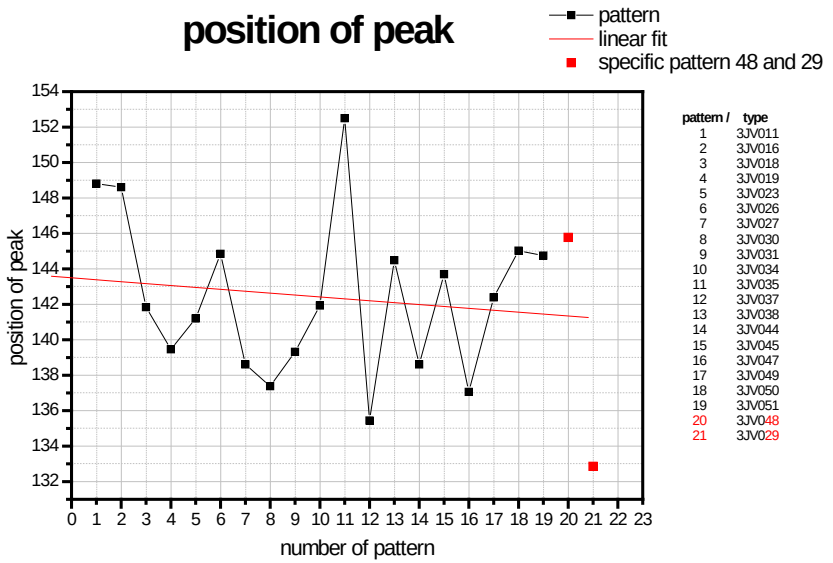

Assembling of the detector head

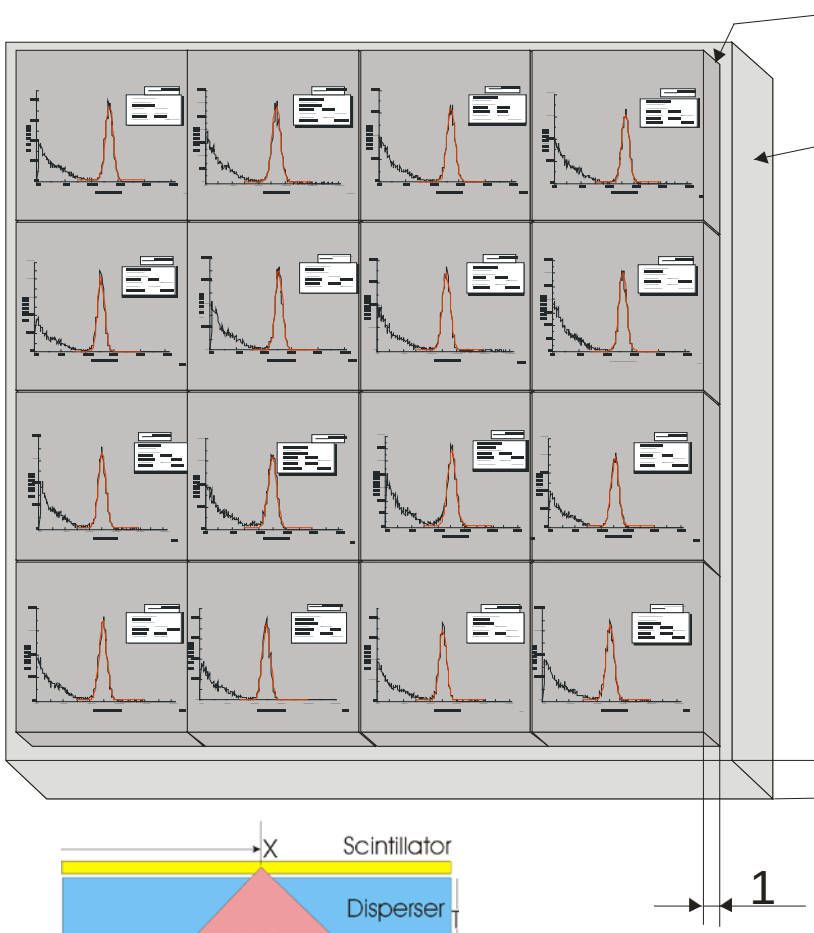

Disperser glass

Complete Scintillator

Assembling of the PMTs

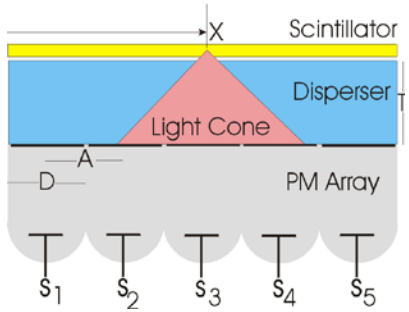

64 PMTs with disperser

Why disperser?

Setup of the remotely controlled test bench

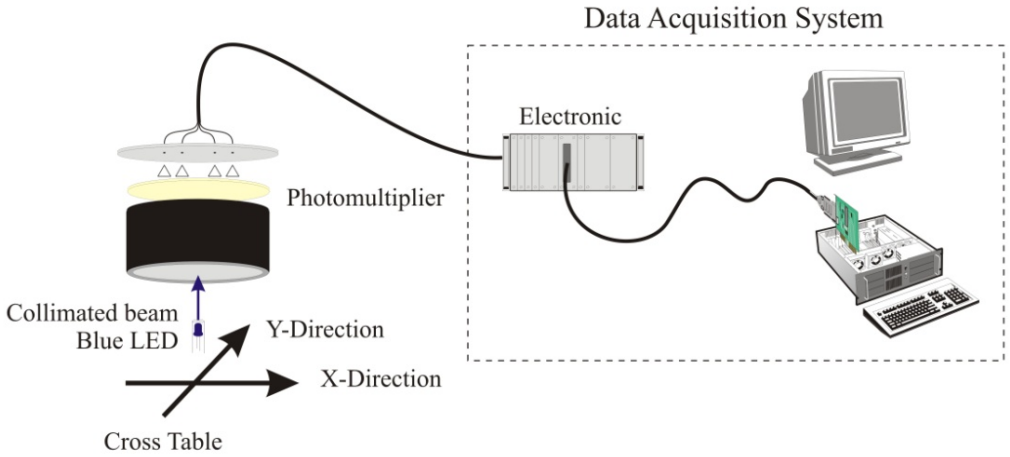

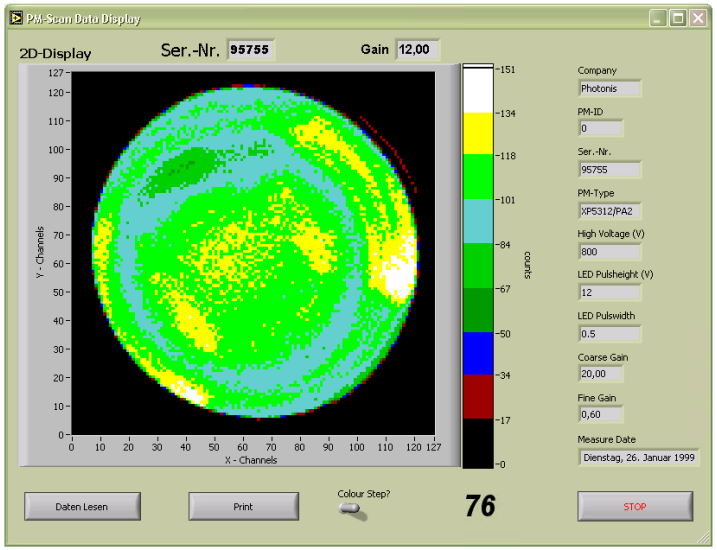

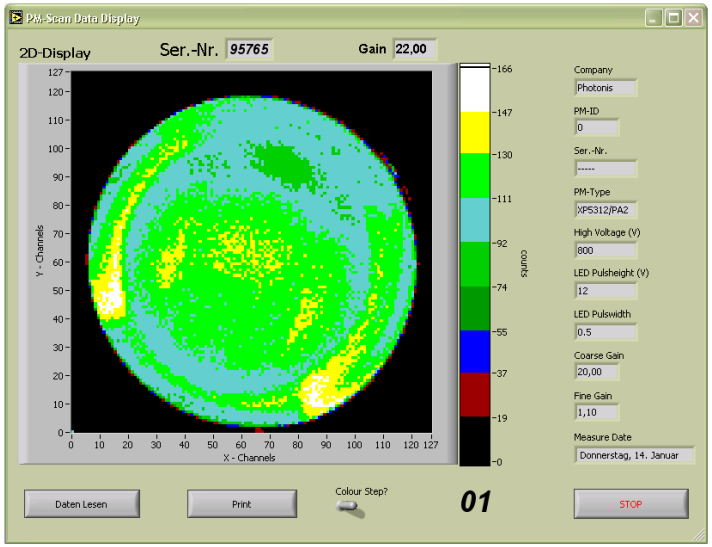

overview of multiplier sensitivity

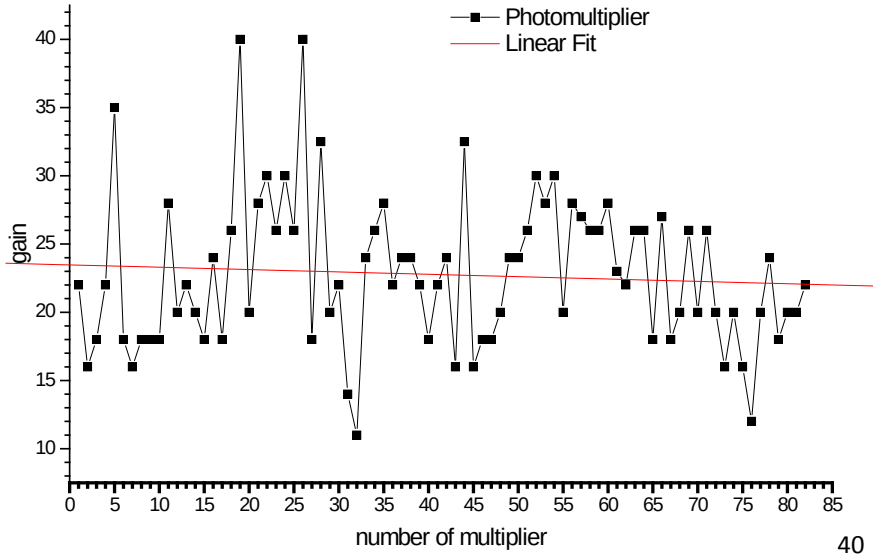

A/B-Reconstruction

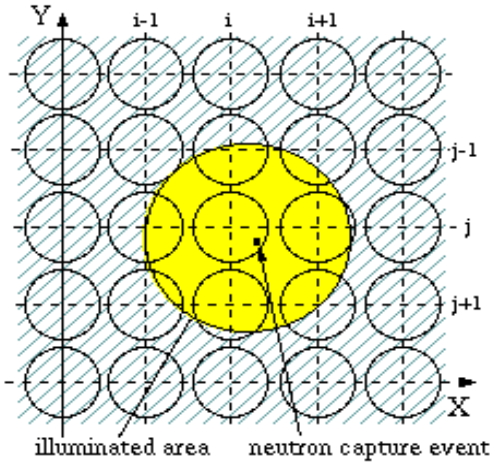

Fixing of the Q-Area:

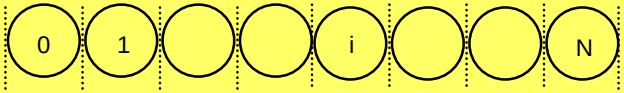

Q= 0/N 1/N .... i/N .... N/N

Aim: $Q_i = a_i + b_i \cdot q_i$

– Definition of the reconstruction parameters as $q_i = \frac{S_{i+1} - S_{i-1}}{S_{i-1} + S_i + S_{i+1}}$

– Identification of a_i and b_i via measuring of q_i at $S_i \approx S_{i-1}$ or $S_i \approx S_{i+1}$:

$a_i + b_i \cdot q_i^L = \frac{i}{N}$ respectively $a_i + b_i \cdot q_i^R = \frac{i+1}{N}$

→ Linear system of equation for calculation a_i and b_i

$x_k \ bzw. \ y_k = Q_{x/y} \cdot M$

Sensitivity correction

- Intensity distribution of the detector is affected by:
  - Size of the scintillator plates, in-homogeneity of the Scintillator‘s, the reflector coating and the photocathode
  - Less linearity of the position reconstruction at the outer face PMTs -> sensitive area approx. 50x50 cm^2
- Calibration measurements and sensitivity correction is useful/needed

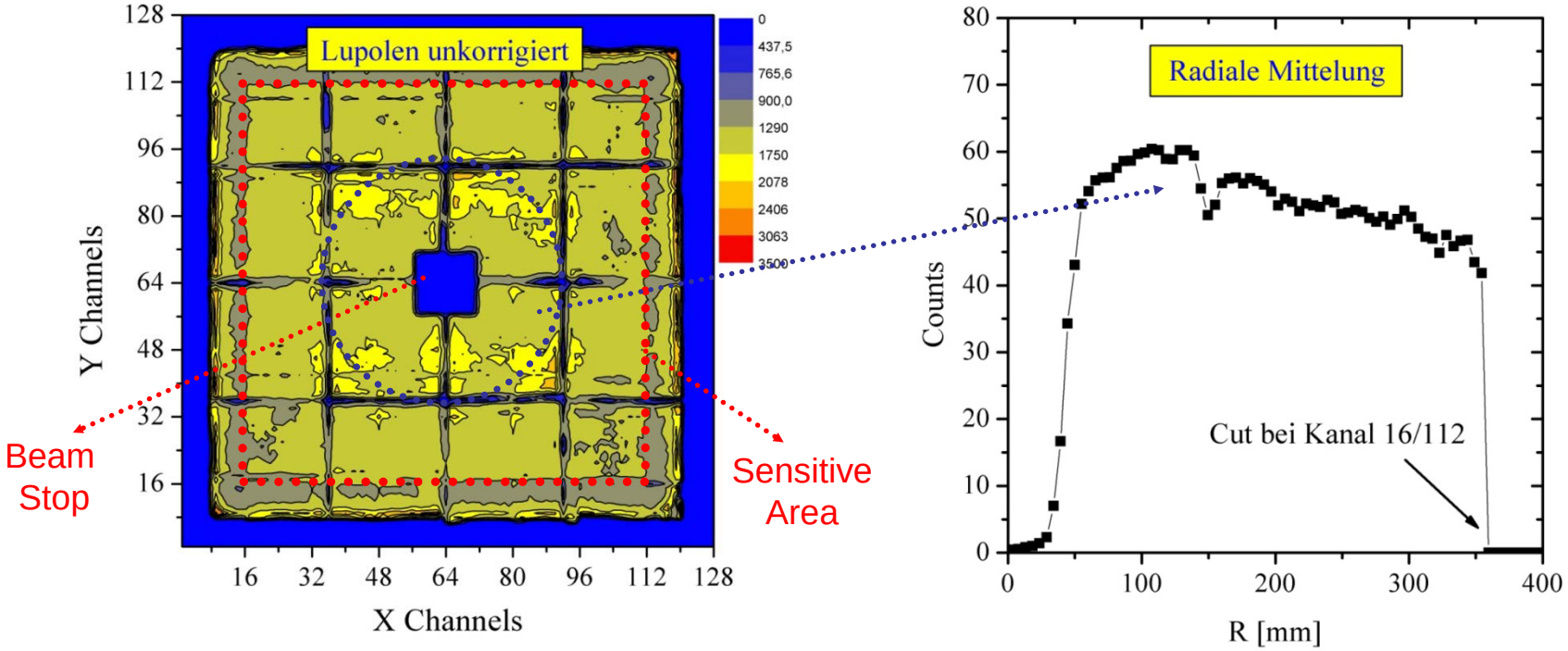

Measurements with a diaphragm

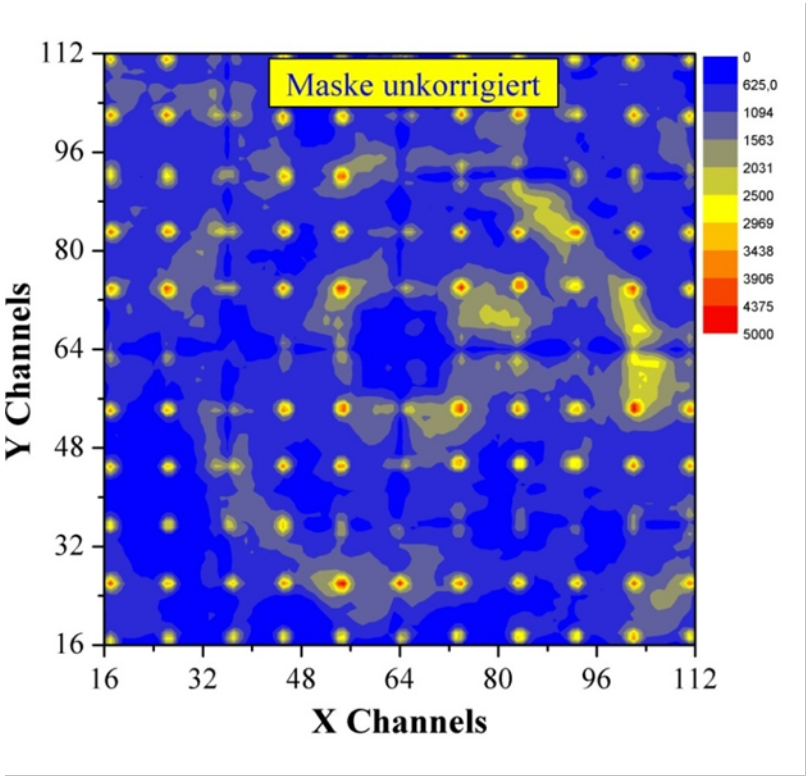

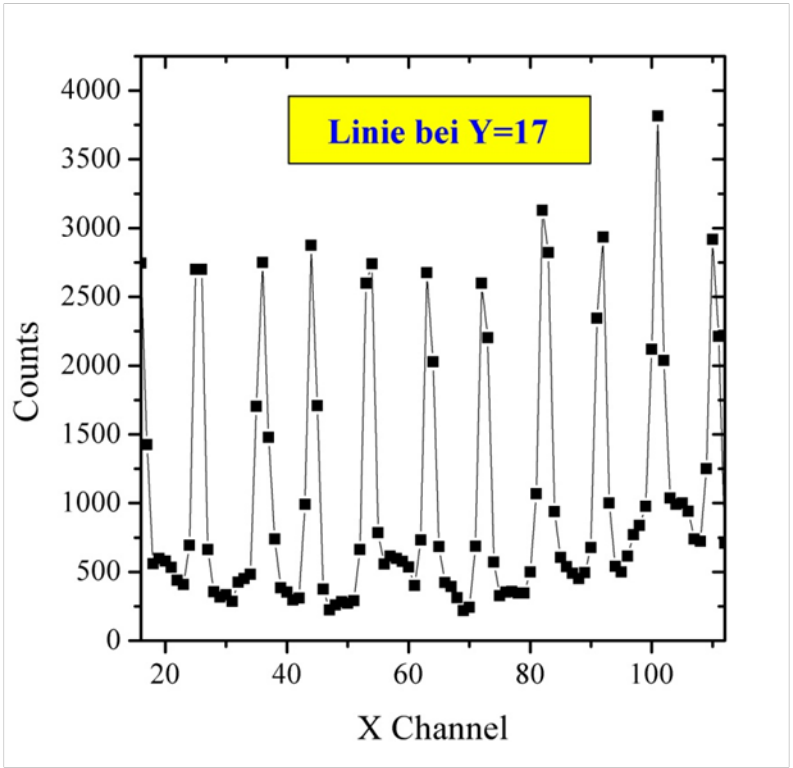

- Thin Al-diaphragm in front of the detector
  - Coated with Boron Carbide, 5mm holes & 5cm spacing
  - Some holes are located directly above the edge of the scintillator plates
  - Definition of von position sensitivity and linearity

Measured – position resolution

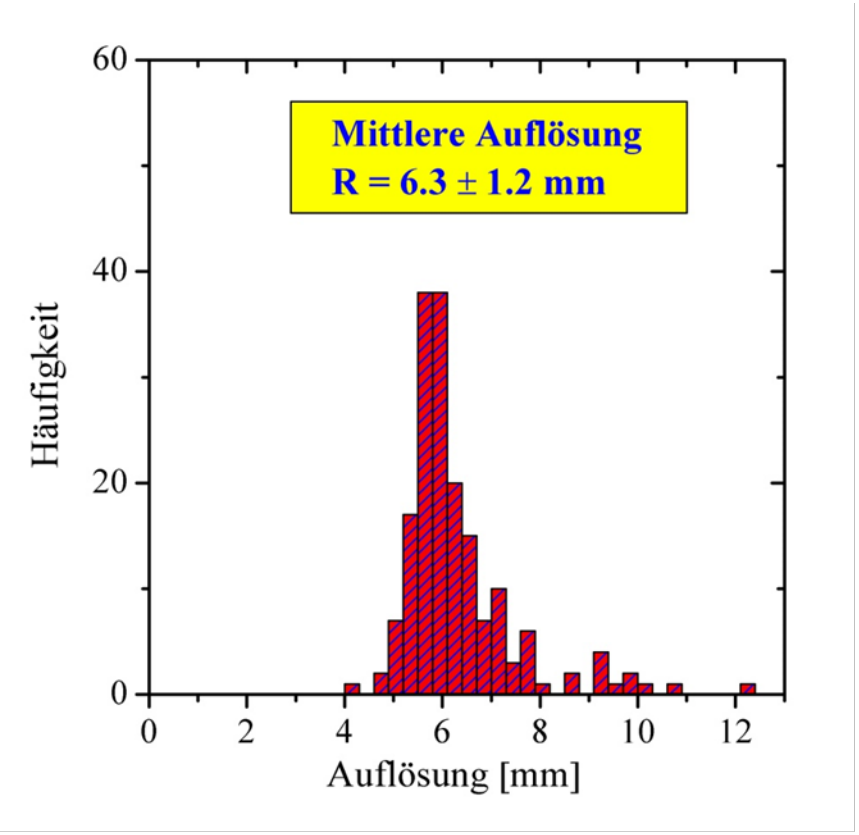

- Position resolution of the detector
  - proportional to the square of the detected light:

$$R = P\frac{D}{\sqrt{N}}$$

  - light reduction at the edge of each scintillator plate
  - calculation was made out of the width of the peak at the holes of the diaphragm

$$\Delta R = \sqrt{P_{FWHM}^2 - D_{Loch}^2}$$

- Position sensitivity improved:
  - Old System 8 mm ↔ new System 6.3 mm

Measured - Linearity

– The difference between actual position and nominal position gives us a number for the non linearity of the detector

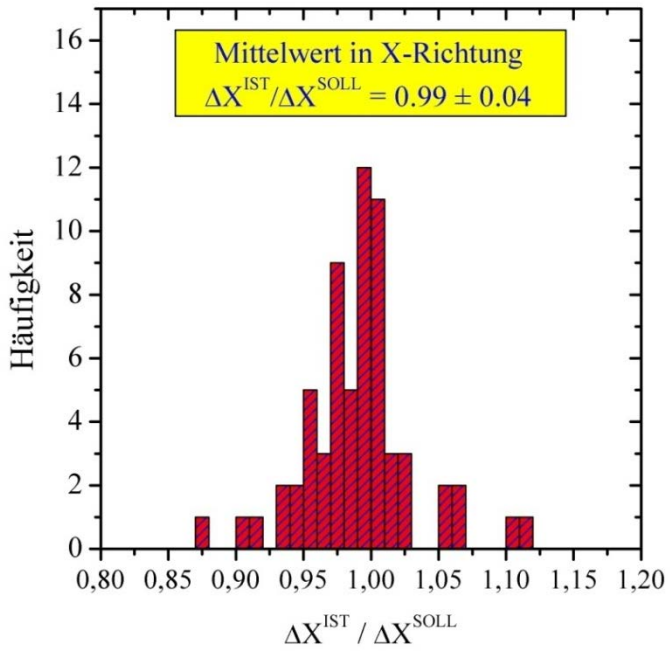

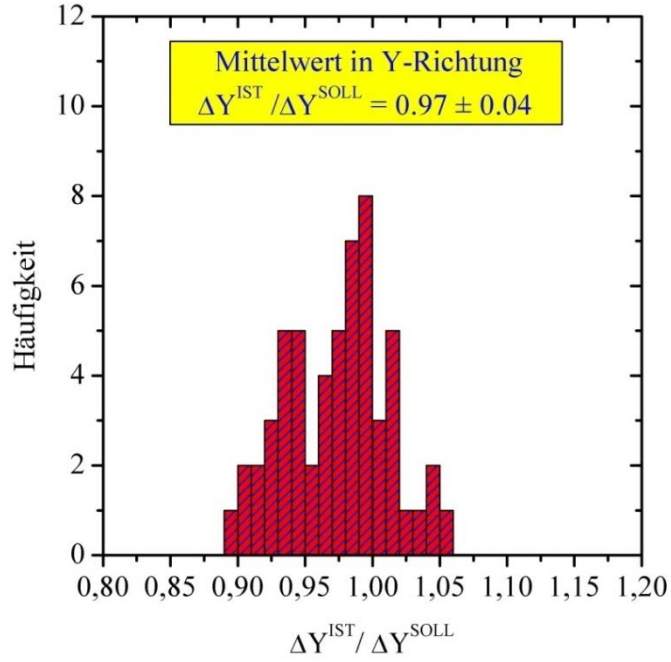

- Linearity of the Detector system was improved :
  - Differential: max $|\Delta s - \Delta s_M| = 11\% \leftrightarrow$ old Detector: 15%
  - Integral: average deviation $s_{actual} - s_{nominal} = \pm 0.1$ channel
    new Detector: 2,8 % ↔ old Detector: 3%

Dead time of the Detector

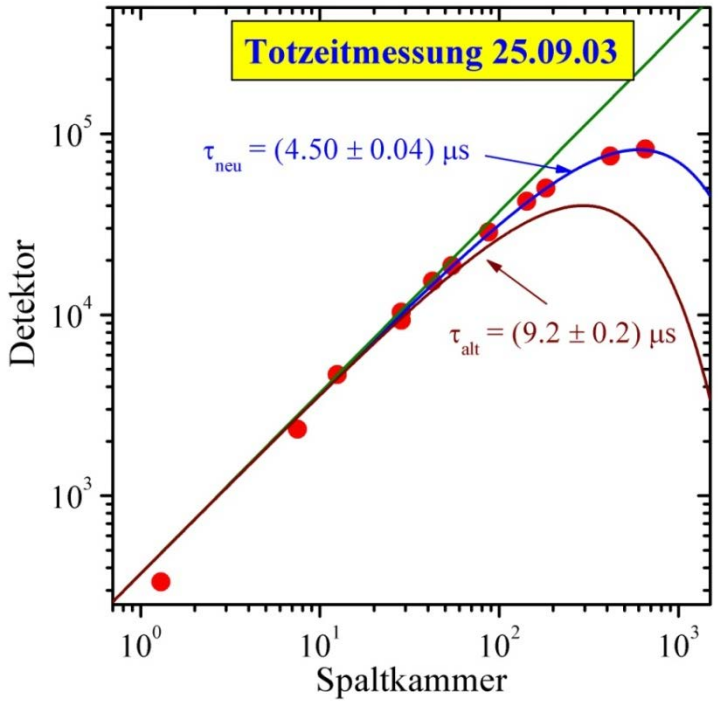

- Measuring the dead time
  - Lupolen probe in the beam line
  - Comparison between fission chamber and Detector
- Paralytic dead time model
  - Dead time of the electronics increases with short pulse sequences
  - Calculation of τ obtained by fitting with:

$$I_D = I_S \cdot e^{-I_S \cdot \tau}$$

G. Knoll

- Dead time could be reduced by 50%
  - old Detector 9.2 µs ↔ new Detector 4.5 µs
  - Further improvements and a reduction to 2-3 µs possible, signal- und event processing

Anger Camera Readout Electronics
- LVD Crate -

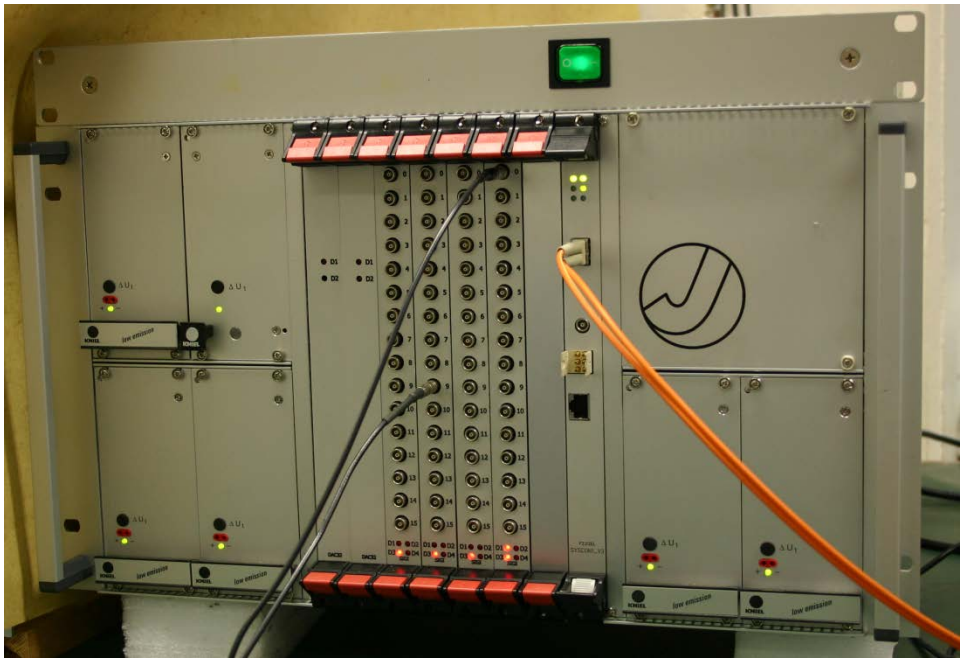

- Driver for Windows XP and Linux available
- C/C++ framework for thread based data processing available
- Advantage of a flexible environment for development and debugging of reconstruction algorithms and data acquisition programs
- Possibility of raw data storage on disk for offline data analysis
- Manufactured for KWS1 & KWS2

Anger Camera Readout Electronics
- Pulse Processing Board -

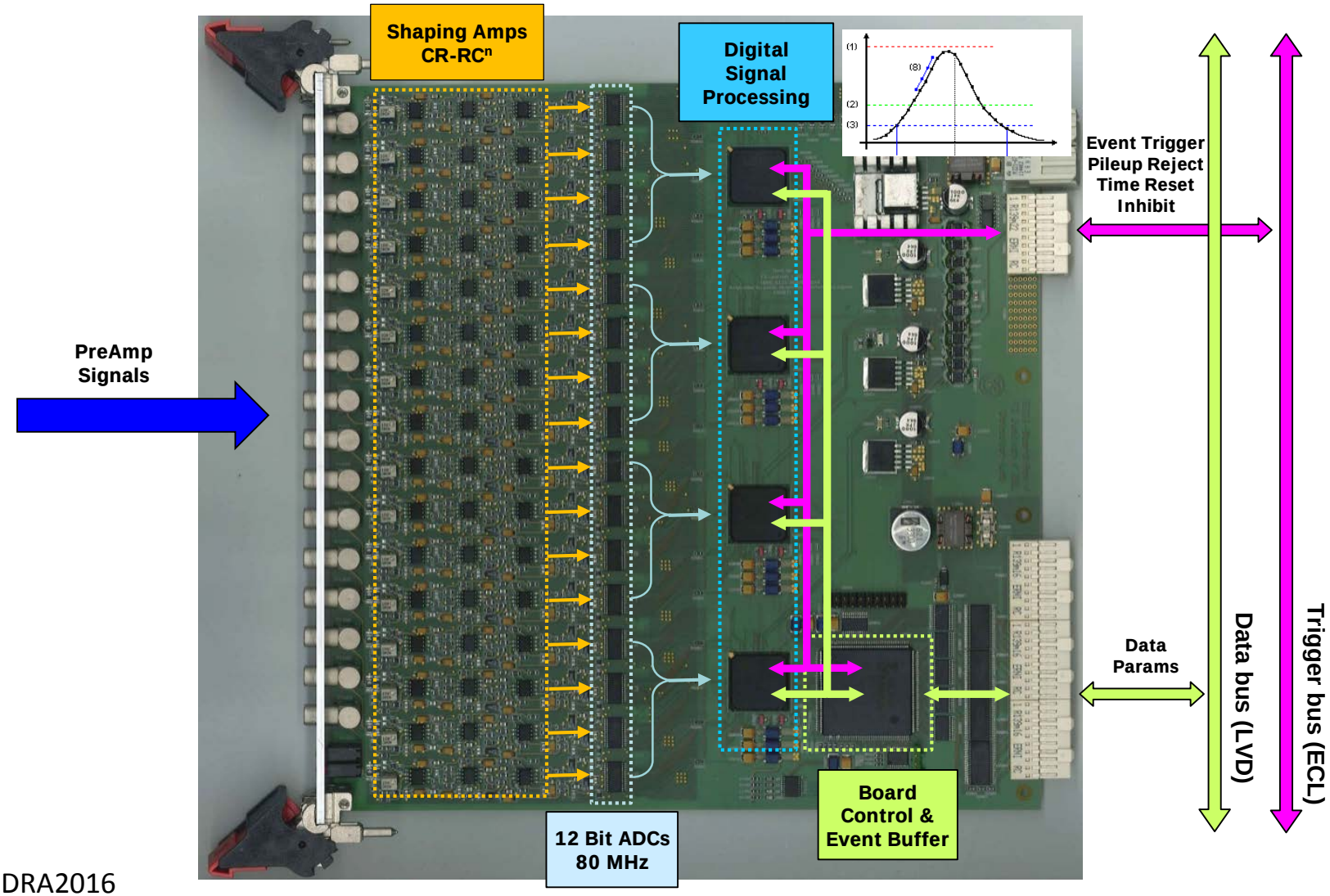

Anger Camera Readout Electronics
Statistical dead time of the detector

- Simultaneous measurement with fission chamber
- Count rate behavior corresponds to paralytic model
- Measurement at different distances with up to 600 kHz
- Fit to paralytic model gives dead time τ: ~ 0.64 µs

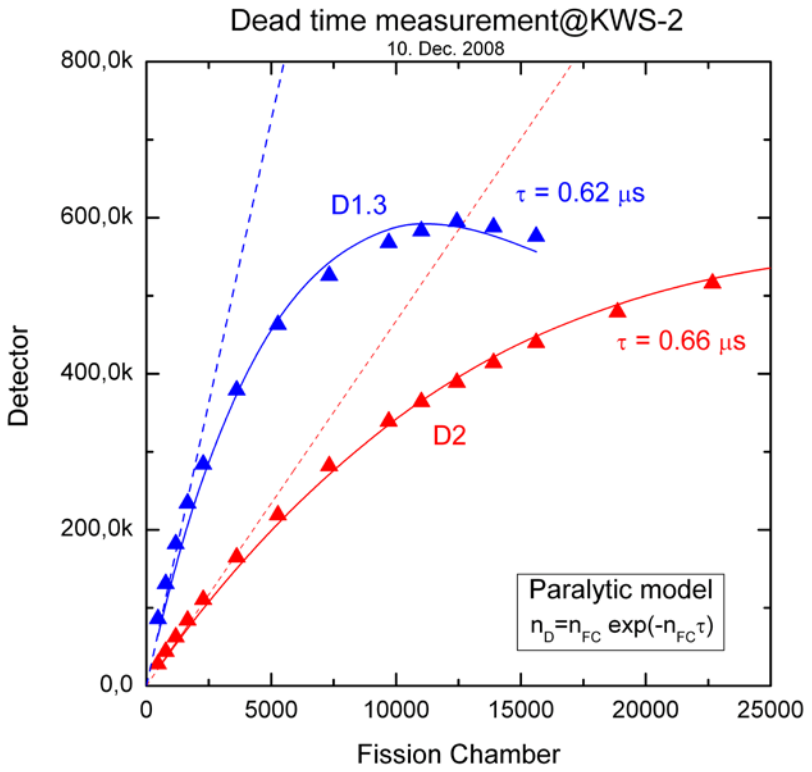

Combination of two position sensitive detector systems

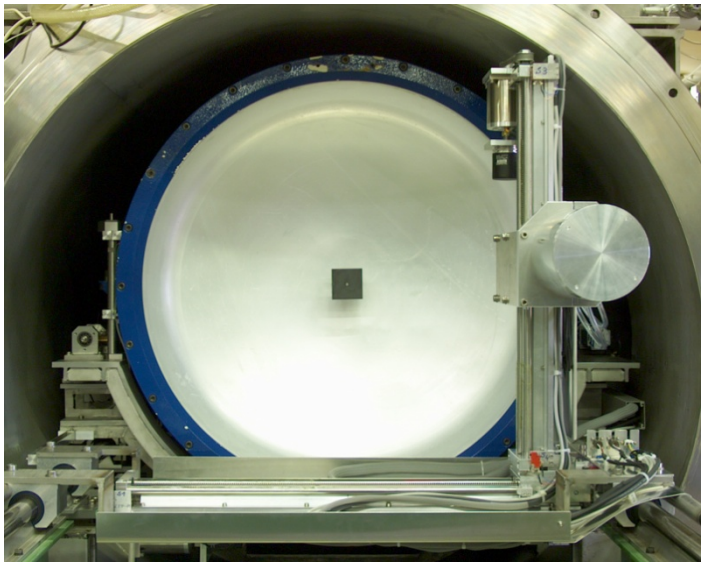

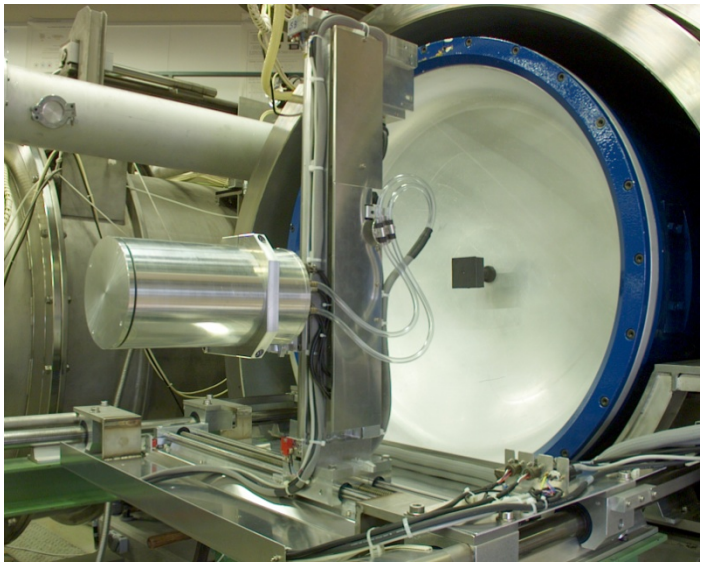

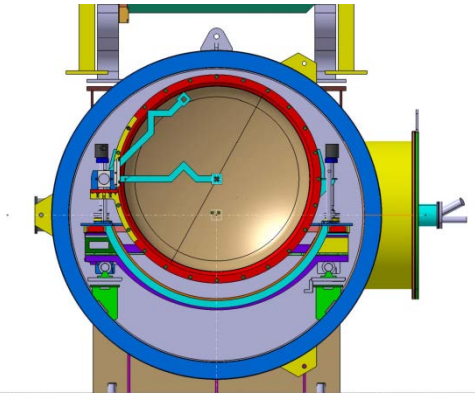

- High resolution KWS with the 2-dimensional Detector on a 2–dimensional motion unit in front of the big Scintillation Detector system
- Small System can be parked outside the sensitive area of the big detector
- Small System can be moved to any position in front of the big system. (Magnifying detector)

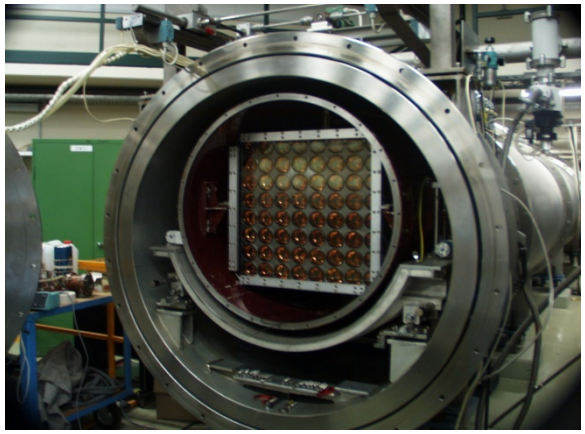

Quelle: H. Frielingaus

Results of test measurements with the combined Detector-Systems

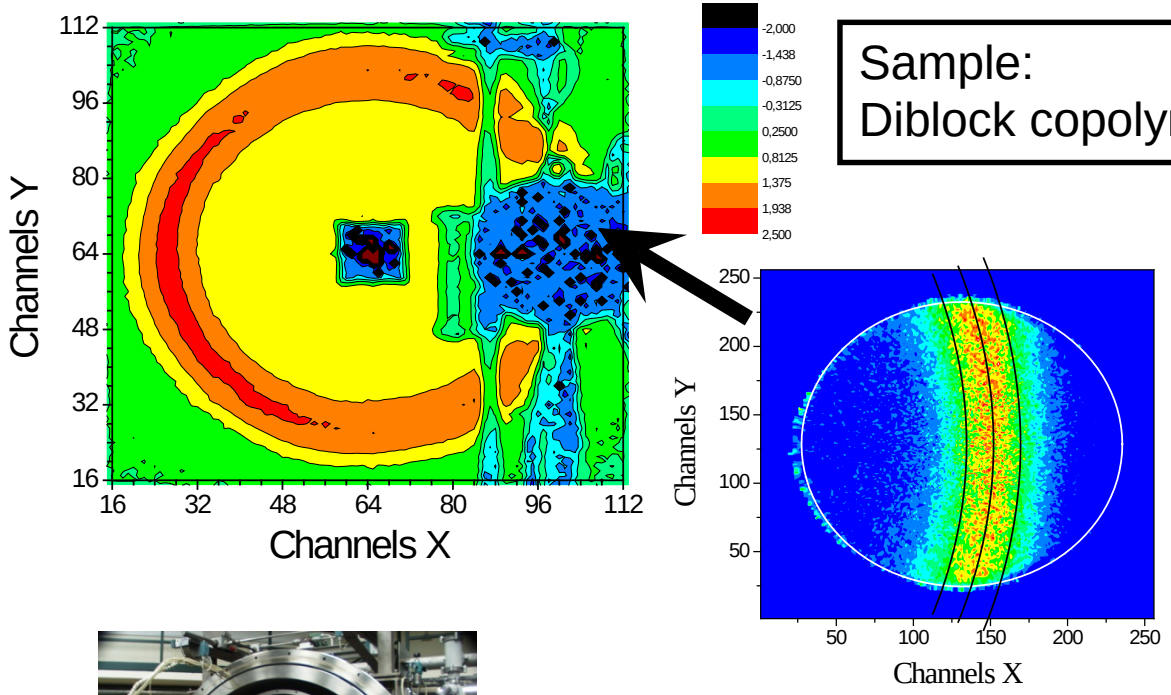

Sample:
Diblock copolymer

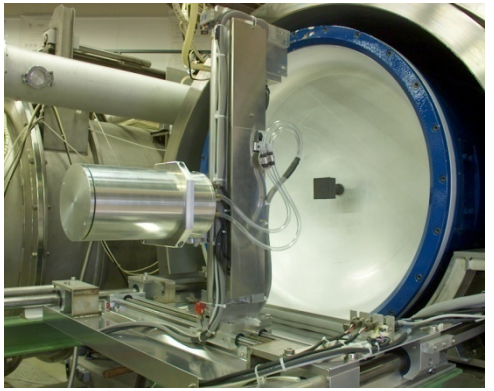

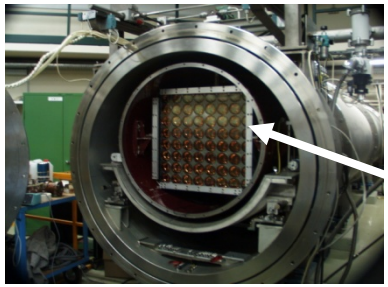

Open vacuum tube with the 60 x 60cm^2
Scintillation detector

Diaphragm with 2mm holes

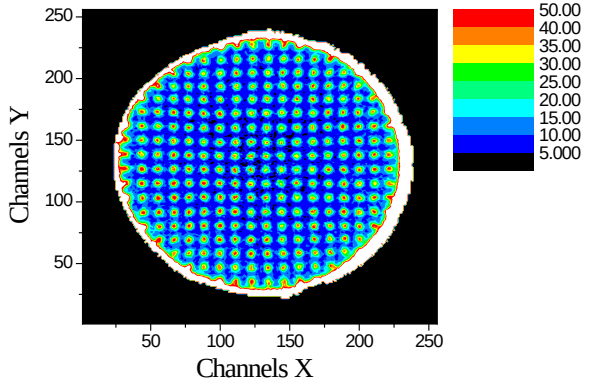

Quelle: H. Frielingaus

Measurements

- KWS-1 Detector was in operation in Jülich from Mai´03 until Mai´06
  - Assembling of the KWS-2 Detector was done July ´04 and it operates until Mai`06
- Neutron Efficiency was improved in comparison to the former detector system
  - Spatial resolution 6.3 ± 1.2 mm, diff. Linearity: 11% , integral: 2.8%
- Maximum Count rate was increased
  - Statistical dead time was reduced by 50%, τ = 4.5 ± 0.04 μs
- Excellent Quality of the corrected spectra's
  - More Stability with the Sensitivity corrections
  - Exact reconstruction of complex two dimensional scatter experiments

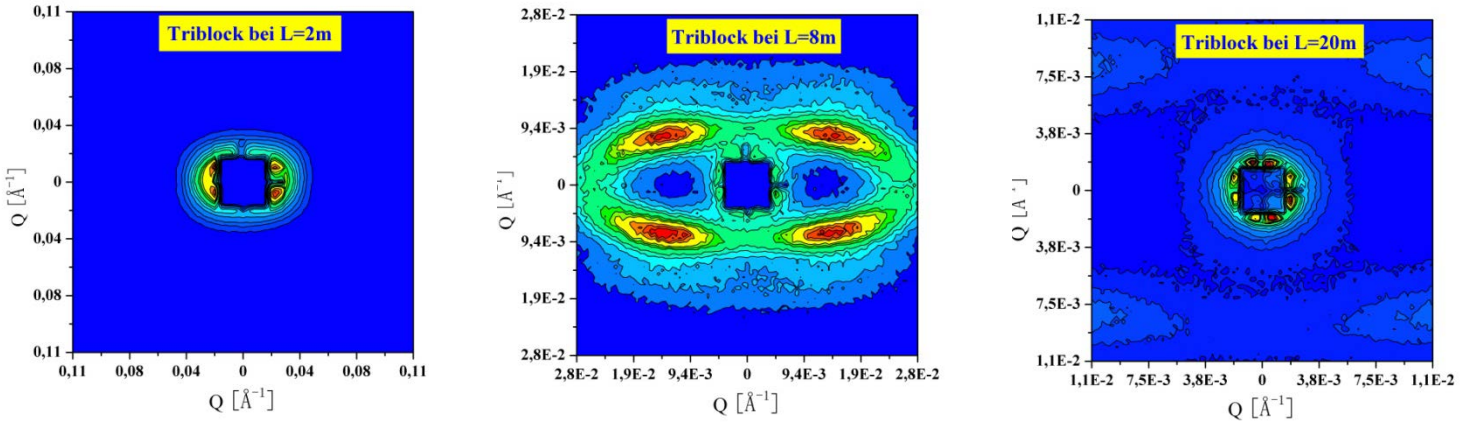

Measruements with a Triblock (styrol-isoprene-styrol chain, 100% expand)

Detectors based on position sensitive PMTs

Neutron Scintillation Detectors

Detector with position sensitive PMT:

- ^{6}Li-Glas scintillator for neutron capture
- Photomultiplier with Mesh-Dynode structure
- Readout via resistore network
- Position reconstruction via division method
- Linear range up to 10cm ∅

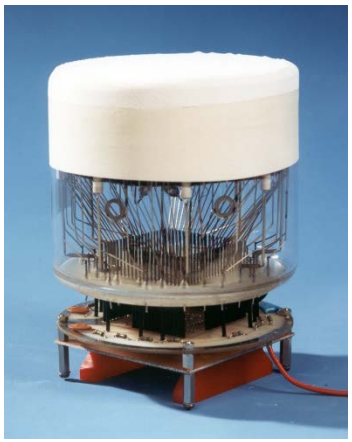

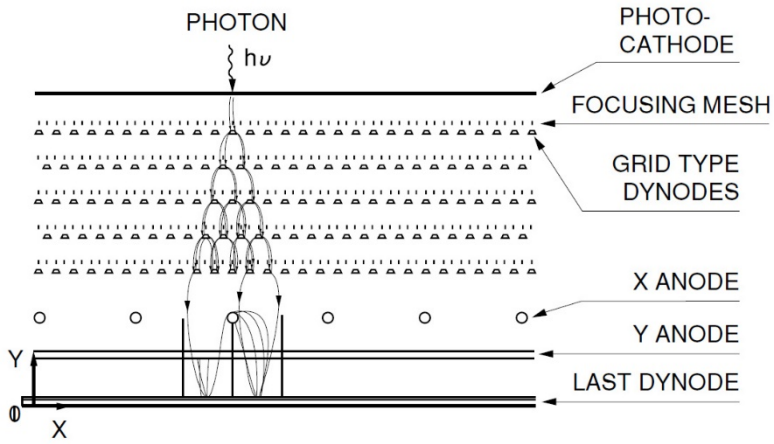

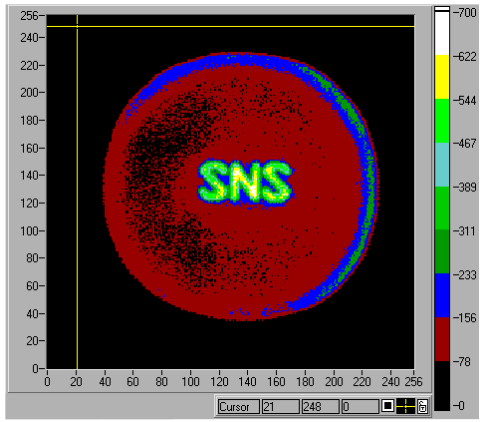

γ-Discrimination:

- Problem because of photocathode inhomogenities
- Software based discrimination for each chanal
- Automated calibration program for adjustment of 65,000 thresholds

Electromechanical Design of the position sensitive PM

Part Number	R3292-02
Type	Head On
Size	132mm
Active Area Diameter or Length	100mm
Min. Wavelength	300nm
Max. Wavelength	650nm
Peak Sensitivity Wavelength	420nm
Cathode Radiant Sensitivity	72mA/W
Window	Borosilicate
Cathode Type	Bialkali
Cathode Luminous Sensitivity	80µA/lm
Cathode Blue Sensitivity Index	9
Gain	1.0E+05
Dark Current	40nA
Rise Time	6ns
Transit Time	20ns
Number of Dynodes	12
Applied Voltage	1250V

Two Anode levels with

- 28 wires in X- and Y-Direction
- 2 Resistor chains
- 4 Output signals

$$Q_x = \frac{X_2 - X_1}{X_2 + X_1} \qquad Q_y = \frac{Y_2 - Y_1}{Y_2 + Y_1}$$

Hamamatsu

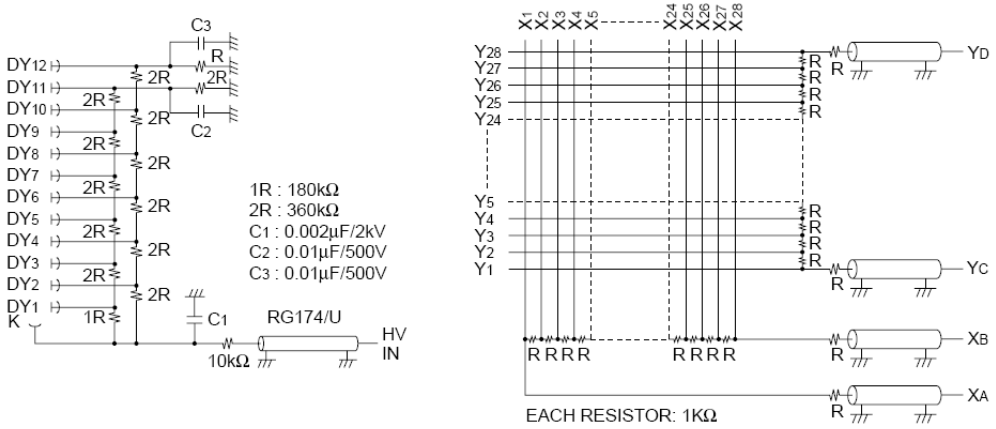

Position Sensitive - PMT Readout Electronics - Block Diagram -

PS-PMT Readout:

- Readout by resistor chain
- Position reconstruction via pulse division method

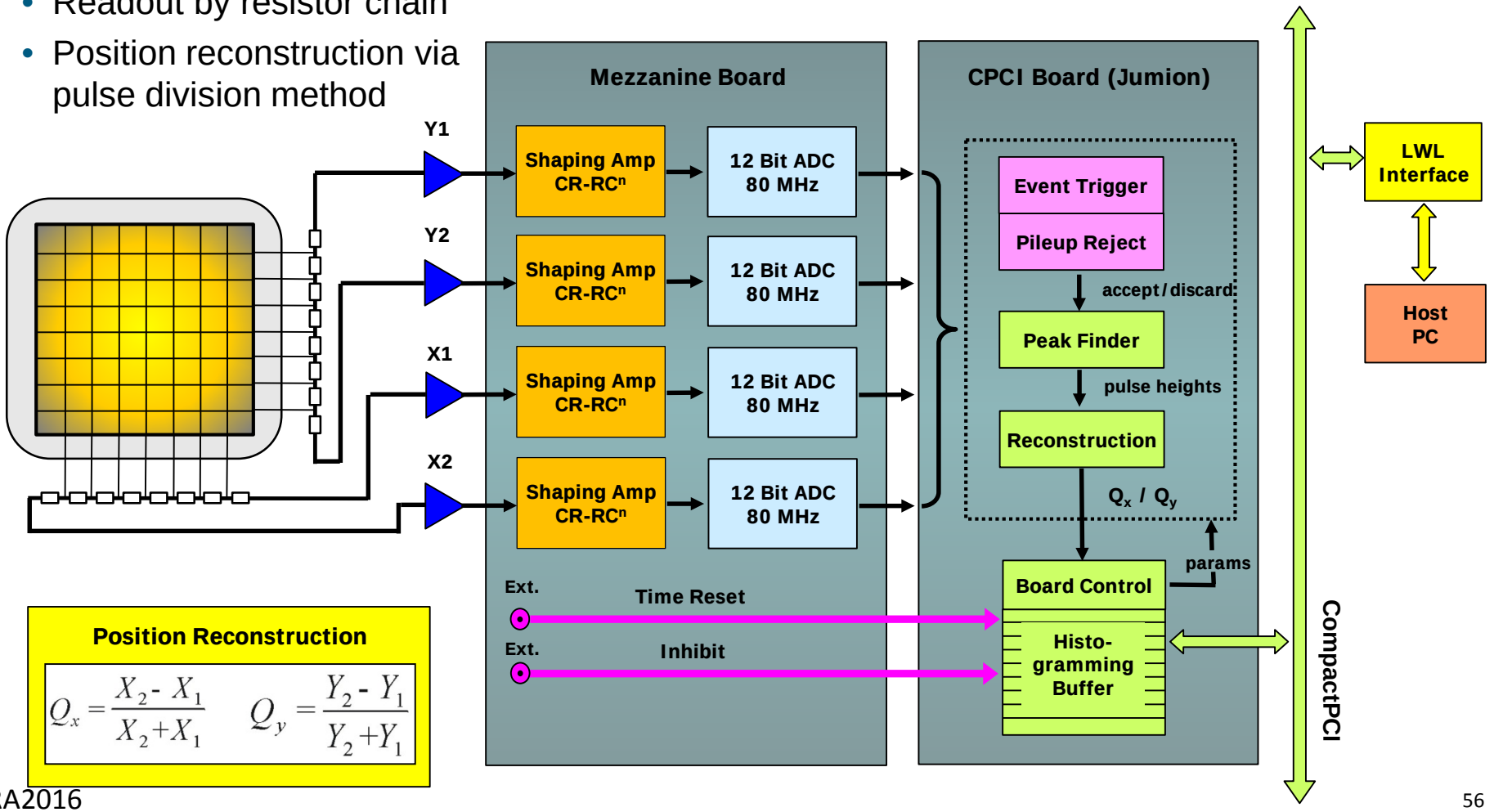

Readout Electronics for PS-PMT
- Jumion + CMC CompactPCI Board -

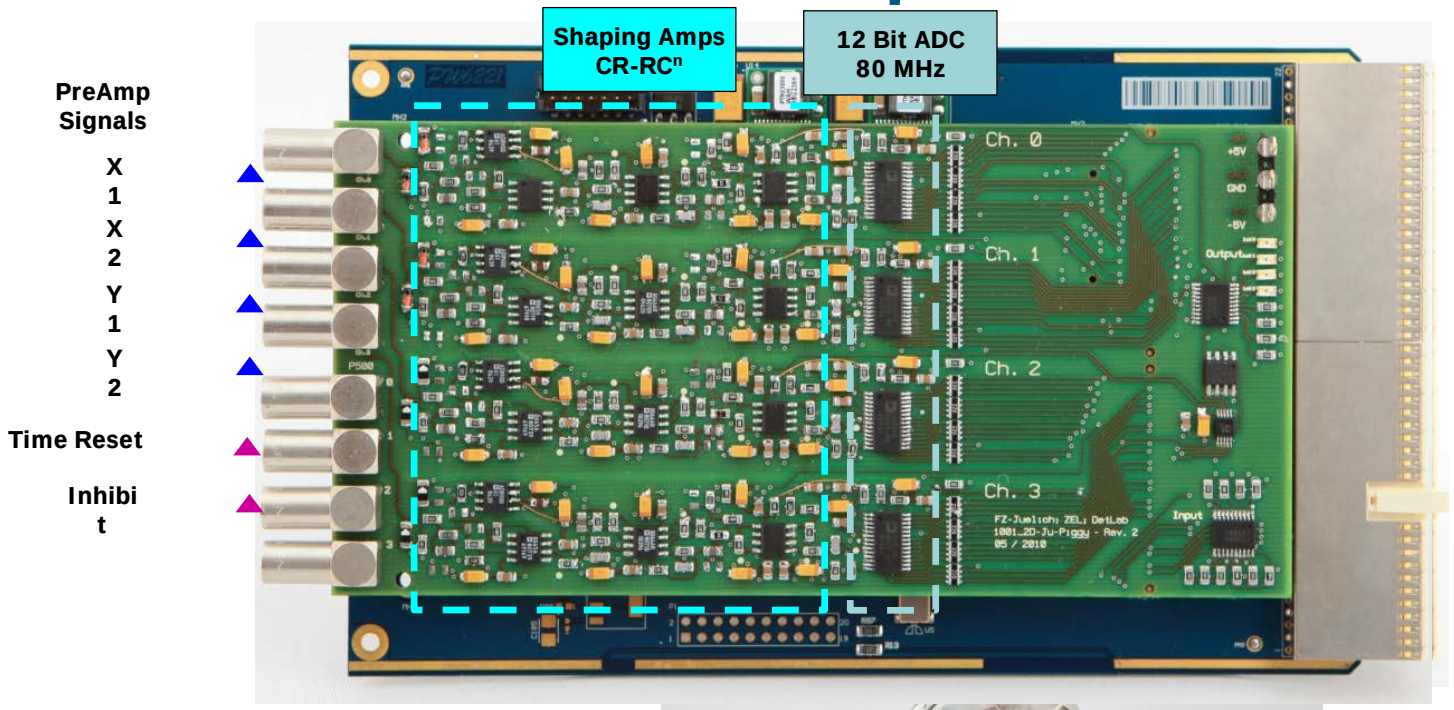

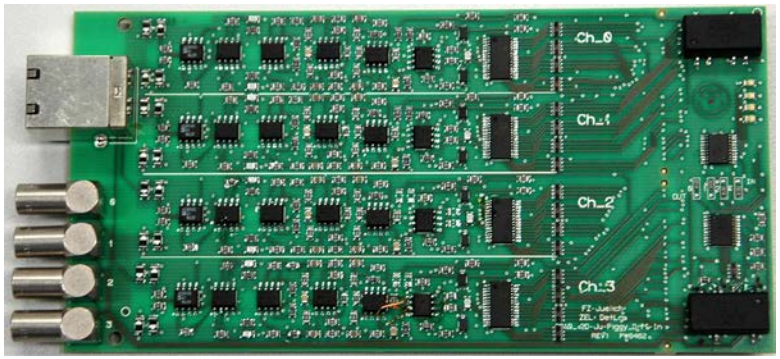

Electronic Parameter

- CMC Board
  - *Pulse width time 800ns*
  - *Four 12bit 80 MHz ADCs*
  - *Digital I/O (TOF, Trigger)*
- Main Board
  - *XILINX SPARTAN3*
  - *CPCI with PLX PCI bridge*
- Read out
  - *Optical Interface to DAQ PC (MXI-3 from NI)*

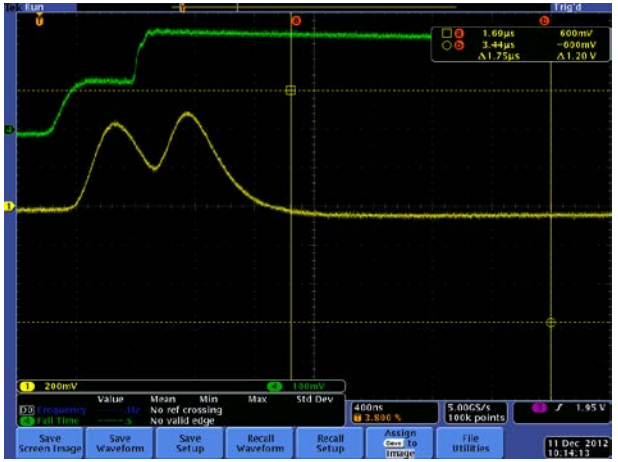

Parasitic Coupling

twisted-pair

without parasitic coupling

single-ended

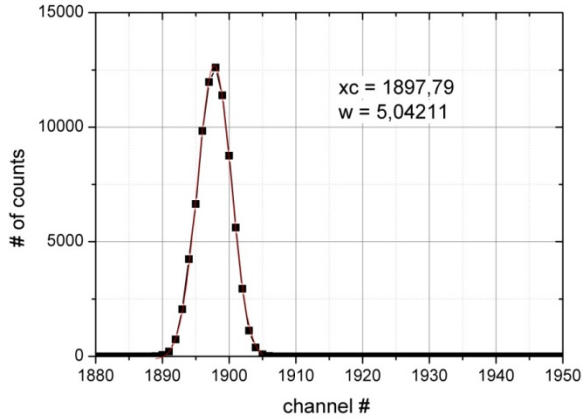

FWHM = 0,260%

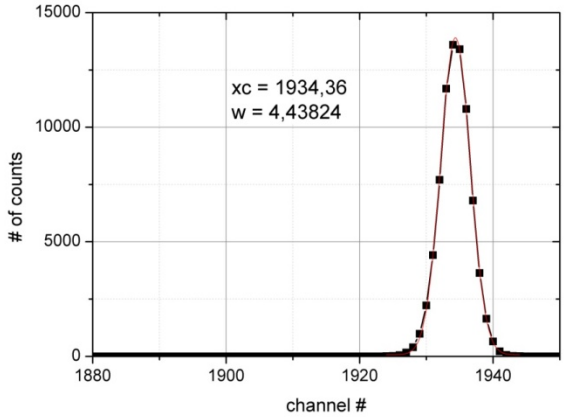

FWHM = 0,229%

with parasitic coupling

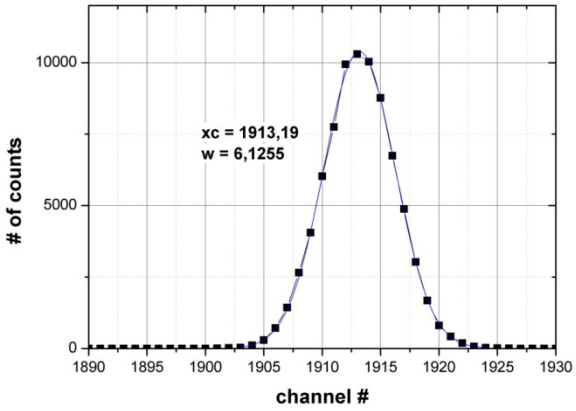

FWHM = 0,320%

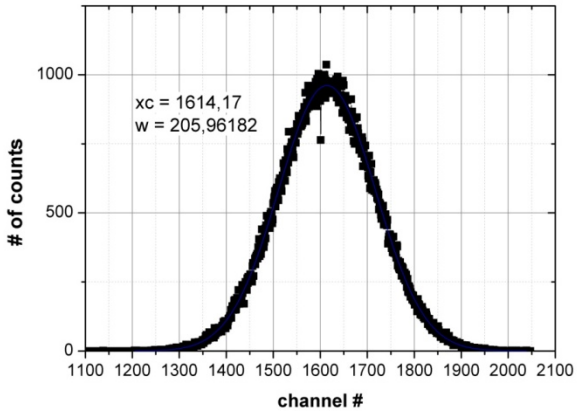

FWHM = 12,76%

Results of test measurements with the combined Detector-Systems

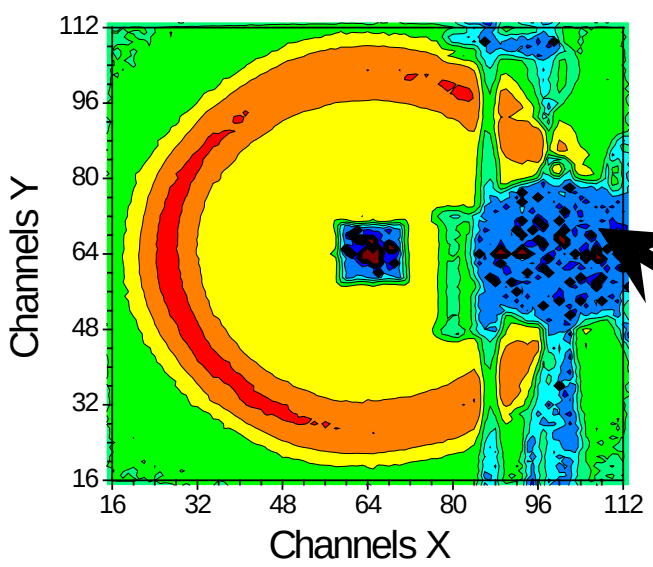

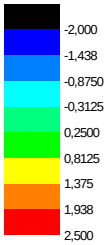

Sample:
Diblock copolymer

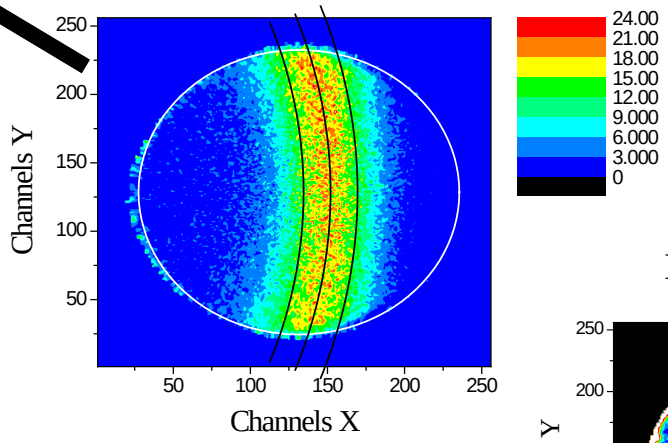

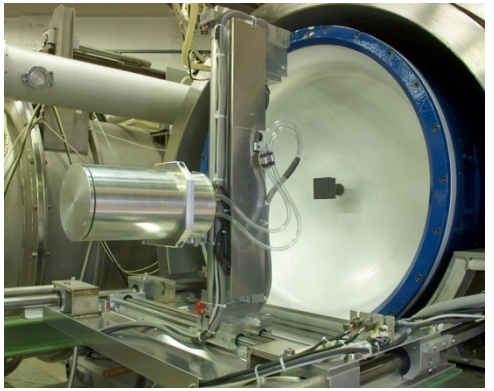

Diaphragm with 2mm holes

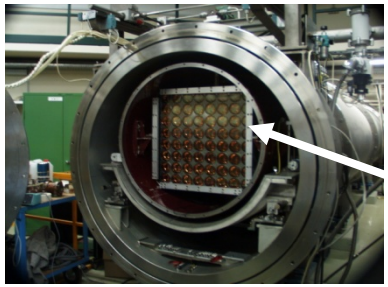

Open vacuum tube with the 60 x 60cm^2
Scintillation detector

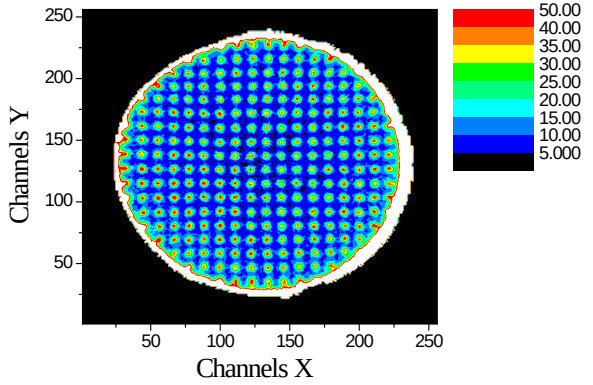

Quelle: H. Frielingaus

Test – Measurements

2-dimensional Image

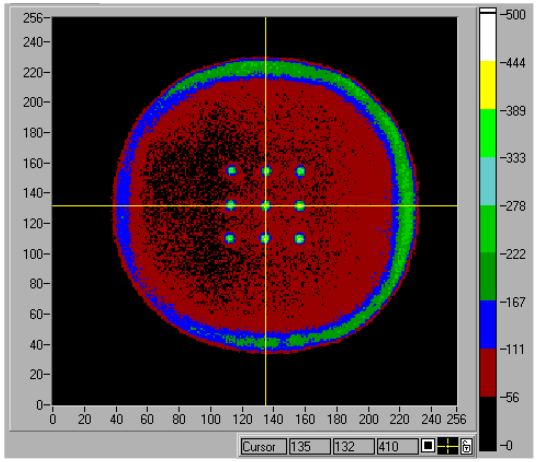

3 x 3 Diaphragm with 2mm holes and 10mm spacing

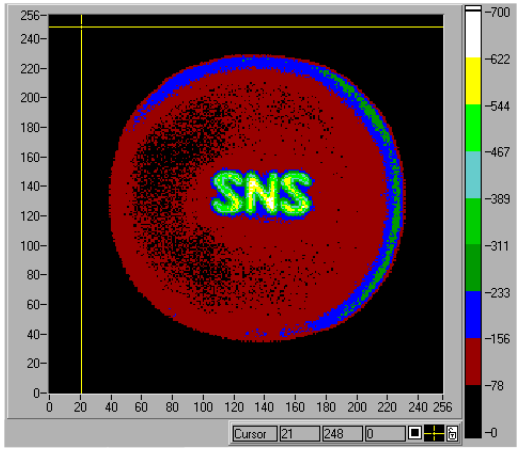

2-dimensional Image

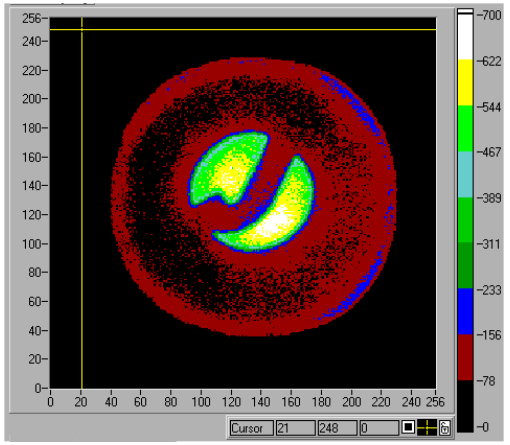

X- und Y-Schnitt

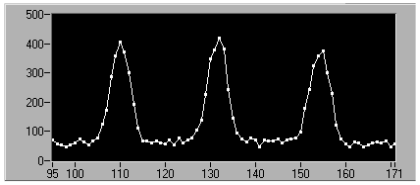

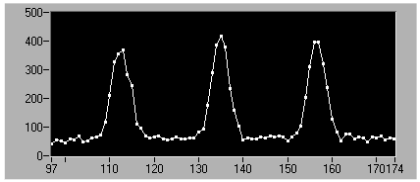

Peaks are clearly separated
-> Spatial resolution < 2mm
-> 0.56 mm per pixel

Setup of the KWS 3

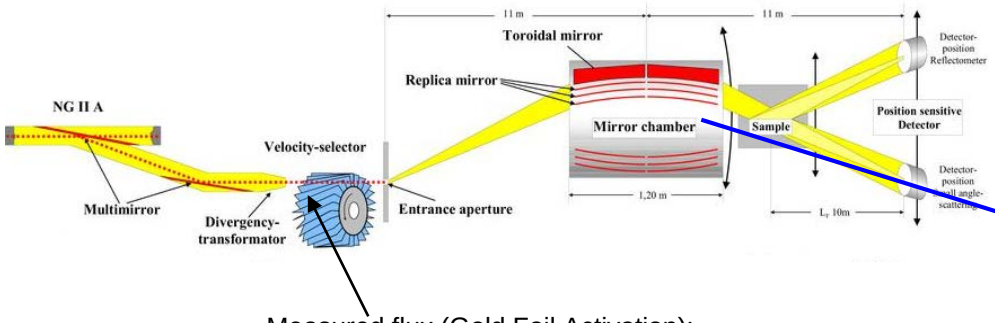

Measured flux (Gold Foil Activation):
Φ = 2 x 106 n/s/cm2

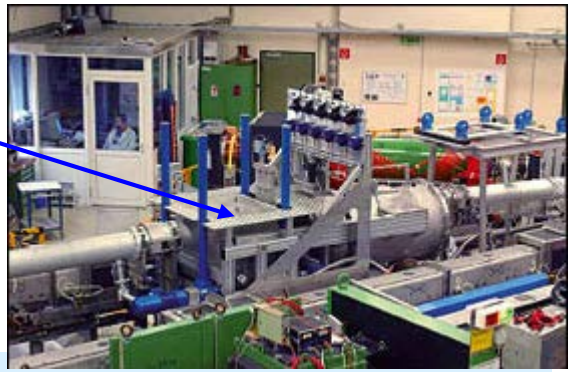

KWS-3 @ FRM-II

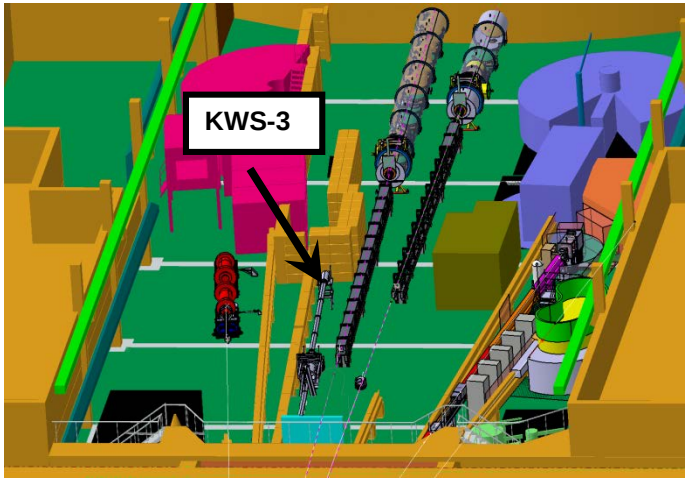

Instrumental Details of KWS-3	
Wavelength	λ = (12.7±0.6) Å (9% FWHM)
Entrance aperture	r_E = 1 to 10 mm
Wave vector resolution given by the opening of the entrance aperture	$\Delta Q = k\, r_E / L$ (k = 2π/λ)
Scattering wave vector range	$10^{-4} \le Q \le 2 \cdot 10^{-3}$ Å^{-1} $10^{-4} \le Q_z \le 0.08$ Å^{-1} in reflectometry mode
Neutron intensity at sample position is proportional to the surface of the entrance aperture:	I = 180 n/s per mm² entrance aperture.
For a wave vector resolution of 10^{-4} Å^{-1} (2 x 2 mm² entrance slit aperture) the intensity is therefore 720 n/s	
Cross section of beam at sample position:	10 cm wide, 2 cm high
Position sensitive detector, 8 cm diameter, 1.5 x 1.5 mm resolution	

Quelle: E. Kentzinger

Setup of the remotely controlled test bench

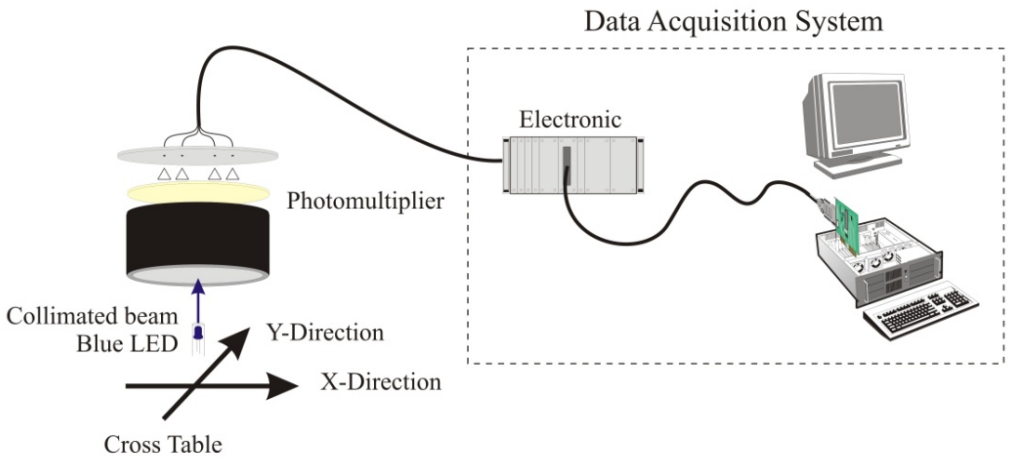

- The test bench has an active scan range of 40cm x 40cm with a collimated 1mm (exchangeable) blue light source
- SPS controlled motion unit
- Position reconstruction is < ±15µm

- Test software allows different figures/scans to test the PMT
- Every parameter are stored in files for each scanned PMT like
  - scan area,
  - temperature in/out-site scan box,
  - pulse height spectra for each pixel and in total

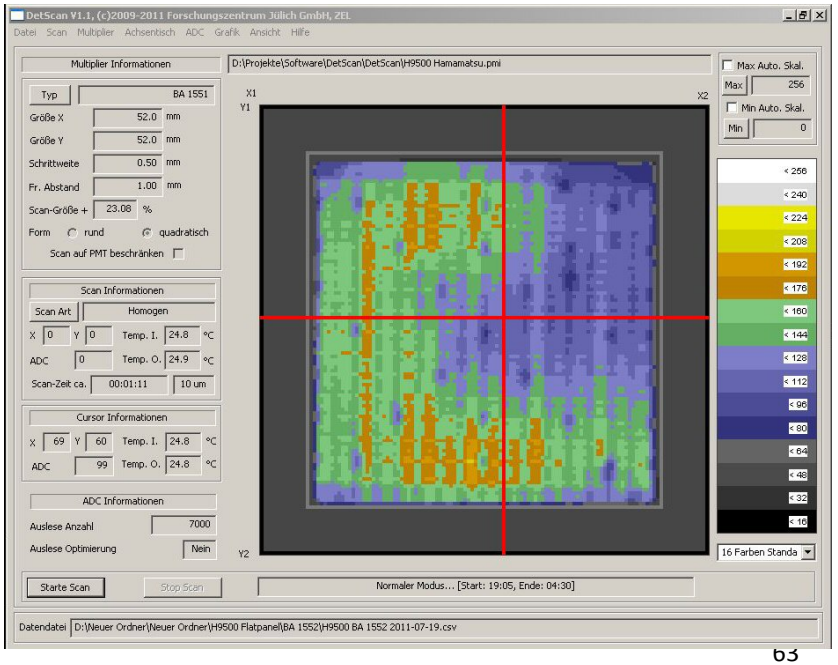

Different data presentations of scanned PMTs

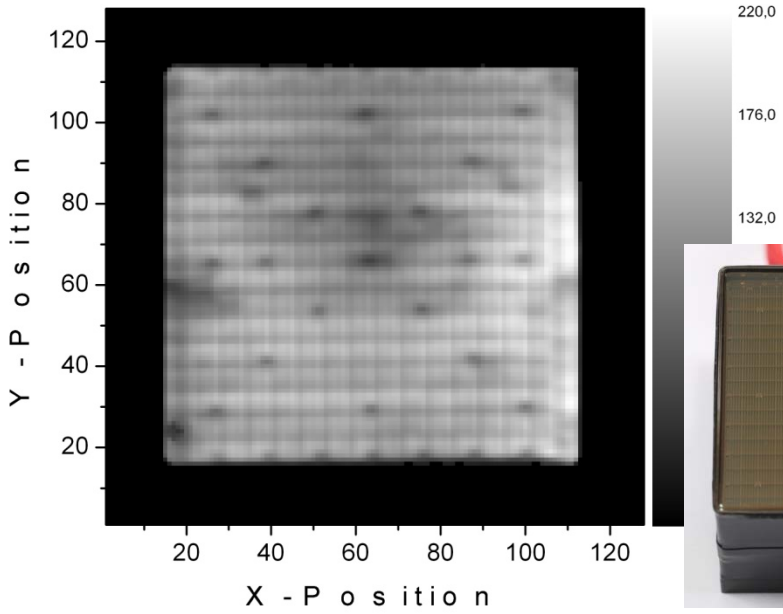

- Two dimensional grey scale plot of a H9500 Ma Tube
- Scanned with blue light
  - # of photons are equivalent as a neutron emitt in a Li-glass scint.
- Pixel structure is very well to see!
- The in-homogeneity is less than 1:3

- Waterfall diagram of a R3292 position sensitive PMT
- The supporting wires for the Mesh dynode are well to see
- The in-homogeneity is less than 1:2,5

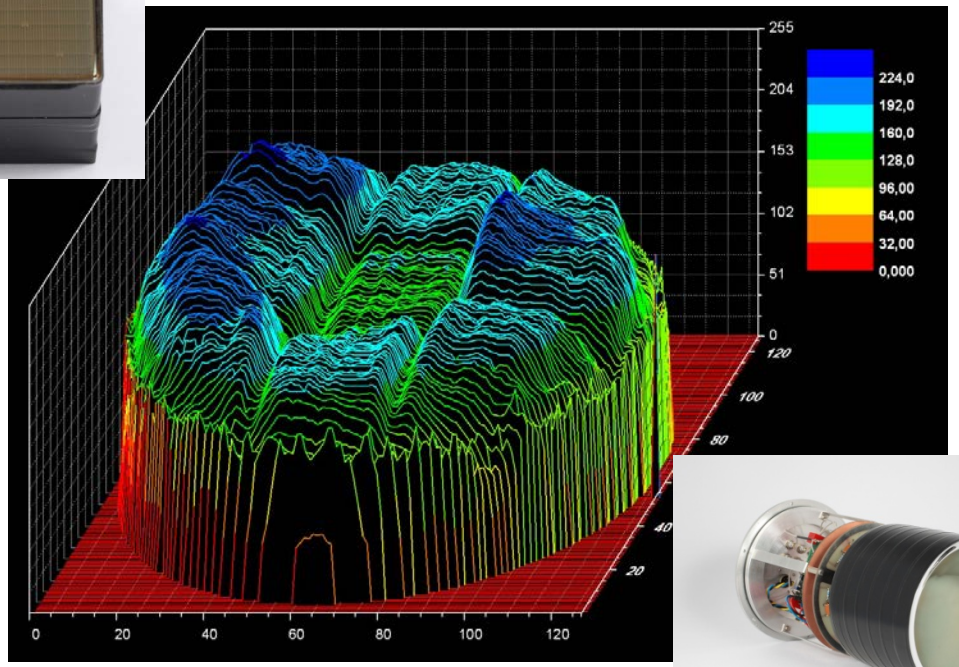

A Multianode PMT adapted to the 2d-readout system

- very high spatial resolution
- high thermal neutron efficiency
- in-house electronic

Innovative Anger detectors with light guides

Wide FOV (field of view) scintillator

Reduce light "footprint"

Reduced Detection Plane

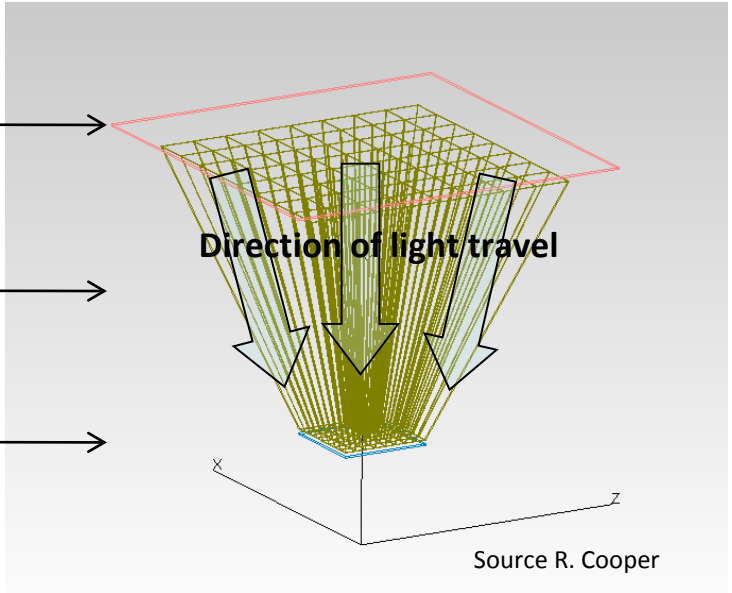

Principle can be used either as Anger camera or as direct view detector

Prototype at FZJ:

- Conical plexiglas light guides
- Mapping of 64 scintillator pixels (100mm^2) to 64 PMT pixels (~33mm$^{2)}$
- Study of light loss characteristics and detector performance
- Further test's were done with the MaPMT due to homogeneity and gain.

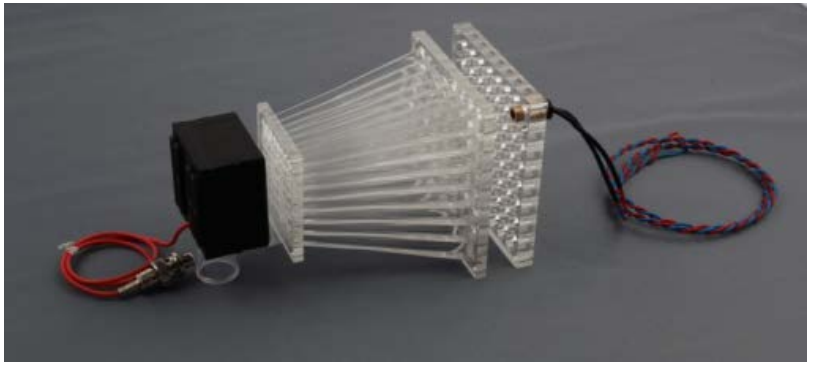

Picture of the PMT with plexiglas light guide and a LED test matrix

Scan measurements of MaPMT together with the plexiglas light guide

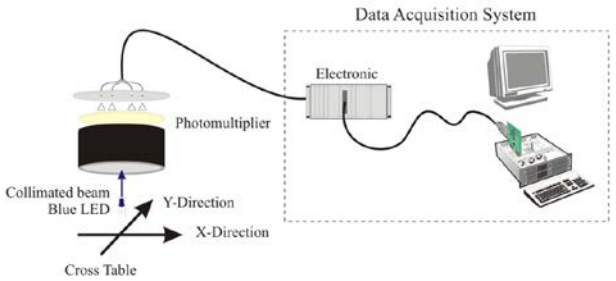

Plot of the scanned MaPMT H8500. The color code is the reference of the inhomogeneity of the photocathode, within a range of 1:3.

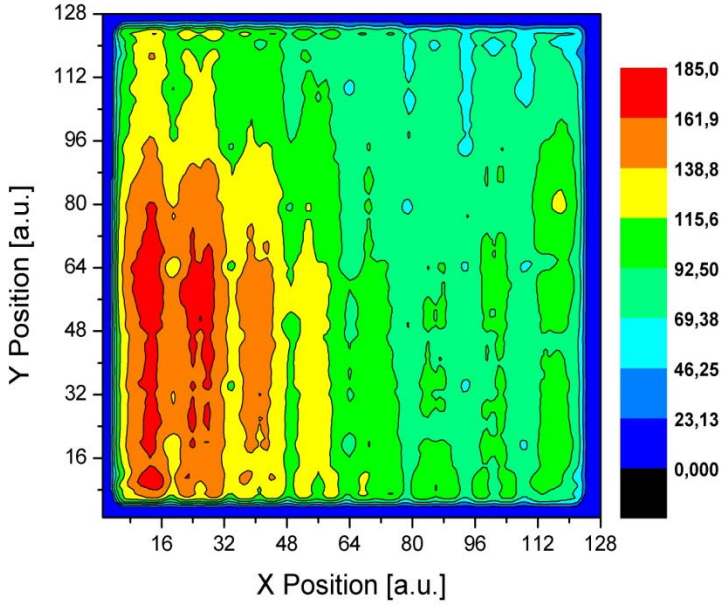

Plot of the scanned MaPMT H8500 together with the Plexiglas rods. The inhomogeneity of the photocathode and the rods need now to further investigate.

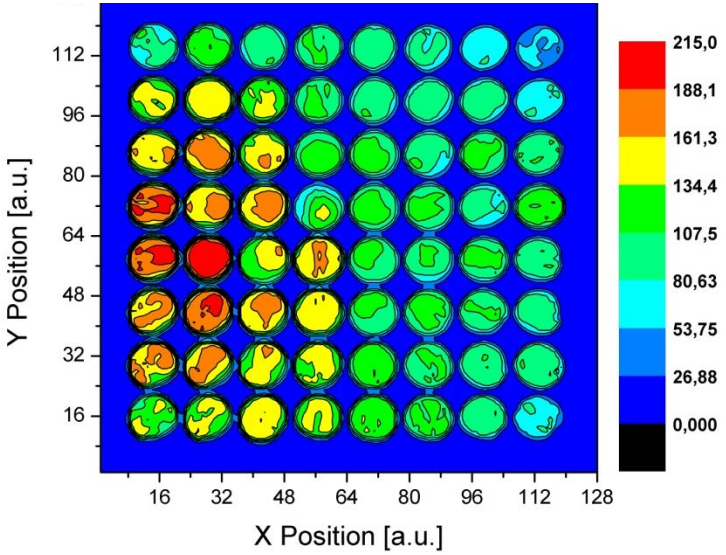

First Wavelength-Shifting Fiber Detector Prototype

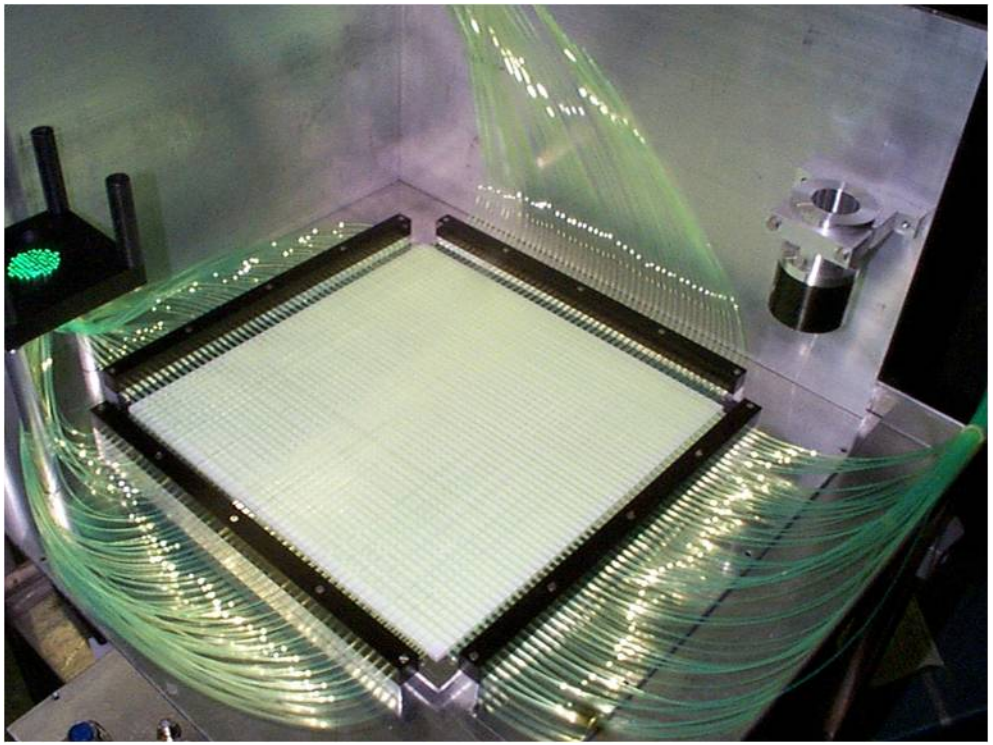

First one I have seen end of ‘90 @ ORNL, USA. Readout was done with two tubes only

Detectors based on Wavelength Shifting Fibers to maximize the size, minimize the costs and replace He-3 technology

- **Option**
  - Detectors with wavelength-shifting-fiber light readout
  - Key issues: large area with minimum dead space, fiber layout, low γ-sensitivity, position resolution, detection efficiency

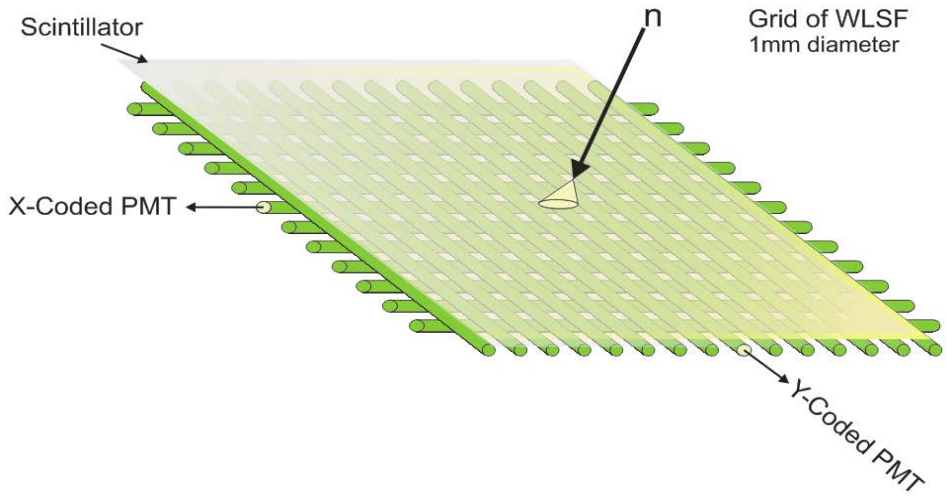

WLSF Detector needs

- Survey of ^{3}He-alternatives showed
  - Apparently, there is a lack of existing and affordable alternatives
  - Emerging technologies are mostly still in the development phase
  - Only the ^{6}LiF/ZnS scintillator with Wavelength-Shifting-Fibers (WLSF) is today applied as alternative for small wavelengths and large areas

- Development of a detector prototype using ^{6}LiF/ZnS-WLSF
  - Validate detector performance for instrument requirements
  - Detector type needs probably shortest time for ready-to-use
  - Large experience at other labs (SNS, RAL, J-PARC)
  - Enhancement of this technology

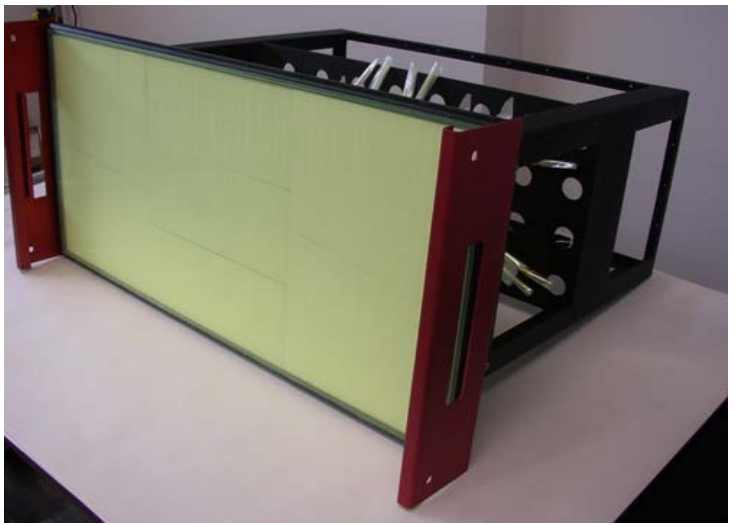

Source R. Cooper

Selection of WLSF from Saint Gobin and their characteristics

BCF 91A and BCF 92 are both WLSFs which fits well to the spectra of the entrance window from the selected PMT.

Standard Sizes and Formulations

Fiber	Emission Color	Emission Peak, nm	Decay Time, ns	1/e Length m*	No. of Photons per MeV**	Characteristics/ Applications
BCF-10	Blue	432	2.7	2.2	~8000	General purpose; optimized for diameters >250µm
BCF-12	Blue	435	3.2	2.7	~8000	Improved transmission for use in long lengths
BCF-20	Green	492	2.7	>3.5	~8000	Fast green scintillator
BCF-60	Green	530	7	>3.5	~7100	3HF formulation for increased radiation hardness
BCF-91A	Green	494	12	>3.5	N/A	Shifts blue to green
BCF-92	Green	492	2.7	>3.5	N/A	Fast blue to green shifter
BCF-98	N/A	N/A	N/A	N/A	N/A	Clear waveguide

*For 1mm diameter fiber; measured with a bialkali cathode PMT
** For Minimum Ionizing Particle (MIP), corrected for PMT sensitivity

A Typical Round Scintillating Fiber –

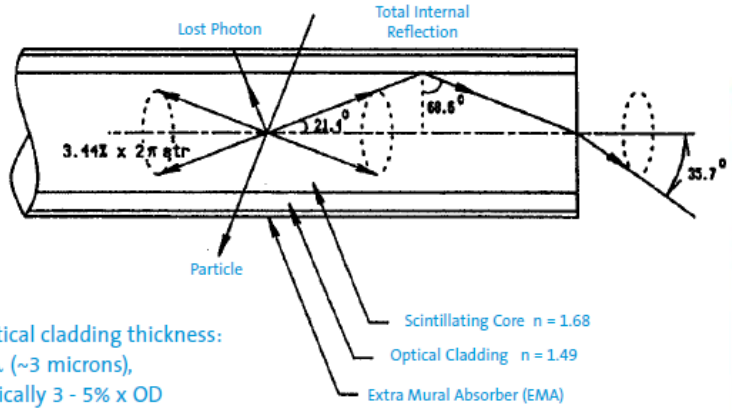

Optical cladding thickness:
>5λ (~3 microns),
typically 3 - 5% x OD

Optical Spectra –

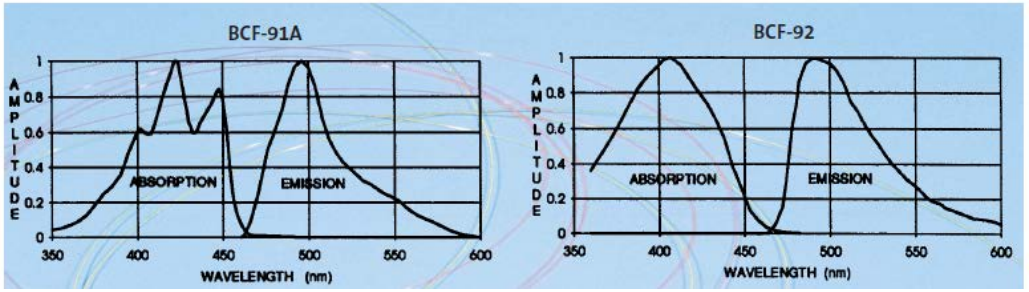

Prospect Saint Gobin

Selection of WLSF from Kuraray and their characteristics

Absorption and Emission Spectra

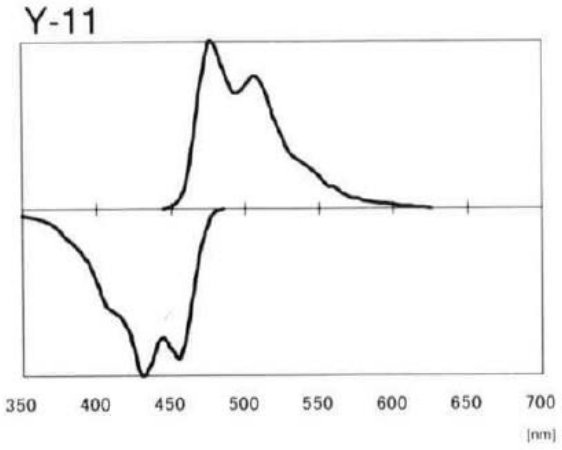

Design of Multicladding

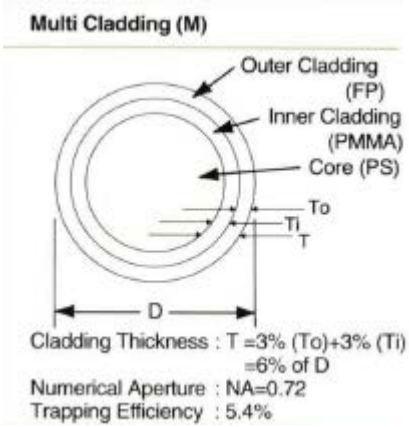

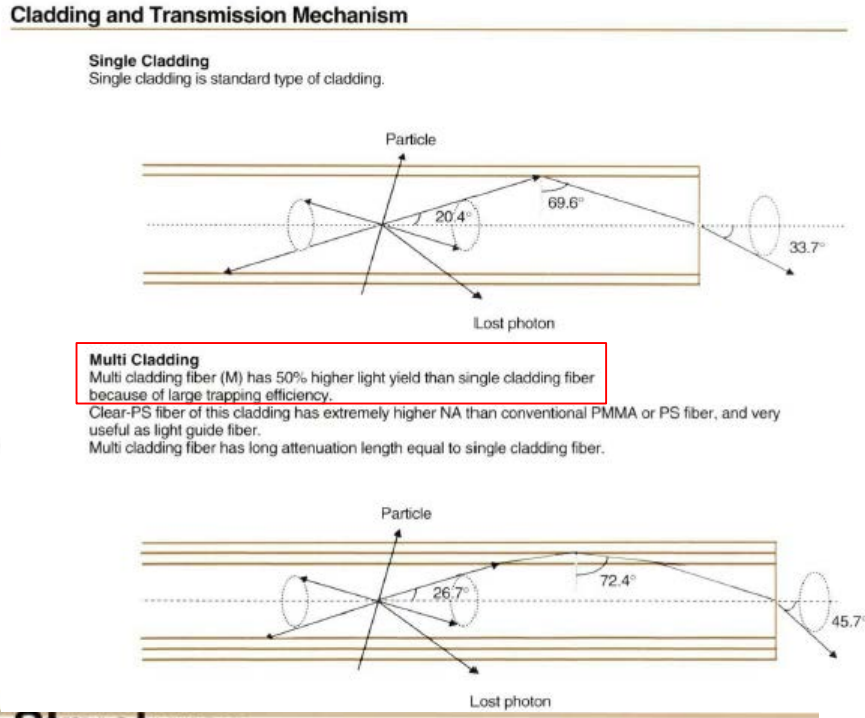

- The Y-11, might fit best to the spectra of the entrance window of the selected PMT.

Materials and Structures

Materials

		Material	Refractive index	Density [g/cm³]	No. of atom per cm³
Core		Polystyrene (PS)	n_D=1.59	1.05	C : 4.9×10²² H : 4.9×10²²
Cladding	for single cladding inner for multi cladding	Polymethylmethacrylate (PMMA)	n_D=1.49	1.19	C : 3.6×10²² H : 5.7×10²² O : 1.4×10²²
	outer for multi cladding	Fluorinated polymer (FP')	n_D=1.42	1.43	

^{6}LiF/ZnS:Ag Scintillator Characteristics

Technical Data

Name: ^{6}LiF/ZnS:Ag

Common Designator: ND

Formula: ^{6}LiF/ZnS:Ag blend 4:1 ratio

Physical Characteristics:
- phosphor type particle blend
- particle size range(s) 1 .5/5um
- density

Optical Characteristics
- refractive index

Absorption Characteristics
- X-ray very low
- UV broad band
- IR n/a
- neutron high for thermal neutron
- electron n/a
- alpha/beta alpha detection mechanism

Emission Characteristics
- colour blue
- peak emission 450nm
- spectrum type broad band
- decay to 10% 80us
- afterglow low level

Other Characteristics
- intrinsic efficiency phosphor 25%
  ^{6}Li cross section approx 40mb
- phosphor type ^{6}Li 3_H no interaction – band gap phosphor
- robustness moderate – photolysis in UV

Emission Spectrum

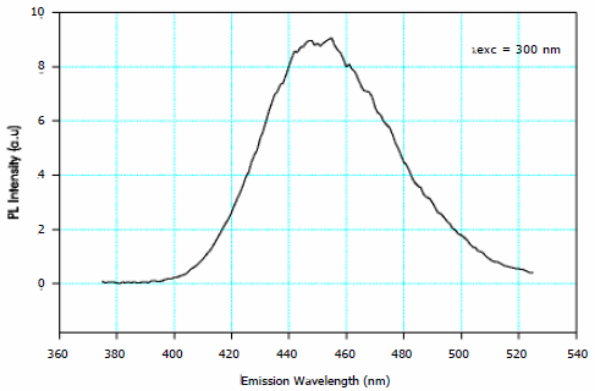

Decay curve

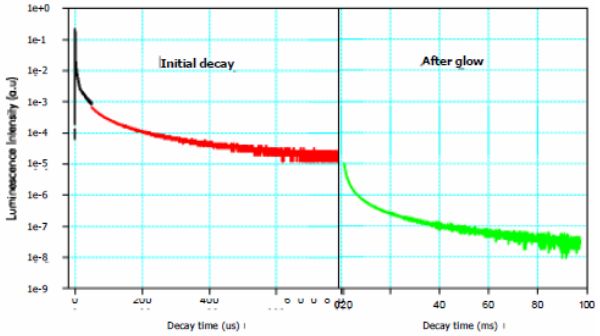

30cm x 30cm Scintillator

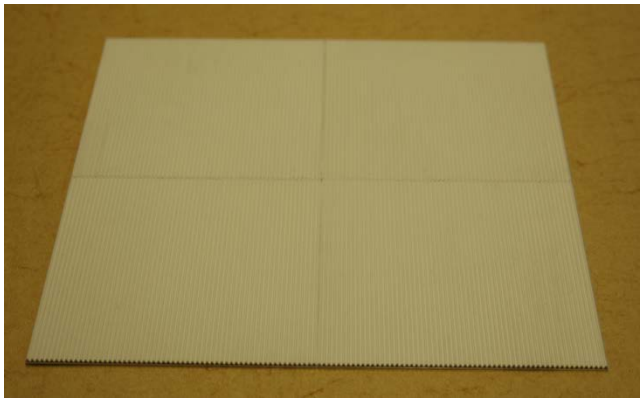

Side view of the Scintillator

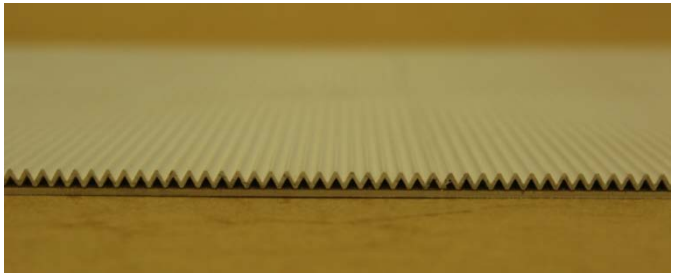

Scintillator is bright and offer a good n/γ discrimination, but it is opaque and has a long decay time

Comparison Measurements of Different Scintillators

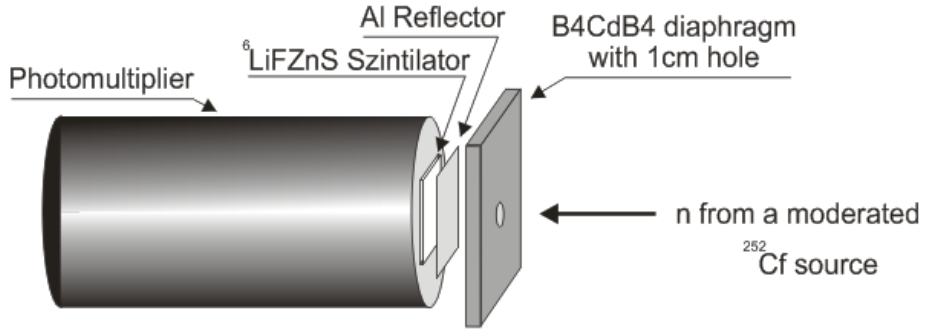

Schematic drawing of the test setup

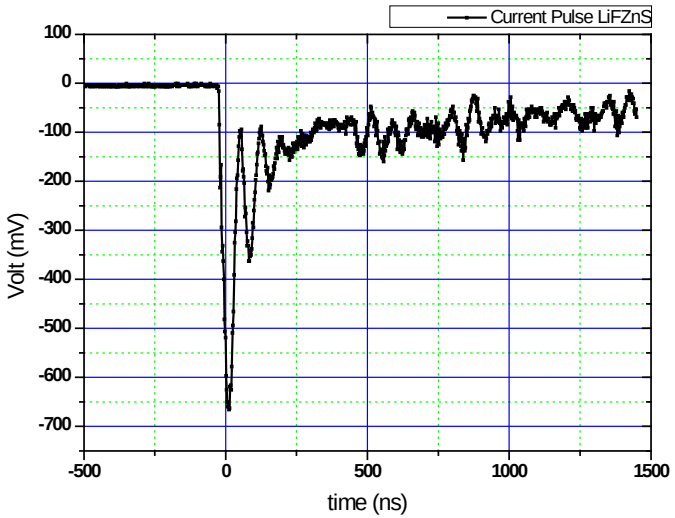

The diagram shows a current pulse of a PMT output measured into a 50Ohm Oscilloscope input.

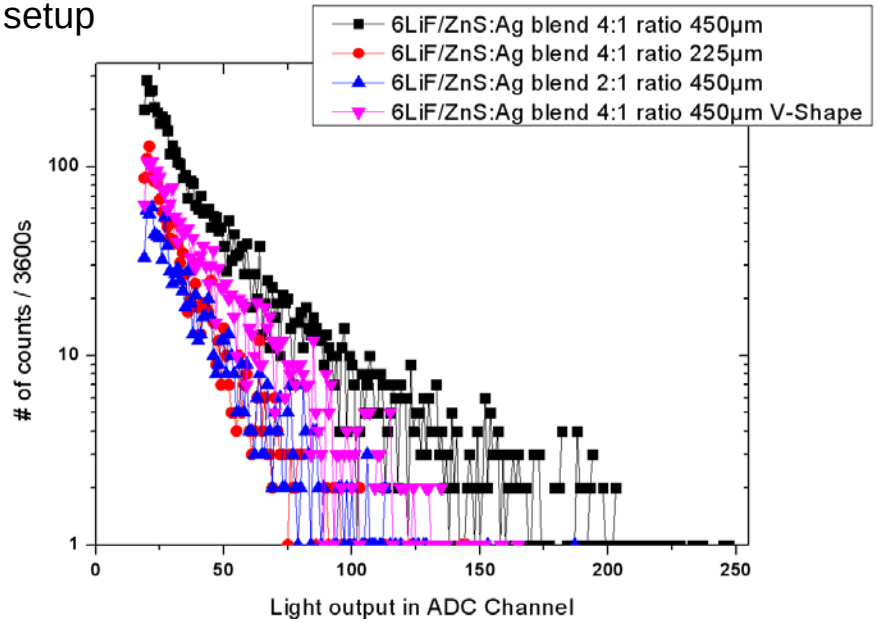

Pulse height distrubtion of different Scintillator types provided by AST

Gamma measurements with the LiF/ZnS-Scintillators

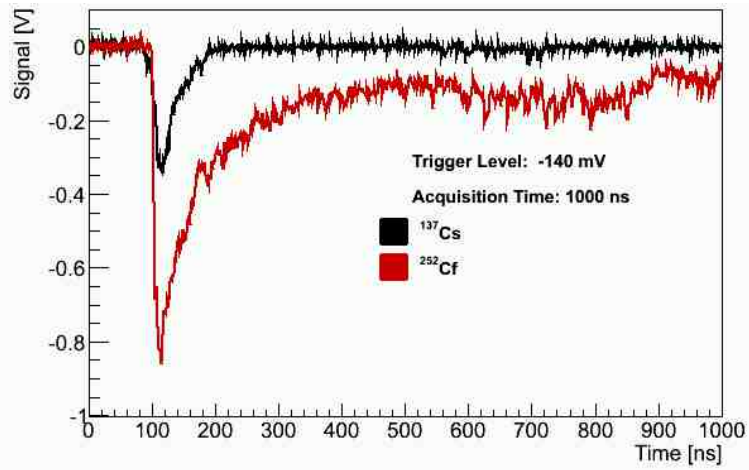

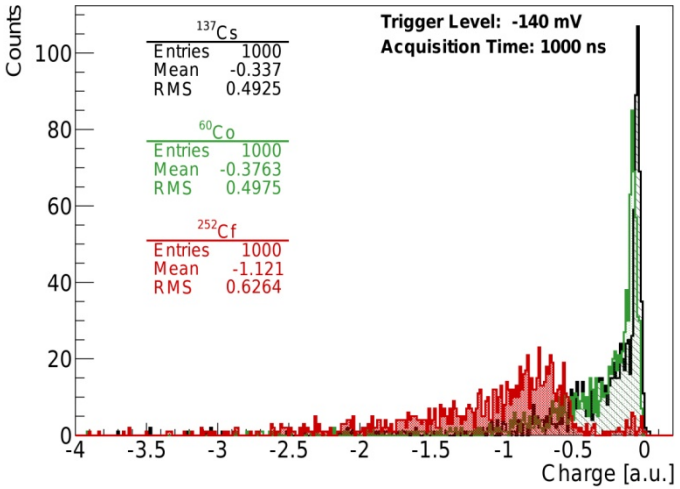

- Determination of Gamma <-> Neutrons:
  - Measurements with ^{137}Cs- and ^{60}Co-sources @ZEA-2
  - Remarkable differences between the two pulses in pulse length and light output
  - The gamma sensitivity measurements need to be double checked

Scintillator

- Requirements for scintillators at WLSF-based detectors:
  - High detection efficiency, low gamma sensitivity
  - High light yield, because of large light loss by WLSF
  - Short decay time -> double pulse resolution, count rate capability
- Two scintillators with high light yield available: LiF/ZnS, B_2O_3/ZnS
  - But both scintillator types are opaque -> limited thickness
  - Detection efficiency is an issue
- Enhancement of detection efficiency by two methods:

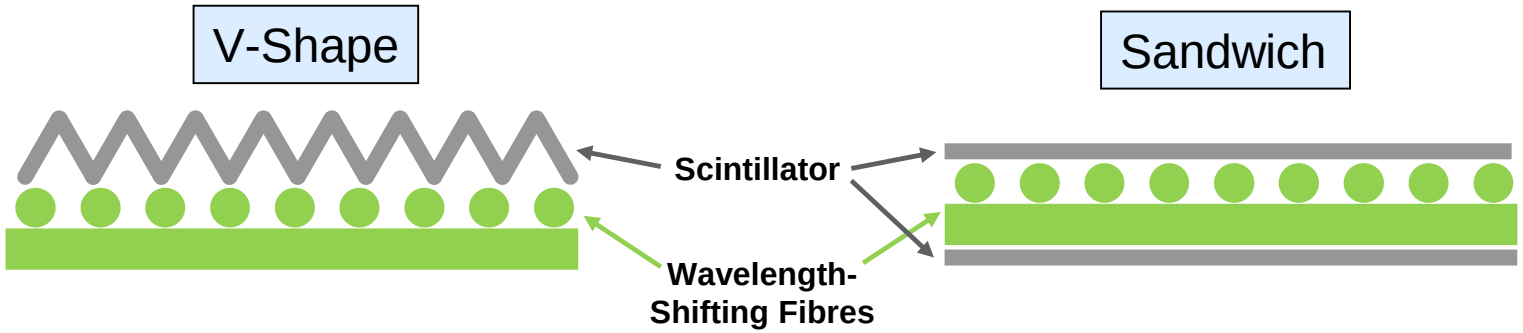

Longer neutron path
$L = d / \sin(\theta/2)$

Higher light output
by thinner scintillators

WLS Fiber Density

- Light loss study at STFC related to fiber density
  - Measurement with 1mm Kuraray fiber in sandwich between two flat scintillators
  - Pitch of 1/2/3/4 mm
  - Relevant to channel count

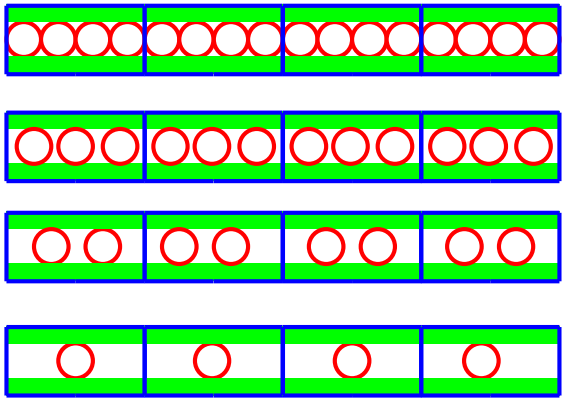

1 mm pitch

2 mm pitch

3 mm pitch

4 mm pitch

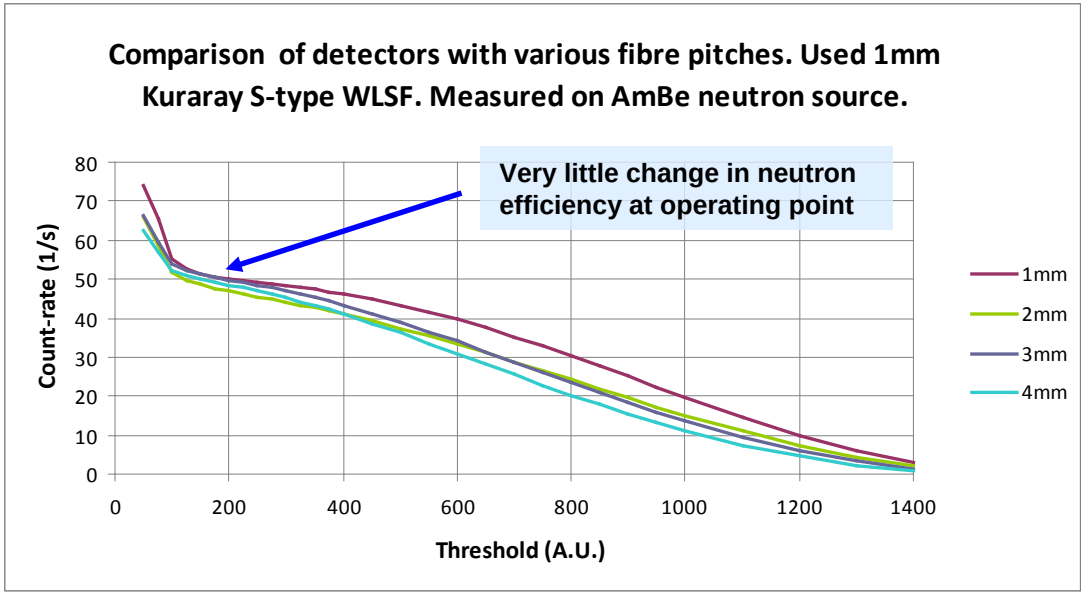

Graphs N.Rhodes, E.Schoonefeld

Scintillator Comparison

- Comparison of flat LiF/ZnS and B2O3 scintillators at J-PARC:
  - thicknesses of the scintillator: AST(2:1) 0.4 mm, AST(4:1) 0.4 mm, *iBIX* scint.: 0.35 mm, *SENJU* scint.:0.3 mm

Scintillator	Efficiency at 1.8Å	Integration:1μs		Integration:8μs	
		Photon	Decay time (μs)	Photon	Decay time (μs)
AST (2 to1)	0.308	9040	0.467	20594	3.18
AST (4 to1)	0.240	8596	0.452	19160	3.13
Old ZnS/B_2O_3 for *iBIX*	0.298	6940	0.371	13328	2.48
New scintillator for *SENJU*	0.358	4718	0.273	7793	2.03

Photo & Graph S.Soyama, T.Nakamura

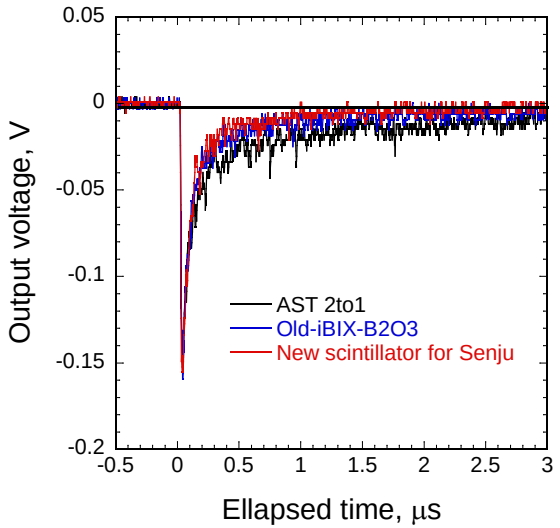

- B_2O_3/ZnS
  - Higher detection efficiency
  - Shorter decay time
  - Thickness typ. 300 um
- LiF/ZnS
  - Higher light yield
  - Thickness typ. 450 um
  - Available in V-Shape

Fibers tests and preparation

- Light loss study of the delivered fibers
  Y11 Type MSJ from Kuraray and
  BCF 91A from Saint Gobin
  have been repeated with delivered fibers!
- Kuraray fibers turned out to have less light loss and better bending properties.
- 250 Kuraray fibers were cut to length and polished on both sides
- A clamping technique was investigated to manufacture the fiber grid in the mechanical prototype

Picture of the test setup for bending the fibers around different diameters in total 360°

Bending Properties and Light Loss have been investigated

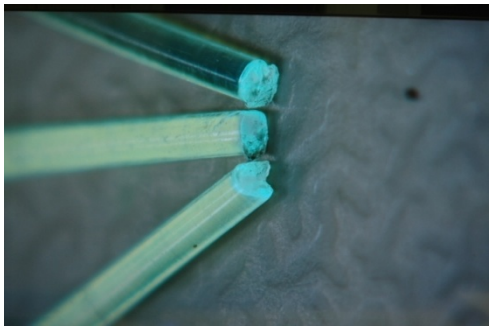

Picture of different cutting methods

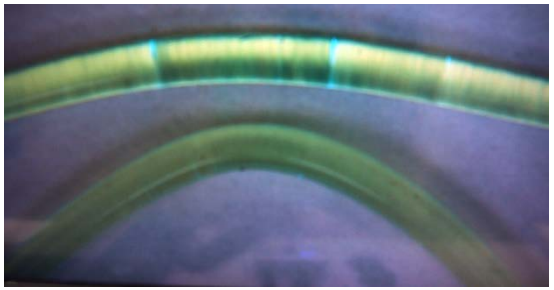

Picture of cold bended fibers

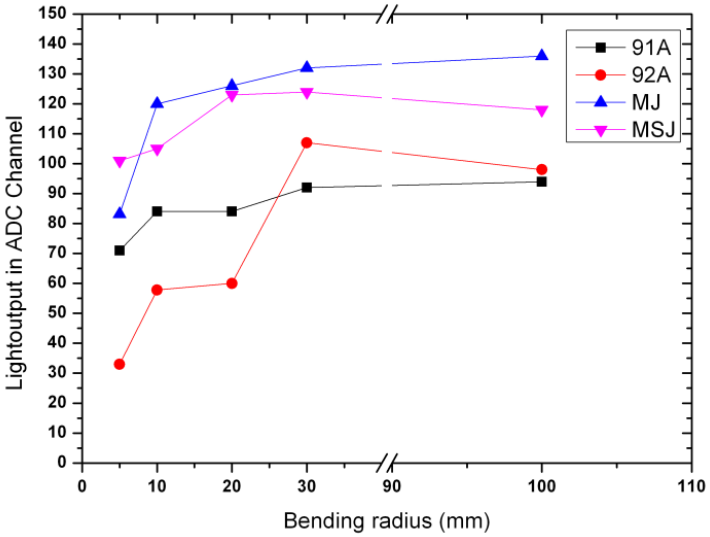

Diagram of different fibers warm bended with different bending radius

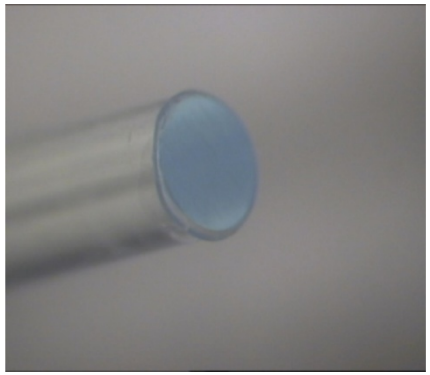

Picture of polished fiber end

Picture of the test setup for bending the fibers around different diameters in total 360°

- large light loss with cold bending due to cracks inside the fibers
- warm bending improved the light yield but may be optimized to get smaller radius
- long term stability needs to be studied with more fibers

Scintillator tests and prototype

- Only weak ^{252}Cf source could be used
- Testing of different scintillator mixtures and thicknesses
  - scintillator of size of 30cmx30cm as showed in the picture ordered.
- Started with manufacturing the fiber grid.
- Measurements with LiFZnS:Ag scintiallator together with WLSF are currently carried out

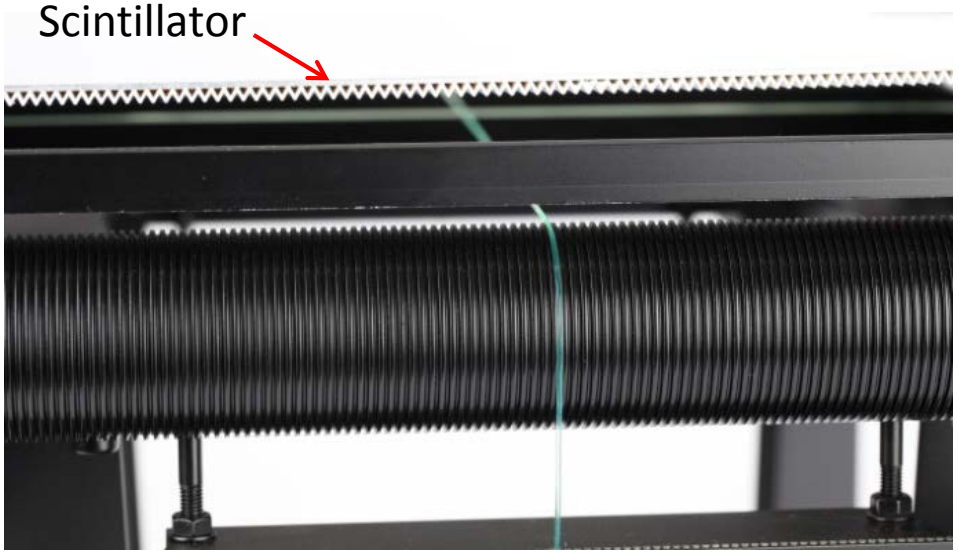

Picture of two crossed fibers below the scintillator together with the mechanical housing

Light Detection and Event Recognition

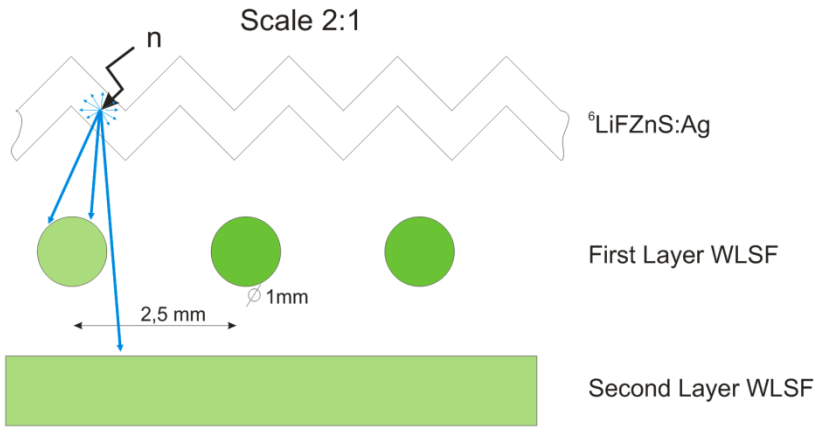

Schematic drawing with the Scintillator on top and the expected light yield spread over the two fiber layers..

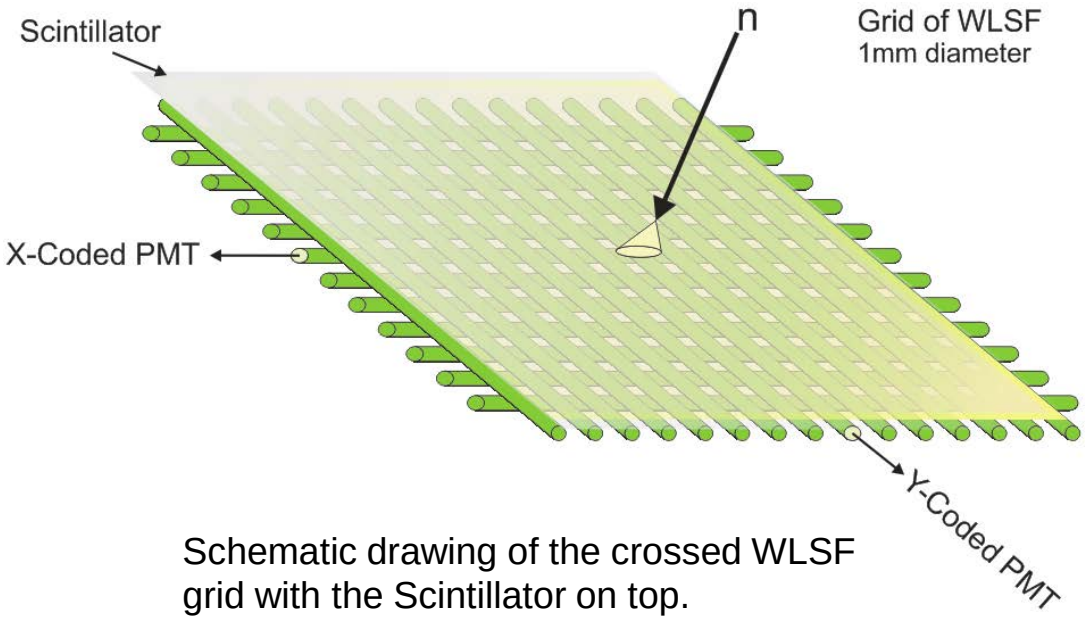

Schematic drawing of the crossed WLSF grid with the Scintillator on top.

- For light detection the use of Flatpanel H9500 PMT is envisaged - one pixel per fiber
- Event position is determined with x and y fibers
- Algorithm for event detection and neutron/gamma discrimination

Hamamatsu H9500 Multianode PMT

CHARACTERISTICS (at 25 °C)

Parameter		Min.	Typ.	Max.	Unit
Cathode Sensitivity	Luminous Ⓐ	40	55	—	µA/lm
	Blue Sensitivity Index (CS 5-58) Ⓑ	5.5	7.5	—	—
	Quantum Efficiency at 420 nm	—	19	—	%
Anode Sensitivity	Luminous Ⓒ	—	55	—	A/lm
Gain Ⓒ		0.1×10^6	1×10^6	—	—
Anode Dark Current per Channel Ⓓ		—	0.1	—	nA
Anode Dark Current in Total Ⓓ		—	26	100	nA
Time Response Ⓔ	Rise Time Ⓕ	—	0.8	—	ns
	Transit Time Ⓖ	—	6	—	ns
	Transit Time Spread (FWHM) Ⓗ	—	0.4	—	ns
Pulse Linearity per Channel (±2 % deviation)		—	0.2	—	mA
Uniformity (Condition Figure 3)		—	1: 5	1: 10	—
Cross-talk		—	5	—	%

- Response time adequate
- Setting the threshold to 50% of a single electron, should minimize the cross talk
- Homogeneity, Cross talk and Single Electron will be the first tests with this PMT type

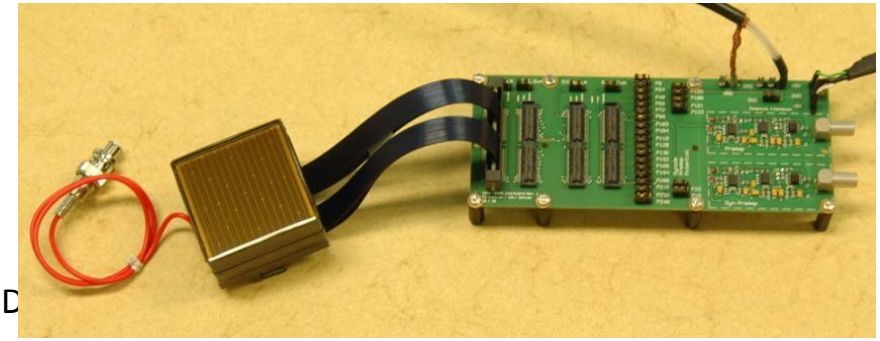

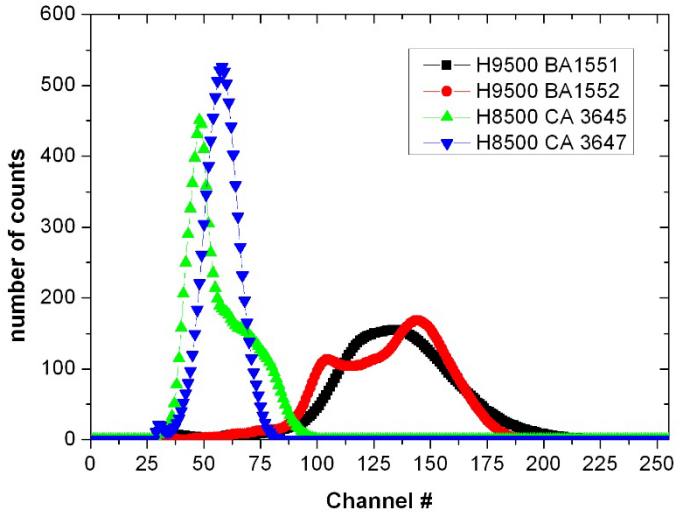

H9500 with a readout electronic board to test selected channels

Measurements at HEIDI instrument

- Neutron wavelengths of 0.8 Å und 1.17 Å
- Transmission measurements with ^{3}He-detector:
  - Scintillator with B_4C-aperture in front of detector
  - Absorption properties of different scintillators

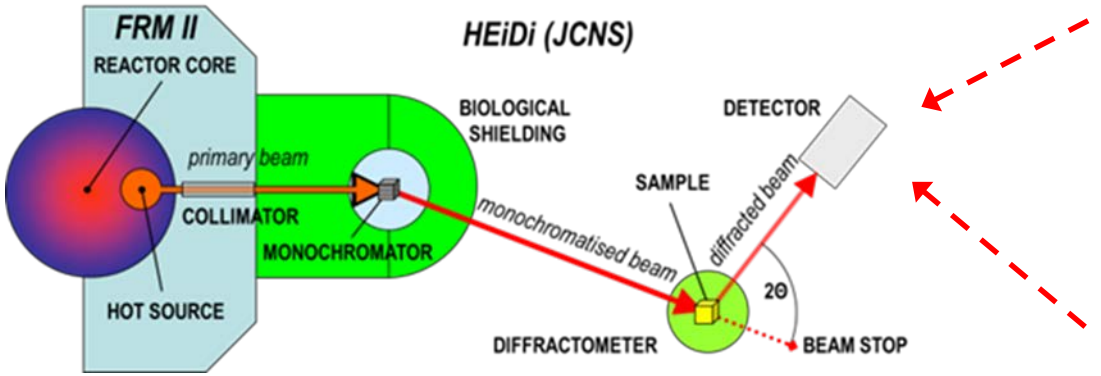

HEIDI ^{3}He-Detector

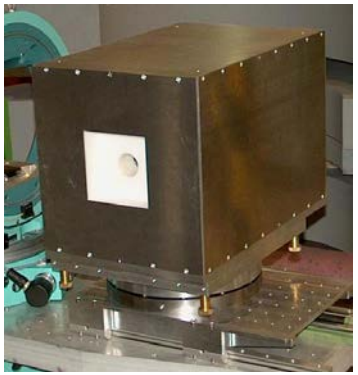

WLSF-Detector prototype

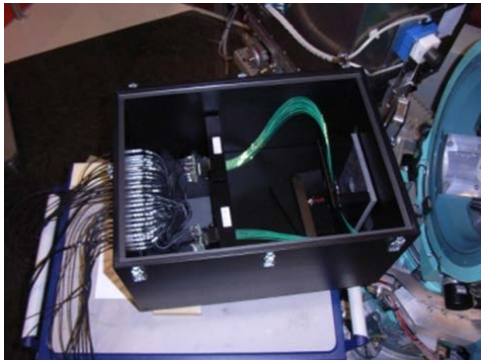

- Measurements with small WLSF-prototype:
  - Development of neutron detection algorithms
  - Determination of light yield, time characteristics, detection efficiency, position resolution

Small WLSF-Detector Prototype

- WLSF-Detector Prototype:
  - Two orthogonal layers with each having 16 WLS-fibers
  - H8711 4x4 MaPMTs from Hamamatsu
  - Fiber pitch 2.5 mm, total area 40x40 mm^2
- Readout-Electronics
  - Discriminator for each channel
  - Time stamping of hits via TDCs (fine) and FPGA (coarse)
  - Disk storage of data on PC
- Measurements:
  - B_4C-aperture for comparison to transmission measurements
  - Measurement of position resolution with additional diaphragm with 2mm holes

Absorption measurements @HEIDI
AST-Scintillators

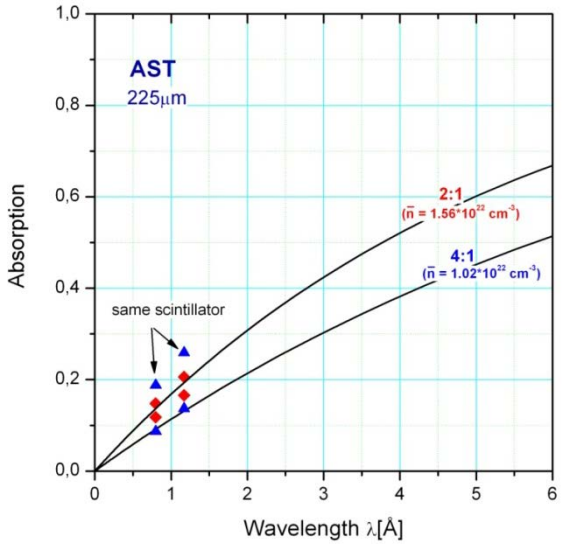

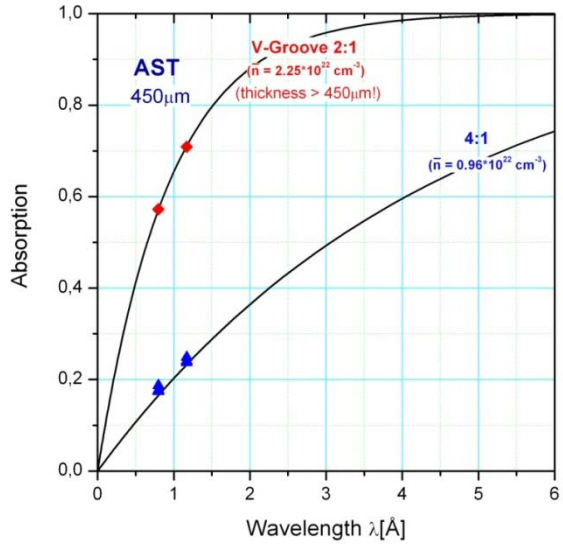

- **Quality of delivered scintillators**
  - confusion due to wrong labeling and via double checking (ZEA-3-Analysis, Chemical) we found out that there was no 2:1 Scintillator with 450µm thickness!
  - even at the same expected composition we got different results
  - V-Shape scintillator is much thicker than expected and has a poor fabrication quality
  - Sandwich-Layout of planar setup gave only 40% Absorption @ 1Å
  - New planar scintillators were tested with an expected efficiency last week @HEIDI

Absorption measurements @HEIDI Elien-Scintillators

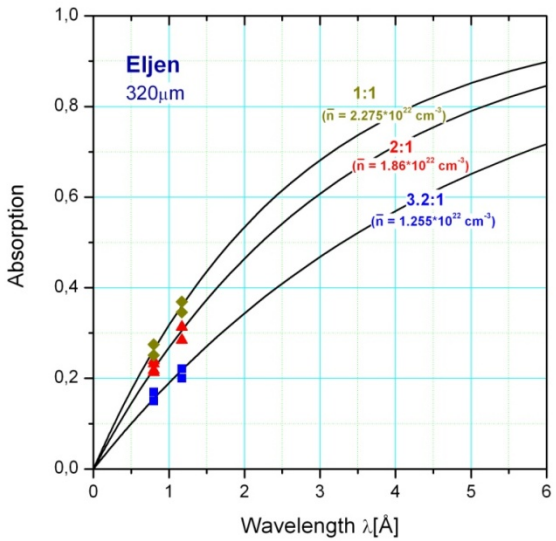

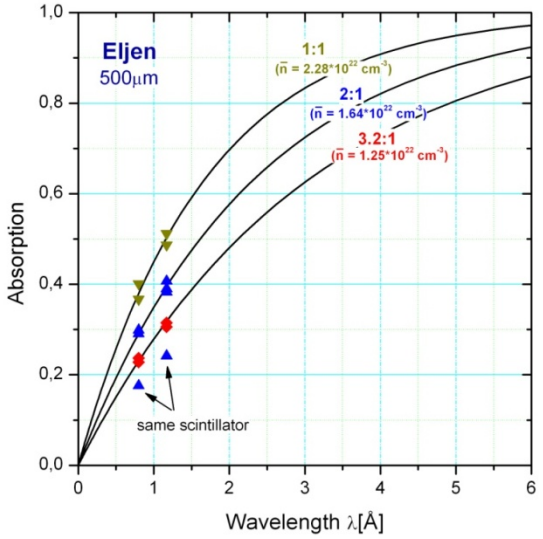

- **Quality control of delivered scintillators**
  - Narrow tolerances of the delivered scintillators at different compositions
  - High number of ^{6}Li atoms results in the higher absorption
  - Sandwich-Layout with absorption of up to ~70% with 1:1 and ~60% at 2:1 composition

Overview of all Eljen-Scintillators

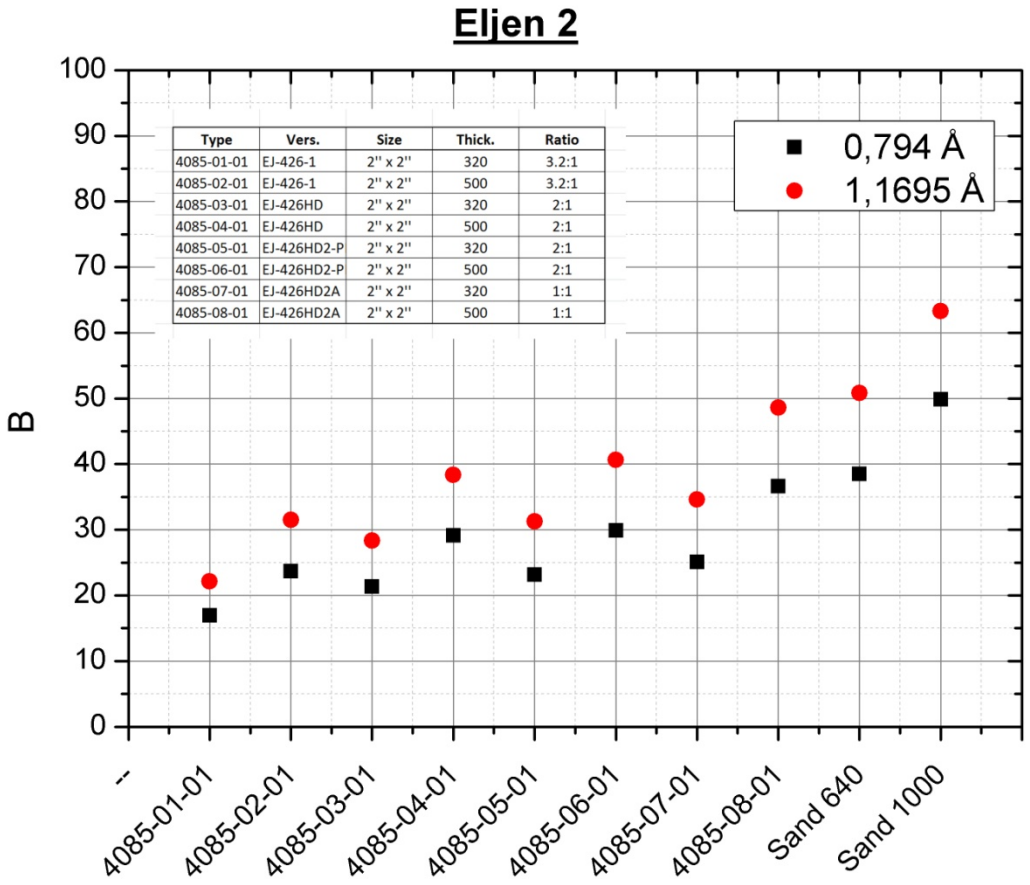

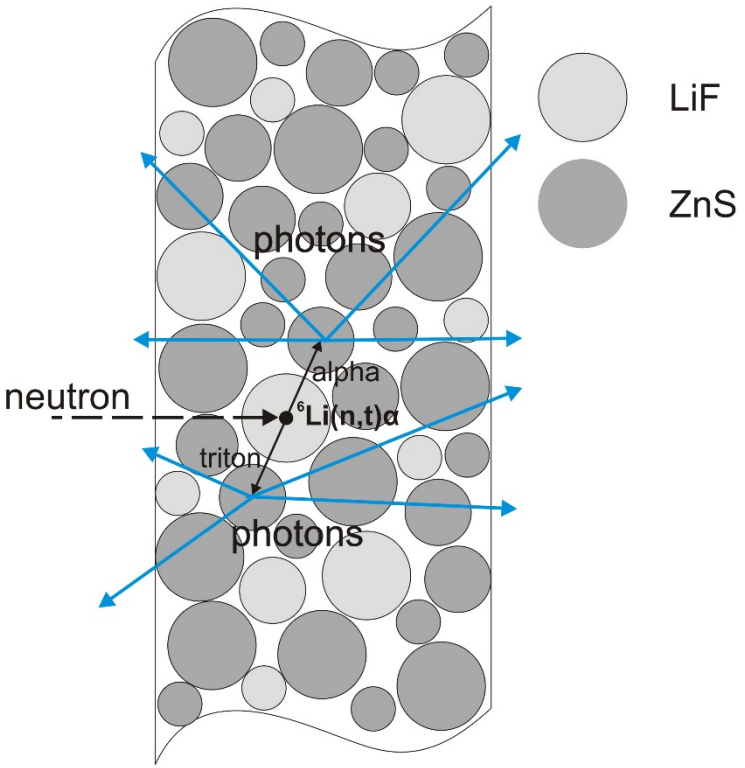

A third set of scintillators were tested last week @HEIDI within the same absorption efficiency as shown above.

Processing of Data

- Detector-Data = Stream of Hit-Time Stamps
- Selection of neutrons according to emission properties of scintillator by:
  1. Time coincidence window: start of event with maximum of light emission
  2. Time delta: End of event characterized by large time distance of succesive hits
  3. Number of hits in an event: corresponds to light yield

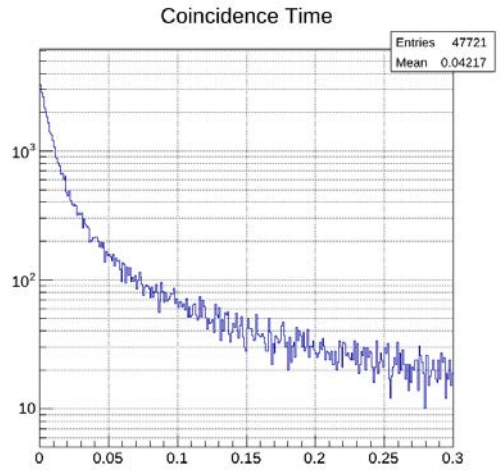

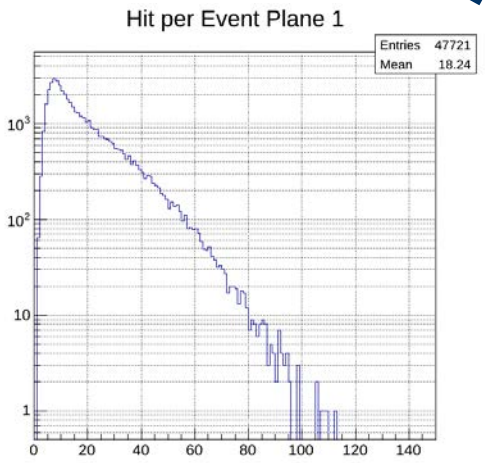

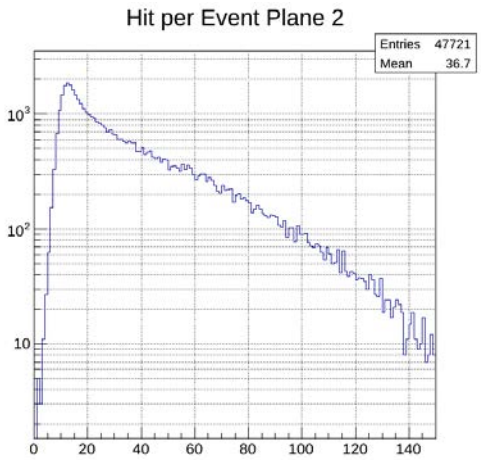

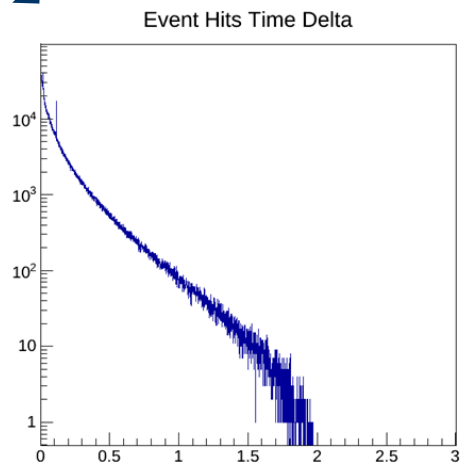

Time Characteristics of Neutron Events

- Time distribution of photon hits in an event:
  - Follows exponential decay law on statistical average (decay time of scintillator)
- Time length of neutron events:
  - Significantly determined by max. time delta of event selection
  - Crucial parameter for local count rate capability
  - 93% of Hit-Time Stamps below 8µs

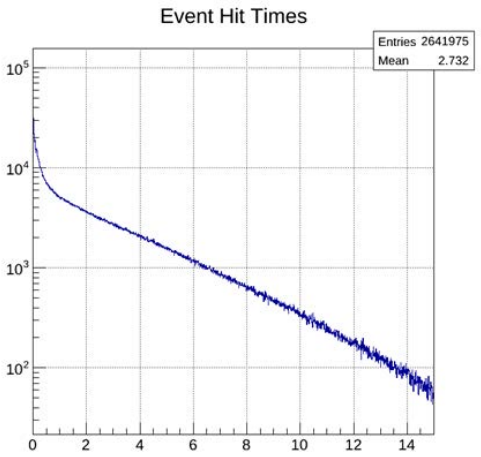

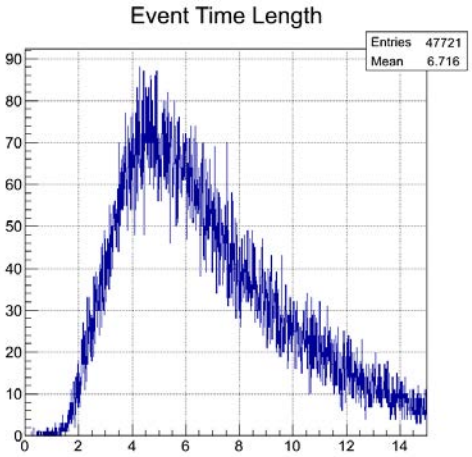

Photomultiplier

- Photomultiplier must be able to detect single Photons
- Initial intention: use of Flatpanel H9500 PMT for light detection
  - Compact device with 16x16 pixels, one pixel per fiber
  - But: probably a bit too less gain for single photon counting (g = $1x10^6$)
- New target: H7546 PMT
  - 8x8 pixels, one pixel per fibre
  - Modified version of this photomultiplier delivers gain up to $3x10^6$

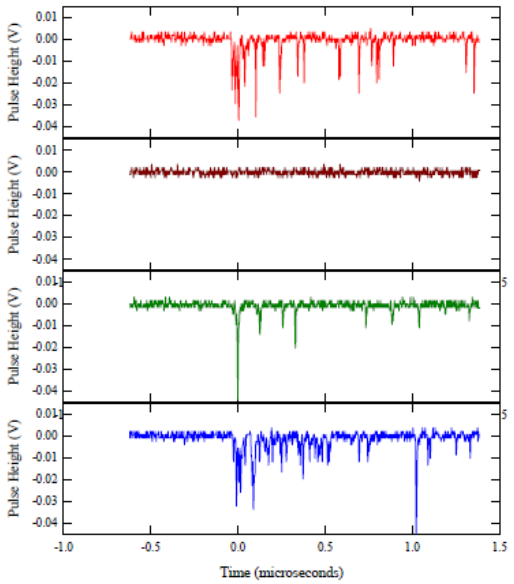

Multianode PMT

- Photomultiplier must be able to detect single Photons
- Initial intention: use of Flatpanel H9500 PMT for light detection
  - Compact device with 16x16 pixels, one pixel per fiber
- But: probably a bit too less gain for single photon counting (g = $1x10^6$)
  - New target: H7546 PMT
  - 8x8 pixels, one pixel per fiber
- Modified version of this PMT delivers gain up to $3x10^6$

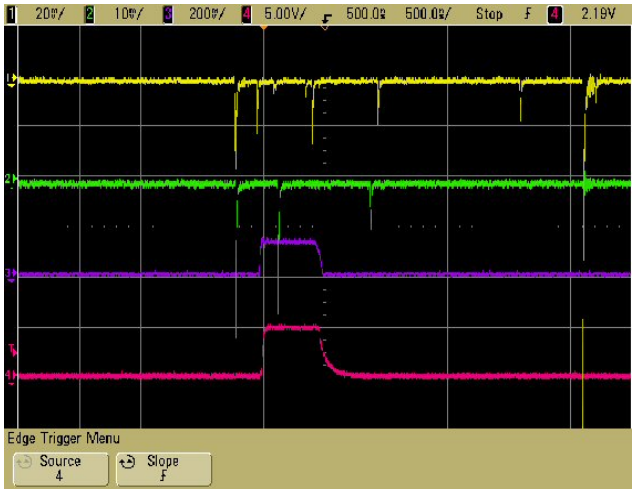

Picture of the measured signals fed into the Aqciris System

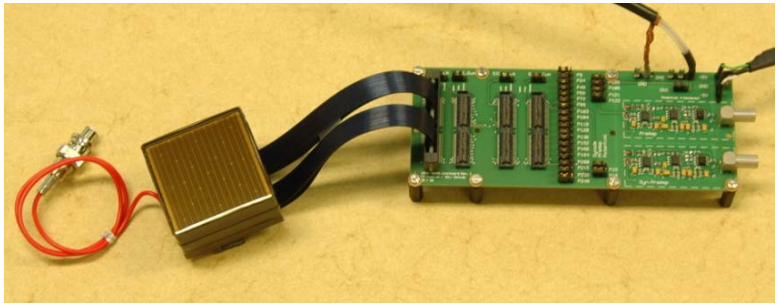

H9500 with a readout electronic board to test selected channels

Picture of the H7546

Readout Electronics

- MAROC ASIC from Omega
  - Variable gain preamplifier 0-4
  - Fast bipolar and unipolar shaper (15 ns) with discriminator for each channel
  - 100% trigger efficiency at 1/3 p.e (= 50fC), Qmax = 5pC
  - Slow shaper with 2 S&H for on-chip Wilkinson-ADC

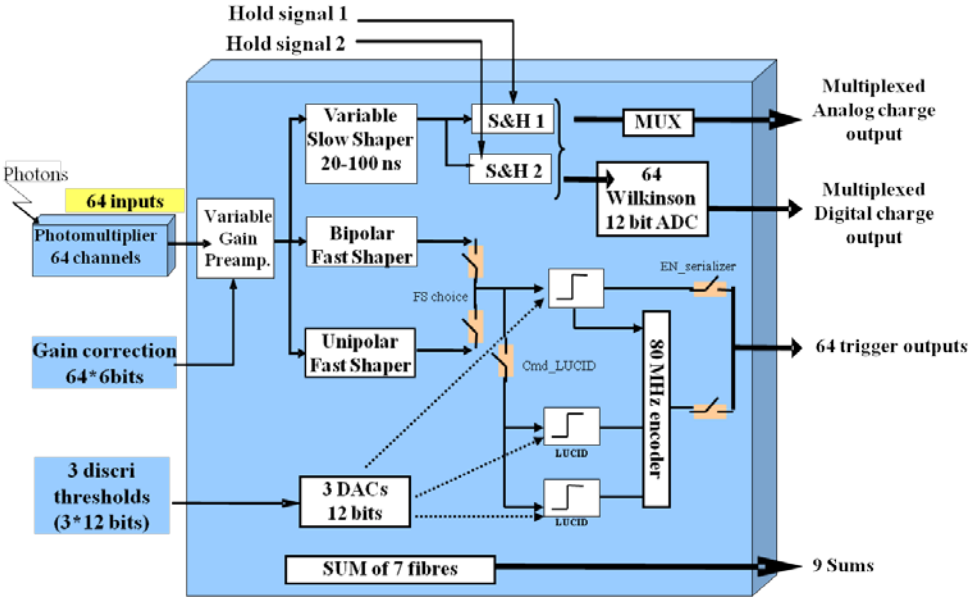

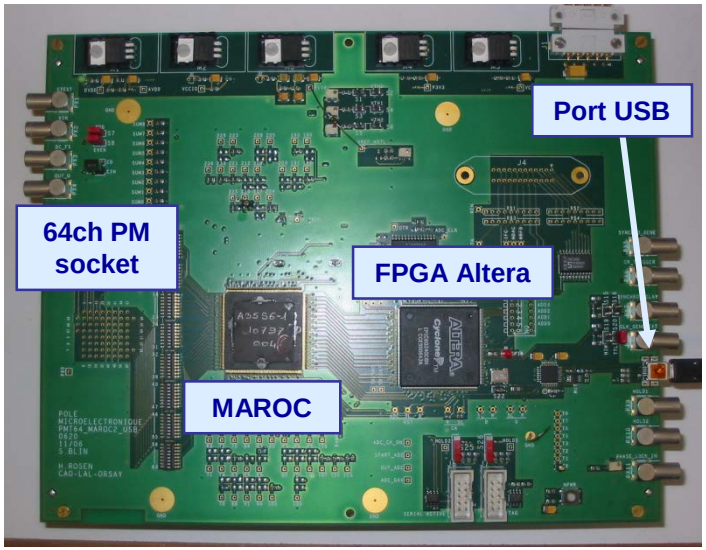

Photo & Graph P.Barillon

- Benefits:
  - Correction of PMT non uniformity
  - 64 trigger outputs for photon counting
  - Analog information for calibration
  - Low Power Consumption: 5 mW/ch.
- Chip is currently tested with evaluation board at ZEA-2

Single and double ended fiber readout

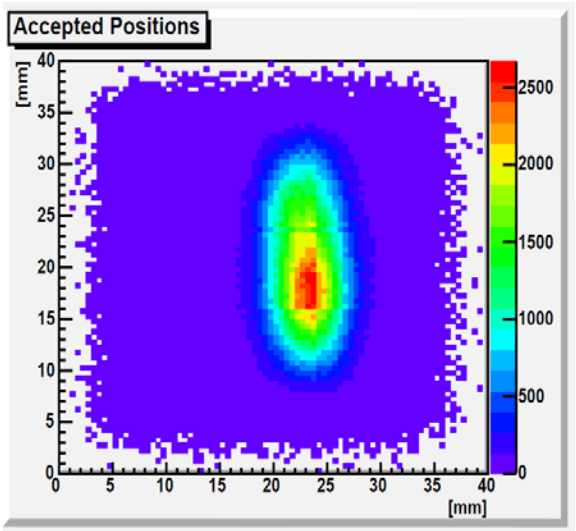

	#Probe	Absorption Density	ZnS	Dicke	1,1695 Å	Theo. Abs. 1,1695 Å	Absorption (Single) 1,1695 Å	Absorption (Double) 1,1695 Å	*He-3 Ereignisse*
	Leermessung								3003601
	Off Reflection								12079
AST	23166	Normal	2	200	17,69%		17,31%	17,54%	
AST	23168	Normal	2	300	25,74%		24,81%	25,27%	
AST	23173	Normal	2	400	29,70%		28,80%	29,07%	
AST	23174	Normal	3	200	15,38%		15,18%	----	
AST	23178	Normal	3	300	19,92%		19,50%	19,88%	
AST	23182	Normal	3	400	25,23%		24,37%	24,92%	
Elien	4318-01-01	EJ-426-1	3.2	320	21,41%		20,59%	21,08%	
Elien	4318-02-01	EJ-426-1	3.2	500	30,57%		29,47%	27,65%	
Elien	4318-03-01	EJ-426HD2	2	320	27,96%		27,47%	26,56%	
Elien	4318-04-01	EJ-426HD2	2	500	39,69%		37,91%	38,48%	
Elien	4318-07-01	EJ-426HD2A (1-1)	1	320	33,33%		32,24%	32,47%	
Elien	4318-08-01	EJ-426HD2A (1-1)	1	500	46,73%		43,01%	46,20%	
Elien	4085-02-01	EJ-426HD	3.2	1000	31,51%	52,45%	49,86%	51,44%	
Elien	4318-02-01	EJ-426-1			30,57%				
Elien	4085-04-01	EJ-426HD	2	1000	38,17%	62,71%	60,91%	60,72%	
Elien	4318-04-01	EJ-426HD	2		39,69%				
Elien	3862-08-01	EJ-426HD2A	1	1000	51,25%	74,03%	72,64%	73,61%	
Elien	4318-08-01	EJ-426HD2A (1-1)	1		46,73%				
Elien	4085-03-01	EJ-426HD2	2	640	27,73%	47,94%	46,50%	46,81%	
Elien	4318-03-01	EJ-426HD2	2		27,96%				

Measurements:

- B4C-diaphrgam in neutron beam Diaphragm with 2cm hole

Position reconstruction:

- Center-of-Gravity Method over the illuminated WLSF

Absorption Efficiency for the WLSF Detector:

- Close to neutron absorption for the measured scintillators
- Comparison with single and double ended fiber readout with adequate results compared to absorption

Difference between one and two scintillators

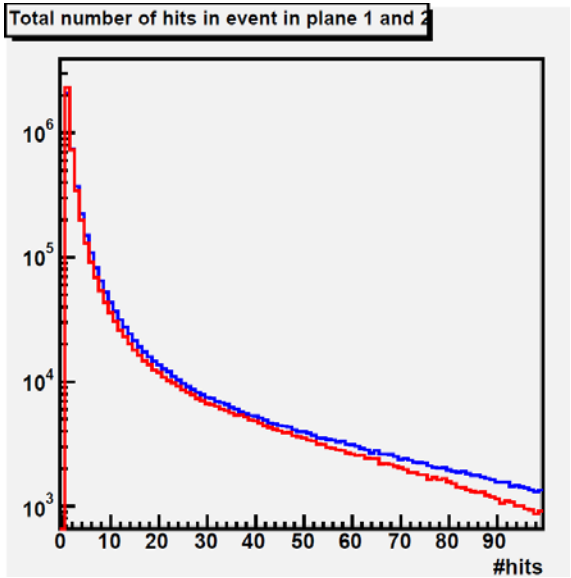

In blue and red one can see the different hits per plane with only on scintillator. The blue curve is the plane located next to the scintillator and red is the second plane with less counts due to less photons

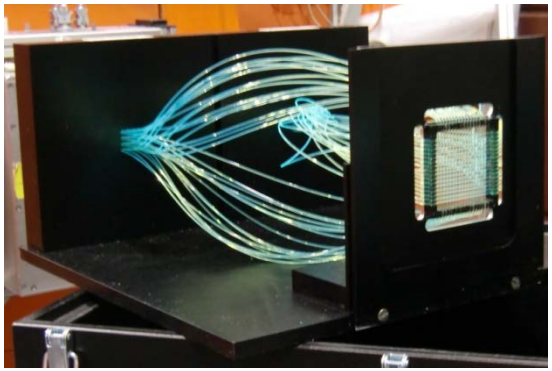

Picture of the double ended fiber readout setup and the orthogonal grid in front but with no scintillator

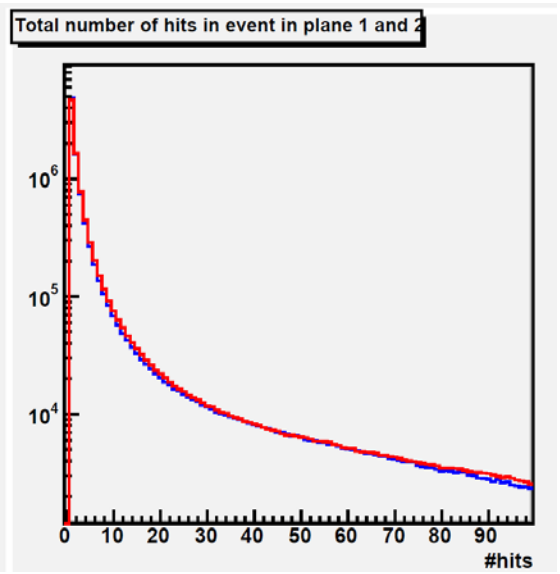

In blue and red one can see the different hits per plane with two scintialltors on each side. Here one can see no different anymore while no „shading“ effect

Position Reconstruction & Detection Efficiency (single)

Measurements:

- Single ended fiber readout
- B_4C-diaphragm in neutron beam
- Diaphragm with 4mm holes and 10mm spacing

Position reconstruction:

- Center-of-Gravity Method over the illuminated WLSF
- 1,727 ±0,17 bin / mm pixel size in the diagram
- Reconstructed Peaks with FWHM of δ = 3,62 ±0,11 bin => δ = 2,10 ±0,06 mm => 4,94 ±0,14 mm

Detection Efficiency:

- Close to theoretical calculation
- Further data analysis will take place in the next couple month

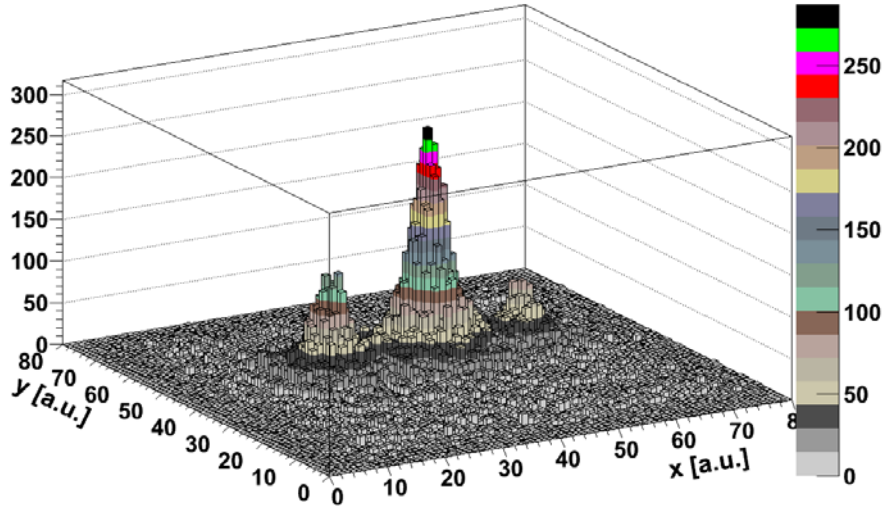

Results of WLSF test measurements @HEIDI

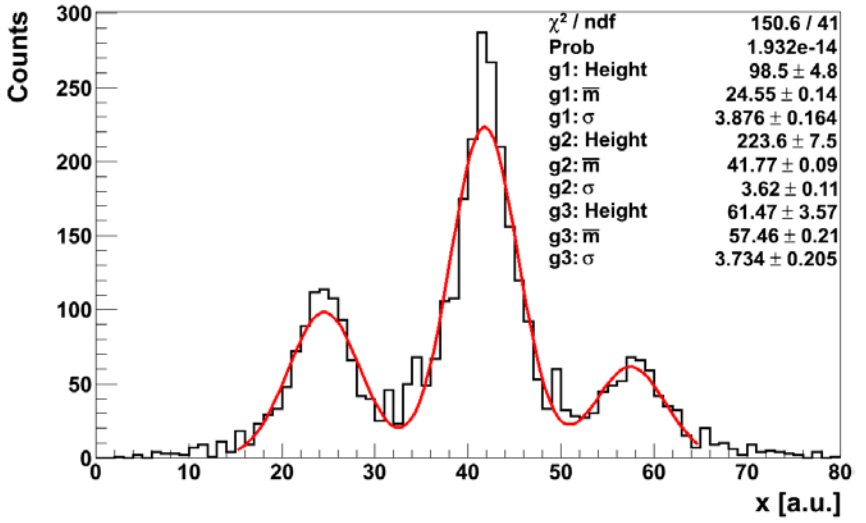

Position Reconstruction & Detection Efficiency (double)

Measurements:

- Double ended fiber readout
- Peak / Valley much better than single ended
- B_4C-diaphrgam in neutron beam
- Diaphragm with 4mm holes and 10mm spacing

Position reconstruction:

- Center-of-Gravity Method over the illuminated WLSF
- Reconstructed Peaks with FWHM of δ = 2,65 ±0,13 bin => δ = 1,62 ±0,08 mm => 3,81 ±0,18 mm

Detection Efficiency:

- Close to theoretical calculation
- Further data analysis will take place in the next couple month

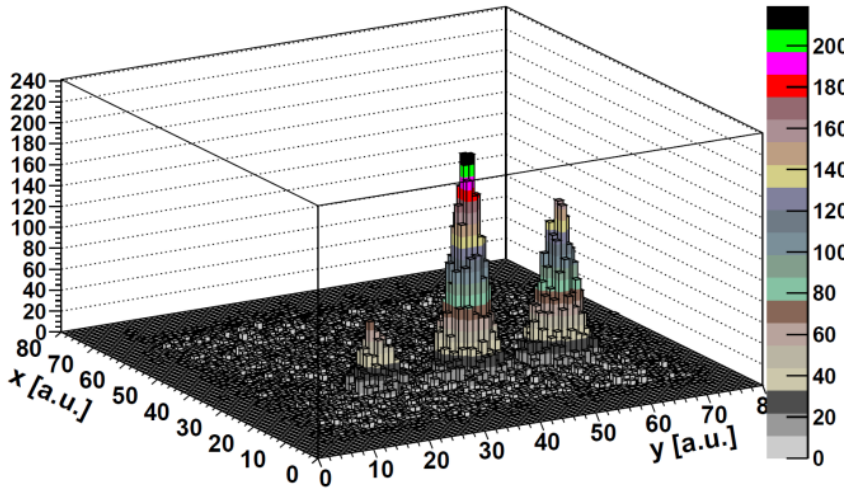

Results of WLSF test measurements @HEIDI

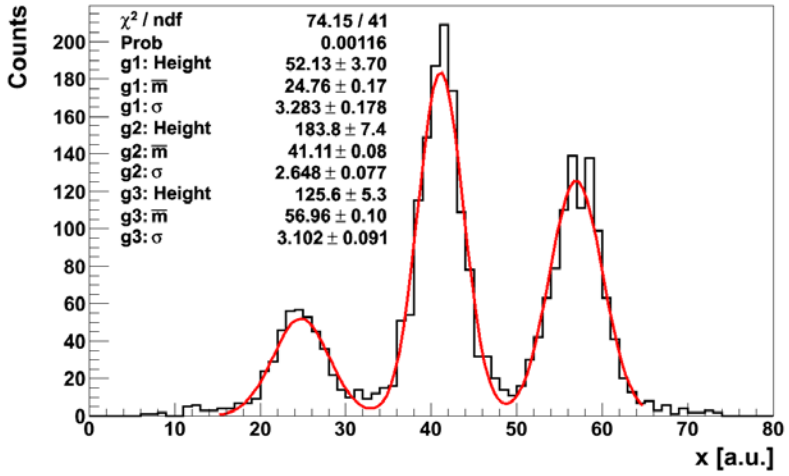

„Big“ WLSF Prototype and next steps

Detector module-Prototype tested :

- 30 cm x 30 cm active area
- 256 WLSF in total for X/Y- direction read out by 4 MaPMTs from Hamamatsu
- First operation with neutrons from a ^{252}Cf-source in 09/12,
- First successful operation with neutrons @TREFF FRM II in 03/13

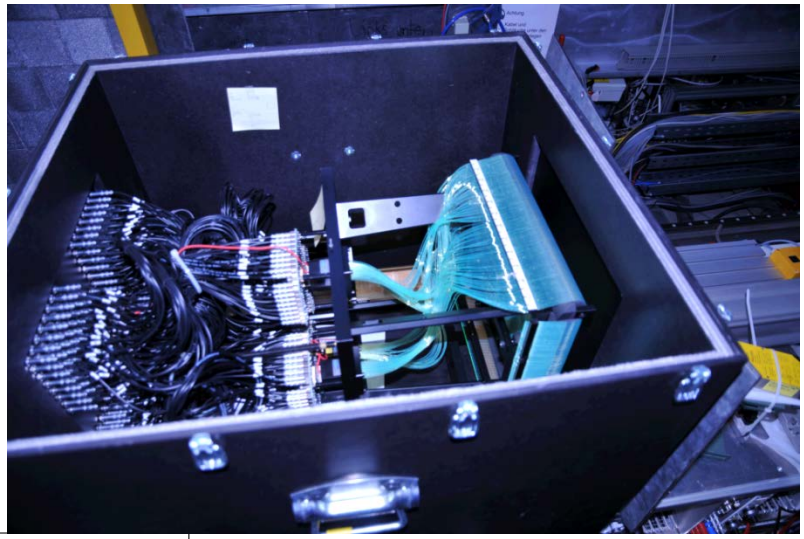

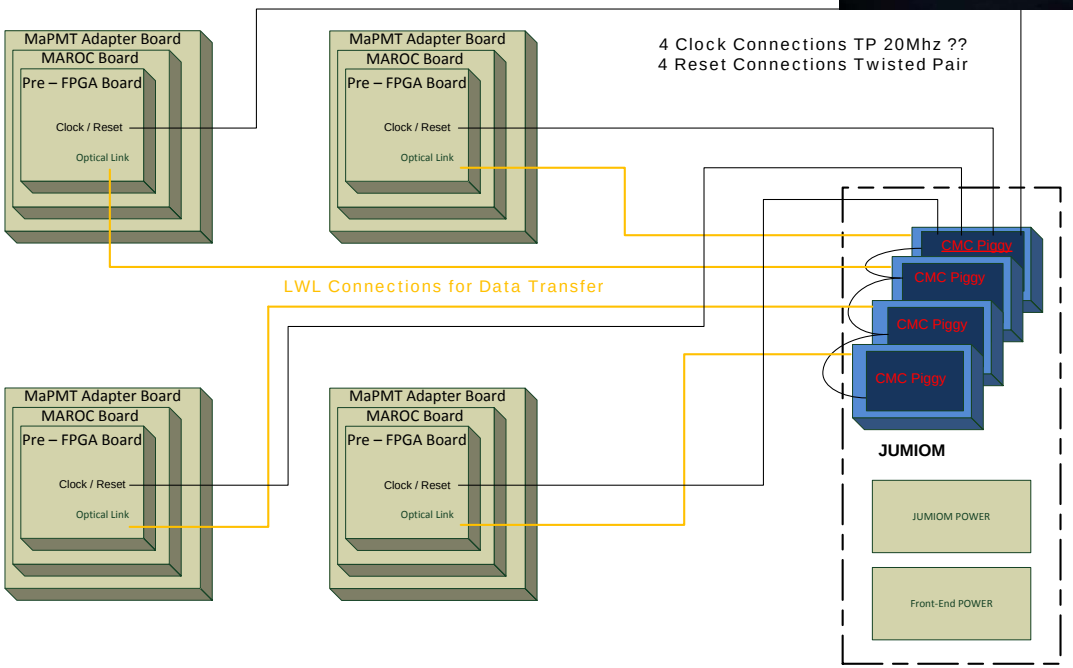

Block diagram of the Chip based read out electronics for one detector segment

Prototype structure

- 32 fibers per layer
- 1mm spacing between fibers

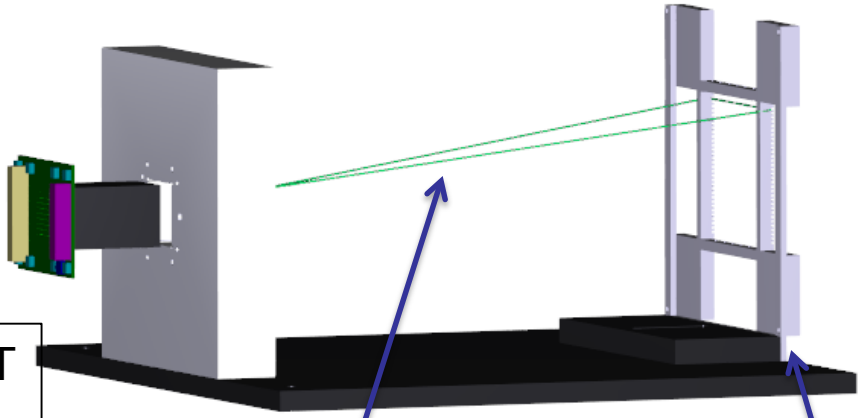

- H7546 Multi Anode PMT
- MaPMT Adapter Board
- MAROC board
- Pre-FPGA Board

Fiber; double ended readout

Fiber grid with scintillator

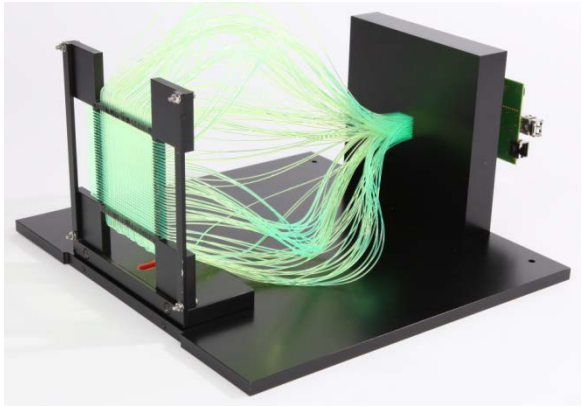

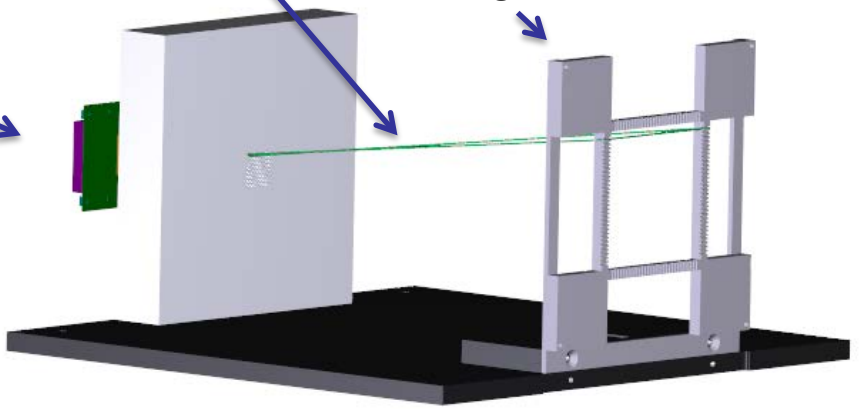

MaPMT readout electronic for 64 channels

- MAROC ASIC from Omega
  - Variable gain preamplifier 0-4
  - Fast bipolar and unipolar shaper (15 ns) with discriminator for each channel
  - 100% trigger efficiency at 1/3 p.e (= 50fC), Q_{max} = 5pC
  - Slow shaper with 2 S&H for on-chip Wilkinson-ADC

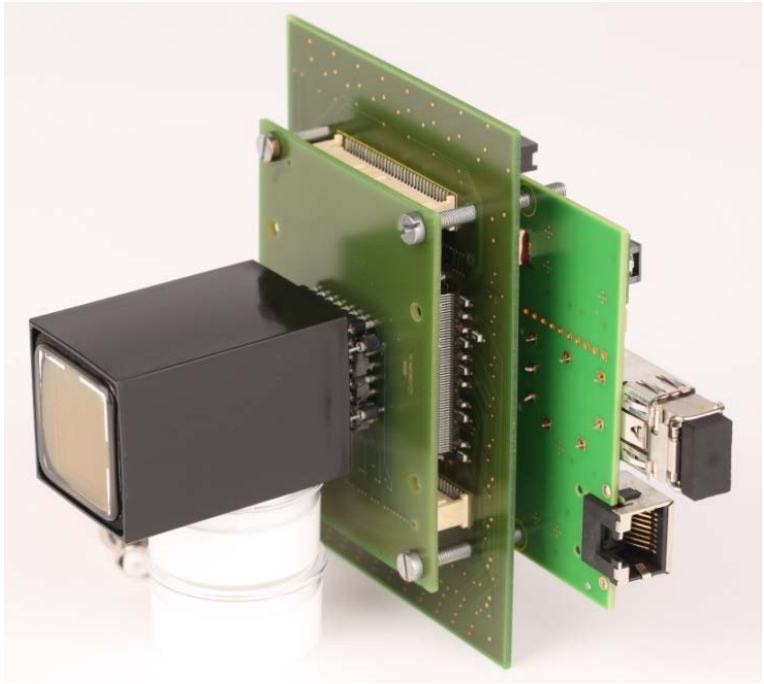

- Benefits:
  - Correction of PMT non uniformity
  - 64 trigger outputs for photon counting
  - Analog information for calibration
  - Low Power Consumption: 5 mW/ch.
- Total electronic with FPGA board and optical link was tested and will be optimized at ZEA-2

SAPHiR Instrument

Detector Requirements

- 2,5 m x 2,5 mm position resolution
- Time resolution <= 1 us
- Count rate a few 10kHz on whole detector area
- 1 -2,5 Angström sensitive wavelength
- >50 % Neutron Efficiency @ 1 Angström
- Sensitive Area ca. 50 cm x 35 cm or ca. 35 cm x 35 cm

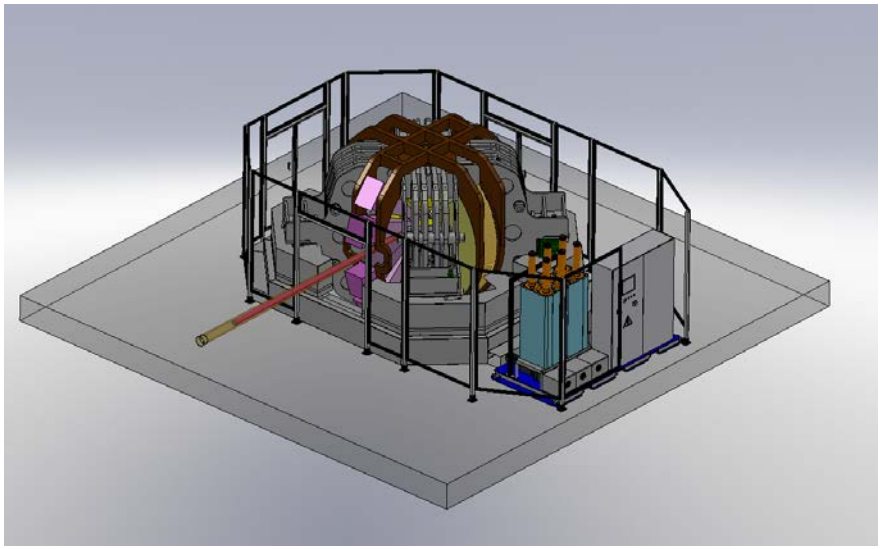

Six Anvil Press for High Pressure Radiography and Diffraction

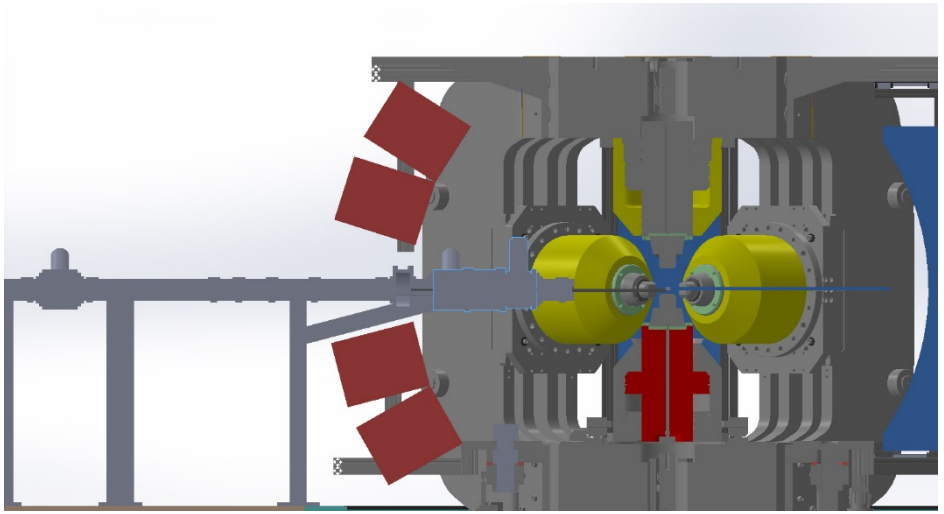

Back Scattered Detector arrangement

Readout Electronic Architecture

- Four Detector Segments
  - Multi Anode PMT
  - MAROC Board
  - FPGA Board
- Synchronized via Clock Sync. Module
  - Start / Stop Measurement
  - Inhibit / Enable Input
  - Sync. Master Clock Input
- cPCI Readout Control Crate
  - Four cPCI In-house PCB
  - Opto Interface to Segments
  - NI Optical Bridge to PC
- Additional Power Crate
- Linux based readout DAQ System

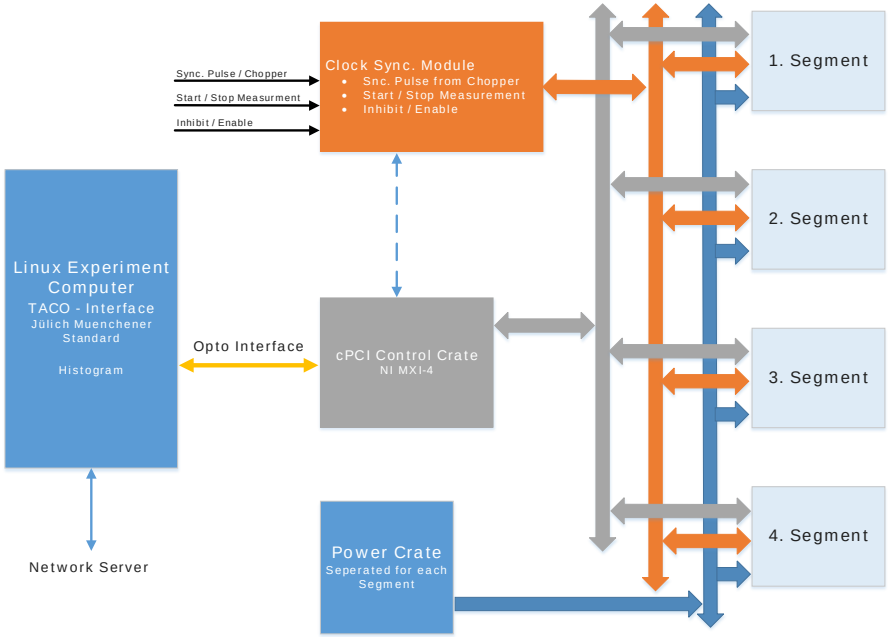

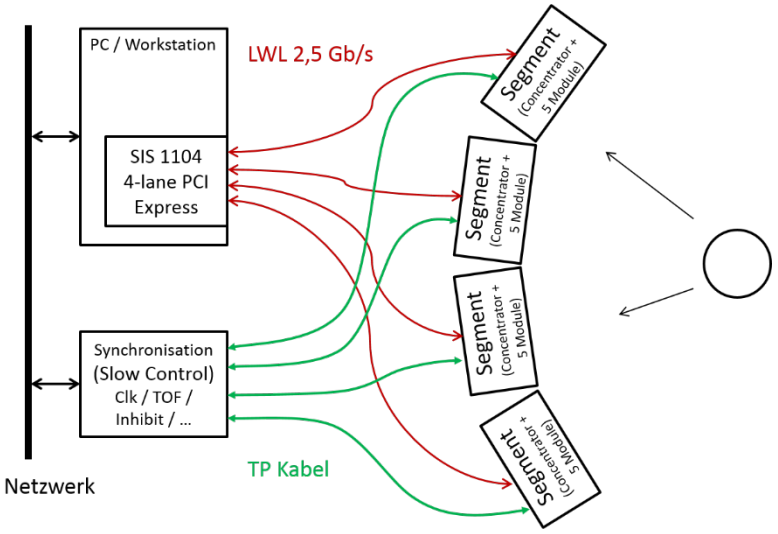

Concentrator Board

- Time stamp 2 ns ; 40bit
- Modules can be used without the Concentrator board
- More flexibility for the mechanical setup
- Cheap FPGA; SPARTAN 6
- Cables from the shelf
  => Serial ATA and TCP

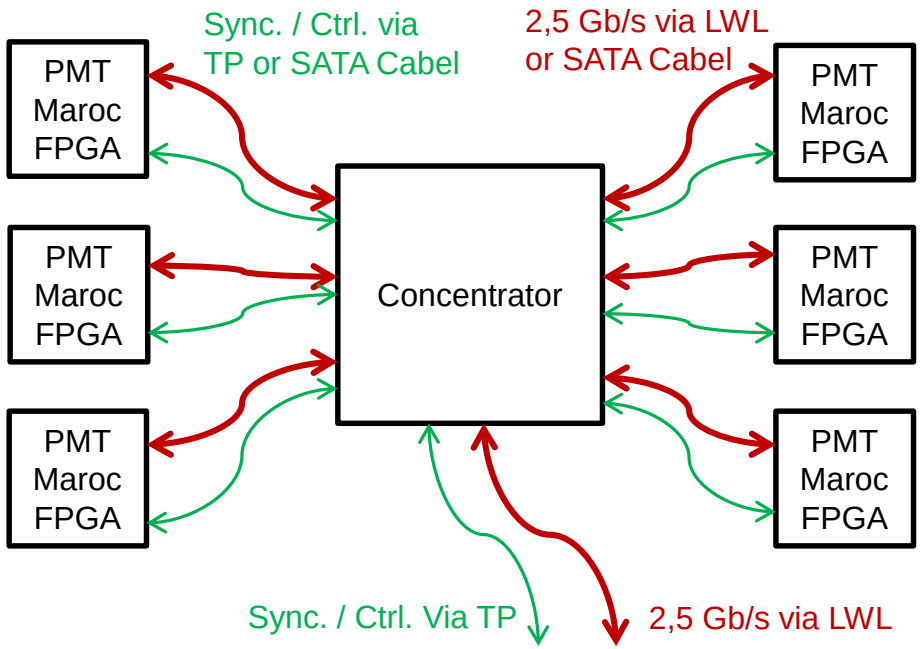

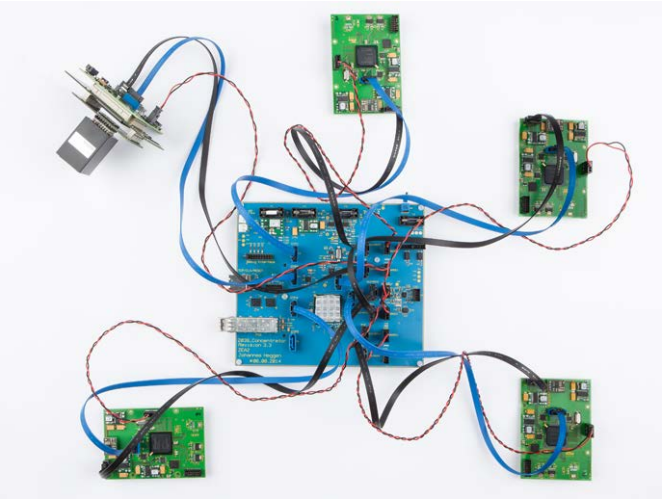

Picture of the Concentrator board with five module connected

Mechanics and fiber arrangement

- Fiber arrangements
  - Double ended readout on one MAPMT Pixel -> higher light detection efficiency
  - Small inner bending radius of 4mm to decrease the dead space for a modular setup to increase the overall sensitive detection area
  - An orthogonal fiber grid for position reconstructing

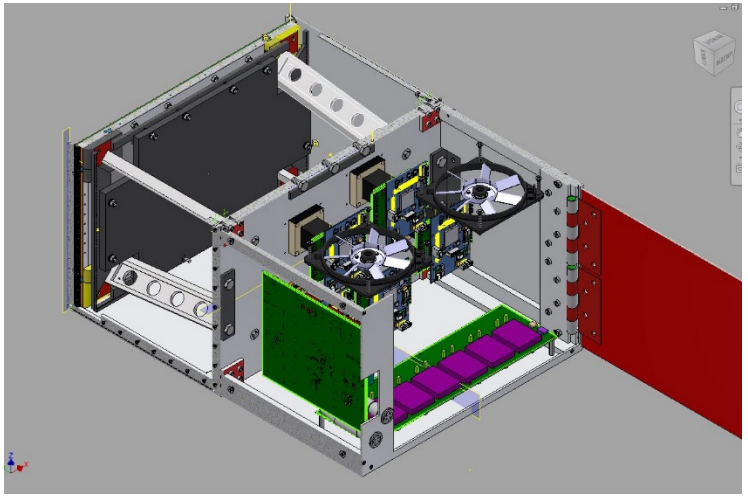

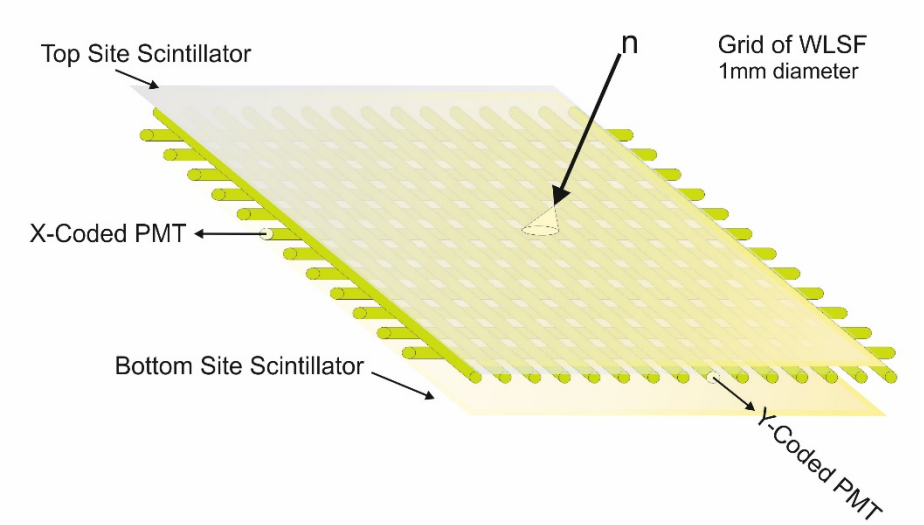

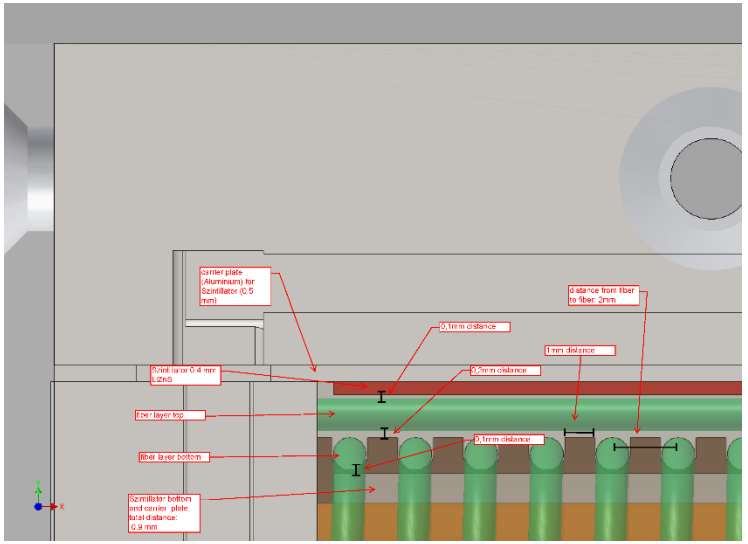

Segment Assembling

- Light tight detector front with ^{6}LiF/ZnS scintillator sandwich and the WLSF, ended on the entrance window of a MaPMT
- Detector segment with all PCB equipped
- Test of the four detector segments in our lab with a ^{90}Sr and the complete readout electronic

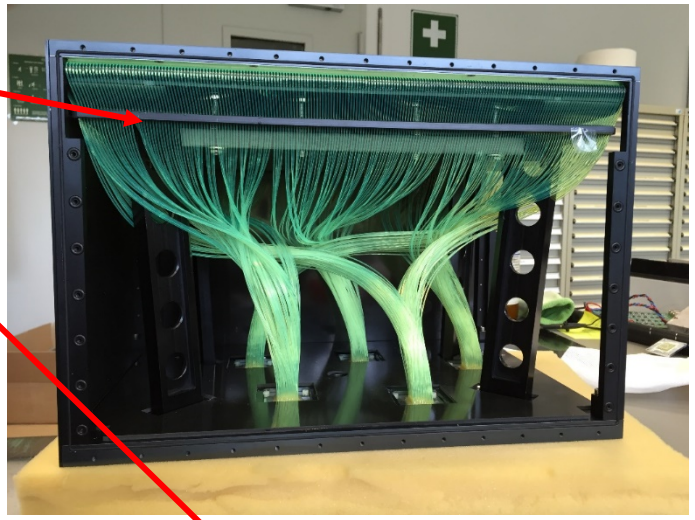

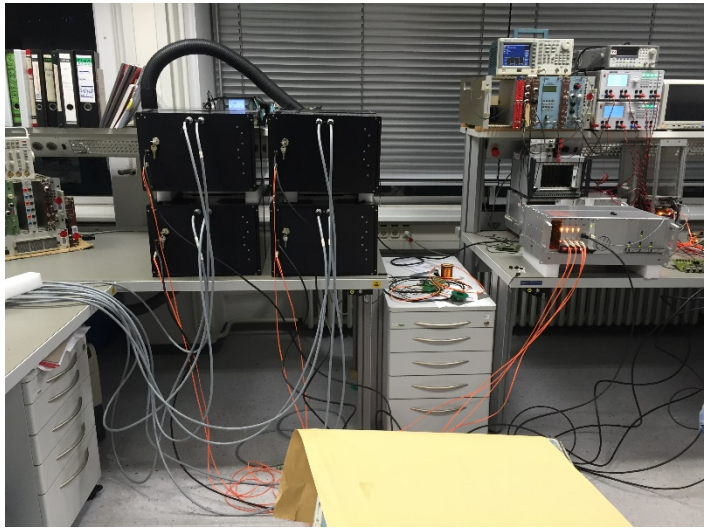

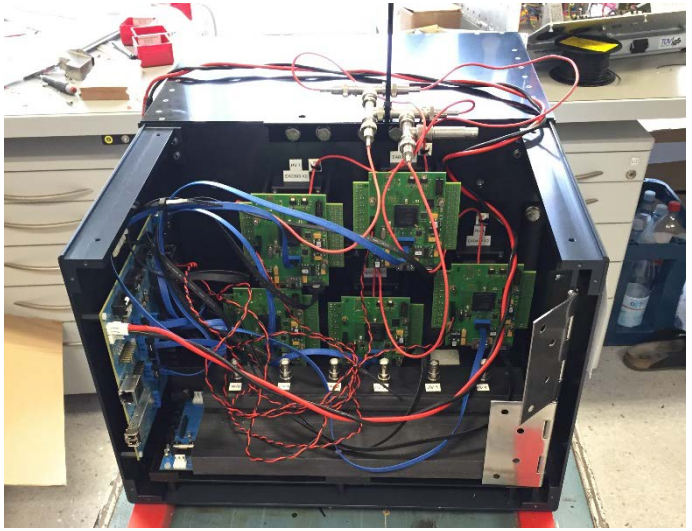

Wedding

- **Installation**
  - Four fiber segments were tested at TREFF beam line, Sept. 2015
  - Two fiber segments were placed in the foreseen position at the SAPHiR Instrument
  - Clock board will be mounted next to the Segments
  - Power supply and readout crate will be installed together with the DAQ PC in an 19 inch rack
  - Instrument will get the He-3 detector banks from our colleagues at FRM-2 beginning 2016
  - Final test's are foreseen with the neutron beam on the instrument, possible in 2016/17

Preliminary Result

Measurements:

- B4C-diaphrgam in neutron beam Diaphragm with six 1 mm holes and 10 mm gap

Position reconstruction:

- Center-of-Gravity Method over the illuminated WLSF

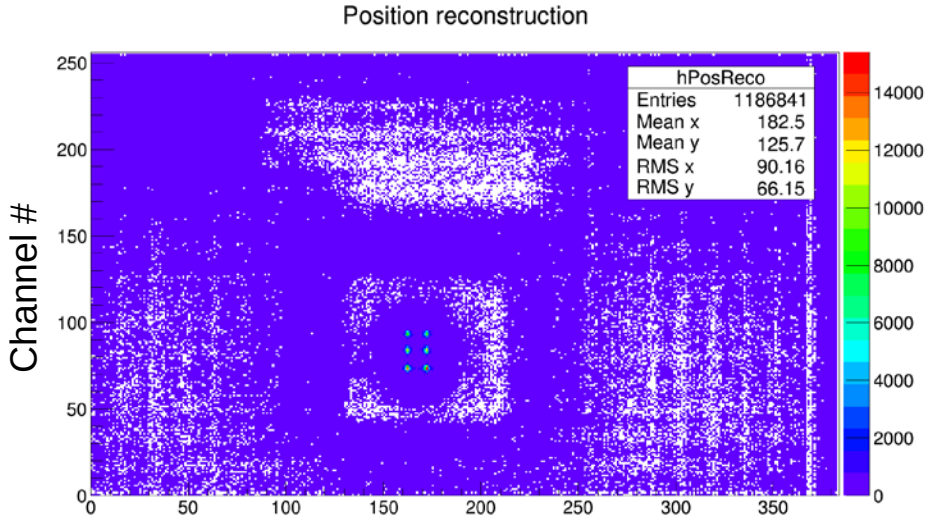

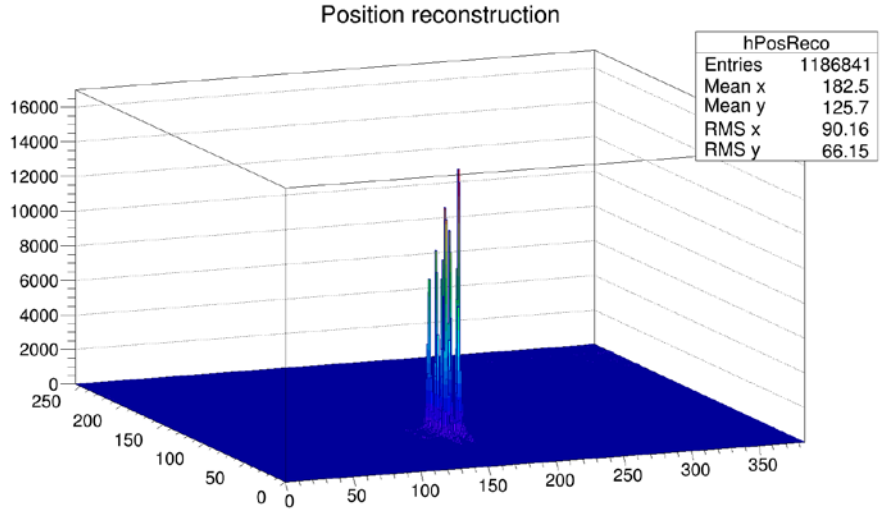

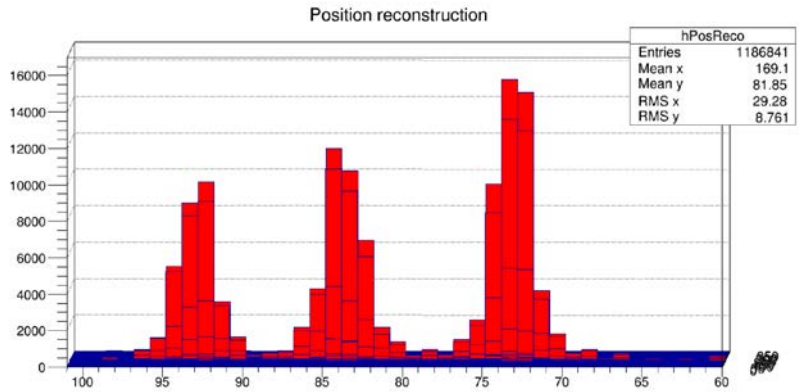

Testsoftware for Windows

- First test's were made with a blue LED
- Control and readout program developed on a Windows 8 system in a Microsoft Visual C environment
  - All parameter can be set and histograms per channel can be measured

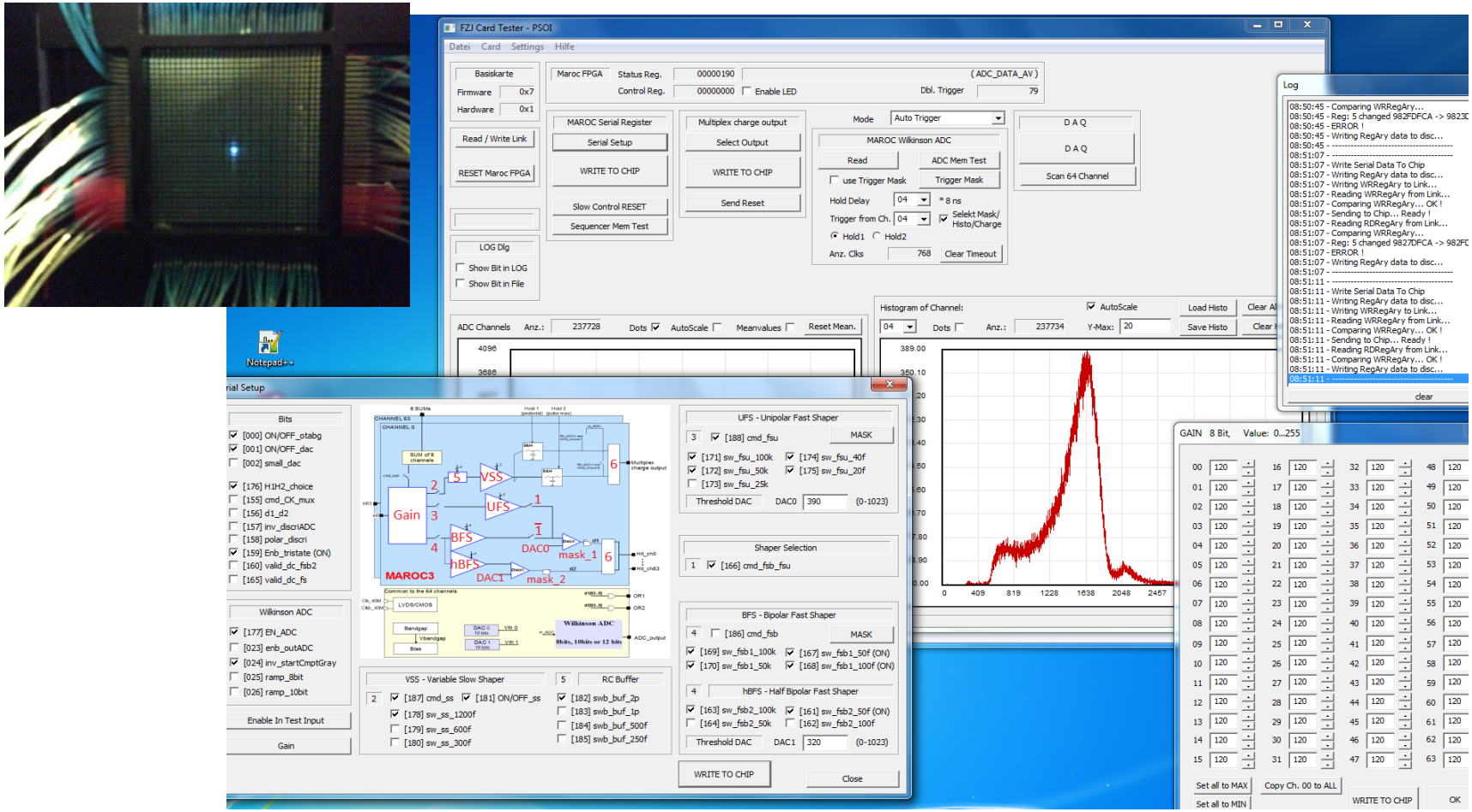

Detector Pulse - Simulator

- Goals:
  - test and optimization of pulse processing for the electronic readout chain
  - 64 trigger outputs for photon counting
  - Analog information for calibration can be easily modified
  - Different test pattern for input pulse simulation can be loaded via 8Mbyte RAM
- Electronic with FPGA board and µC piggy board is in the commissioning phase at ZEA-2

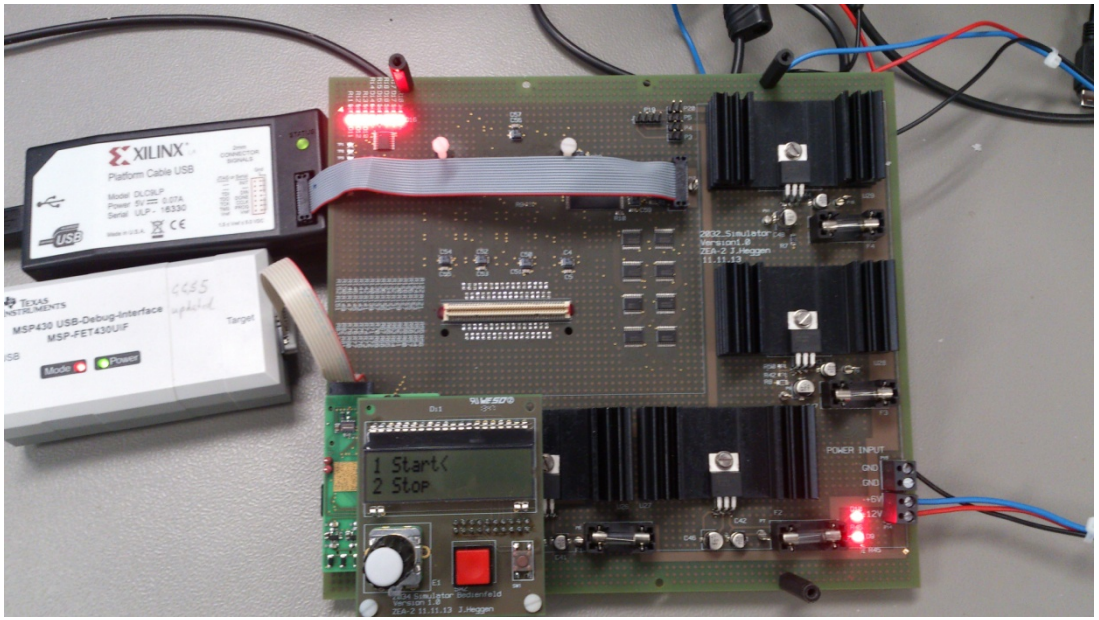

SKADI

SKADI – small-Q, long length scale

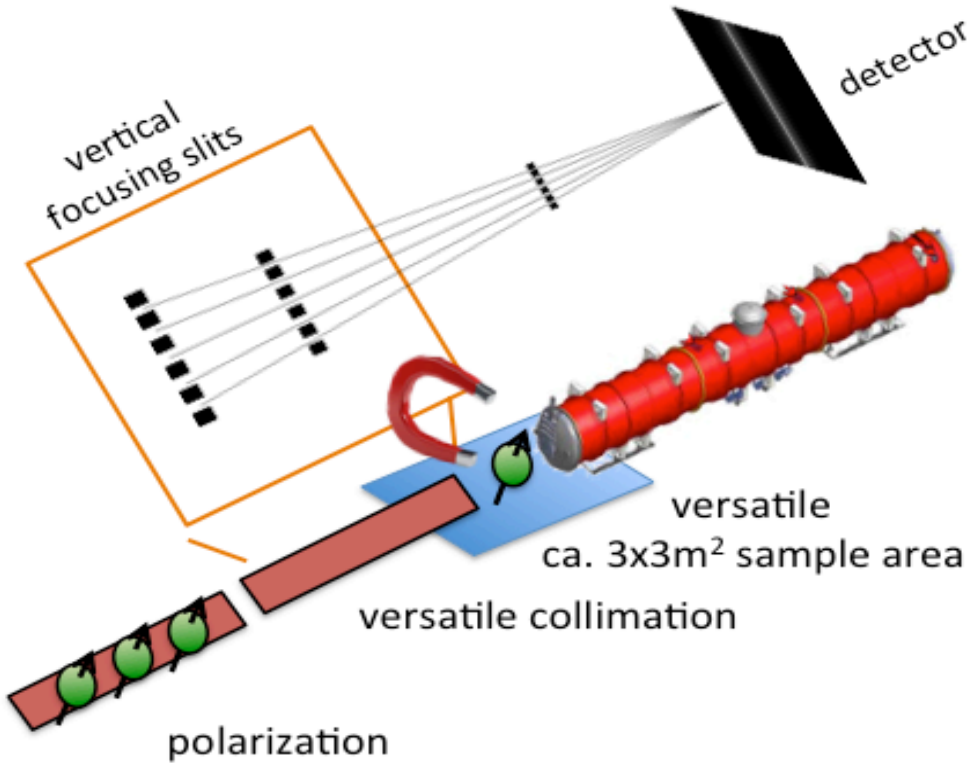

- **Flexibility**
(sample area is approx. 3x3 m^2, and versatile collimation)
- **Very small Q**
accessible through VSANS (using focusing elements)
- **High dynamic Q-range**
(covering three orders of magnitude simultaneously)
- **Polarization**
for magnetic samples and incoherent background subtraction

SKADI Detector Requirements

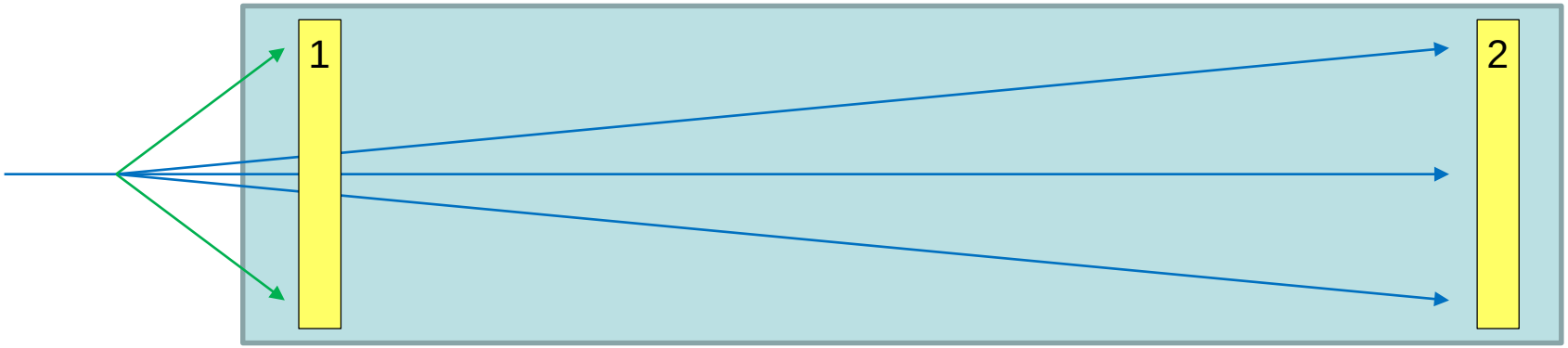

- SKADI goals:
  - simultaneous scattering measurement of large q-range
  - measurement of very low angles
- Usage of 2 detectors at different distance from sample
  - active area of each detector 100 x 100 cm^2
  - first detector with 20 x 20 cm^2 hole in the middle and small amount of dead area around the hole
- Performance requirements
  - detection efficiency ~80% @ 5A, gamma suppression of 10^{-5}
  - count rate capability of ~10 MHz @ 10% dead time
  - position resolution of 6 mm^2, 3 mm^2 down to 1.5 mm^2

SoNDe Project

Develop a large area PSD neutron detector with:

- high-flux capability (gain factor of 20 over current detectors)
- high-resolution of at least 3 mm by single-pixel technique
- efficiency of 80 % or more
- no beam stop necessary
- strategic independence of ^{3}He
- time-of-flight (TOF) capability, time resolution in the µs regime
- modularity

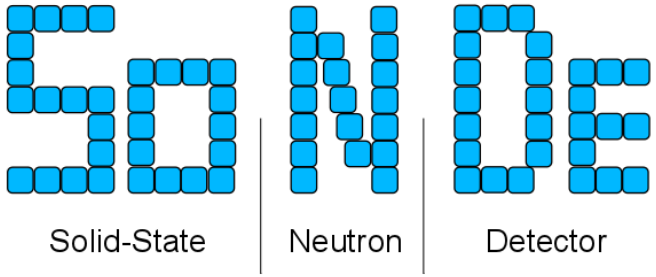

- Started in May 2015
- Consortium of FZJ, LLB, U Lund and ESS
- First tests with 2x2 Demonstrator this Autumn

Readout Electronics Evaluation System

- Required parameter for pulse processing: charge per neutron
  - dependent on number of photons hitting photocathode, quantum efficiency, gain of MaPMT
  - difficult to predict (reflective effects)
  - adjustable to some degree by MaPMT gain
- ROSMAP readout system for evaluation
  - digitization and counting mode available, but only digitization mode used for tests
  - 2x VA32HDR14.3 ASICs for digitization of channels with 10:1 charge splitter for measurement up to 200pC input charge
  - trigger derived from PMT dynode signal
  - 14 bit ADC, data values are delivered with 8 bit resolution via ModBus interface
  - read out rate of ~50 Hz achieved for digitization mode (with python interface)
  - external high voltage supply for MaPMT

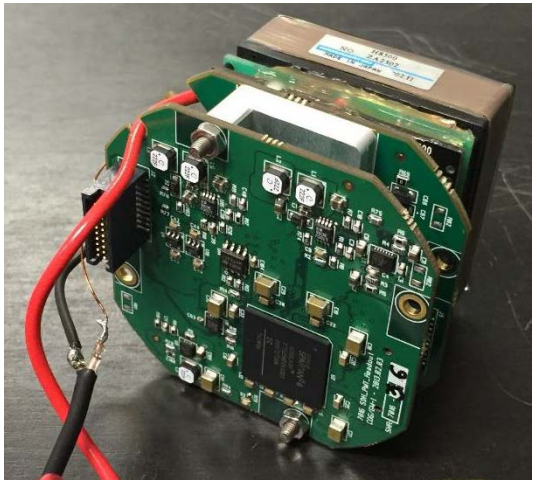

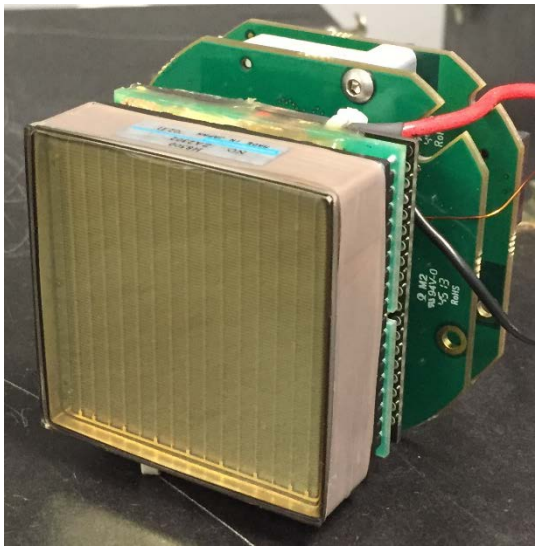

Backend Board

	Realisierungsvorschlag				
Lage:			Stärke(µm) :	Mat.	
	Lötstopplack		20		
1		Cu-Folie	5 + 30 galv.Cu		Signal
	2 x 106	Prepreg	100	IS410	
2		Cu	35		Signal
		Laminat	300	IS410	
3		Cu	35		Signal
	2 x 1080	Prepreg	115	IS410	
4		Cu	35		Signal
		Laminat	300	IS410	
5		Cu	35		Signal
	3 x 1080	Prepreg	190	IS410	
6		Cu	35		Plane
		Laminat	300	IS410	
7		Cu	35		Signal
	2 x 1080	Prepreg	115	IS410	
8		Cu	35		Signal
		Laminat	300	IS410	
9		Cu	35		Signal
	2 x 106	Prepreg	100	IS410	
10		Cu-Folie	5 + 30 galv.Cu		Signal
	Lötstopplack		20		
		Stärke :	2210	+/- 10%	

Thickness of the board 2,2 mm

Screenshot of the 10 Layer board

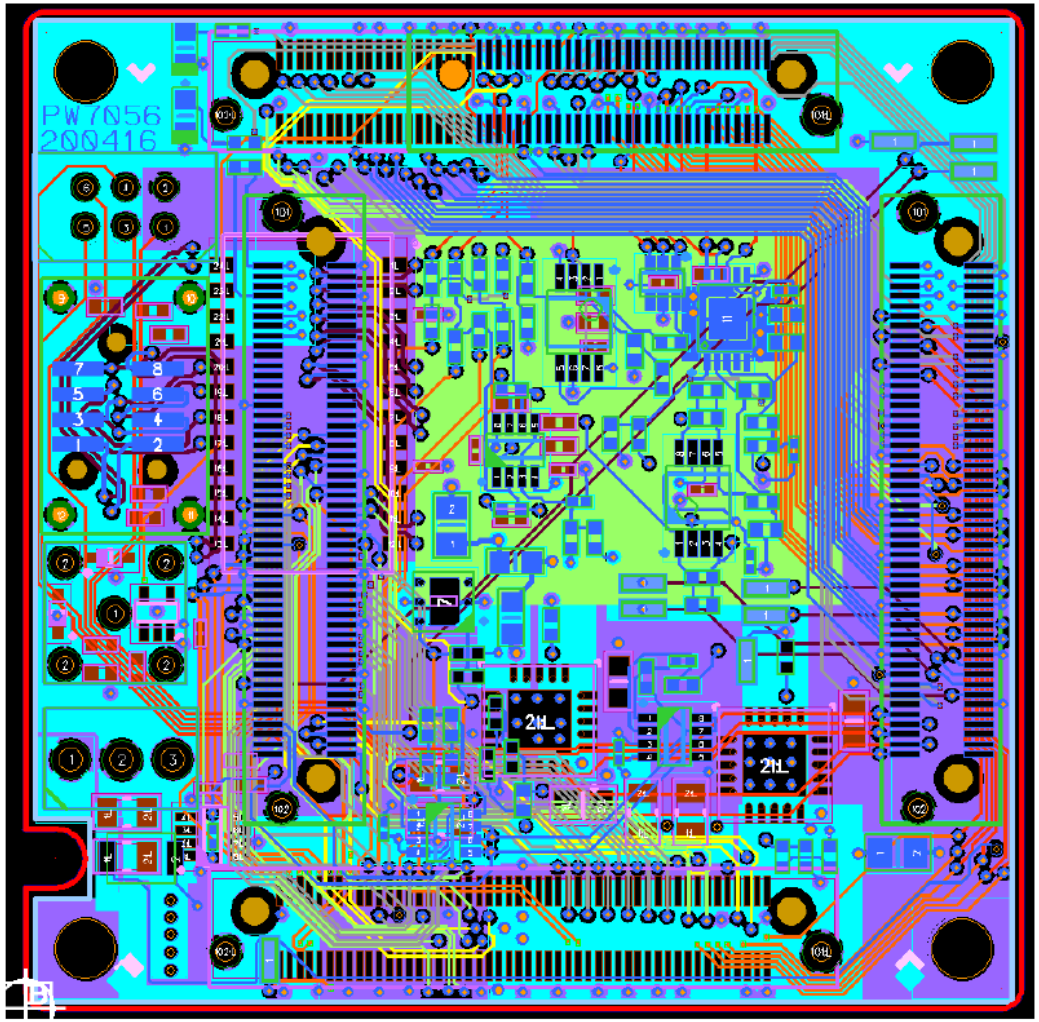

2x2 Demonstrator Test Setup

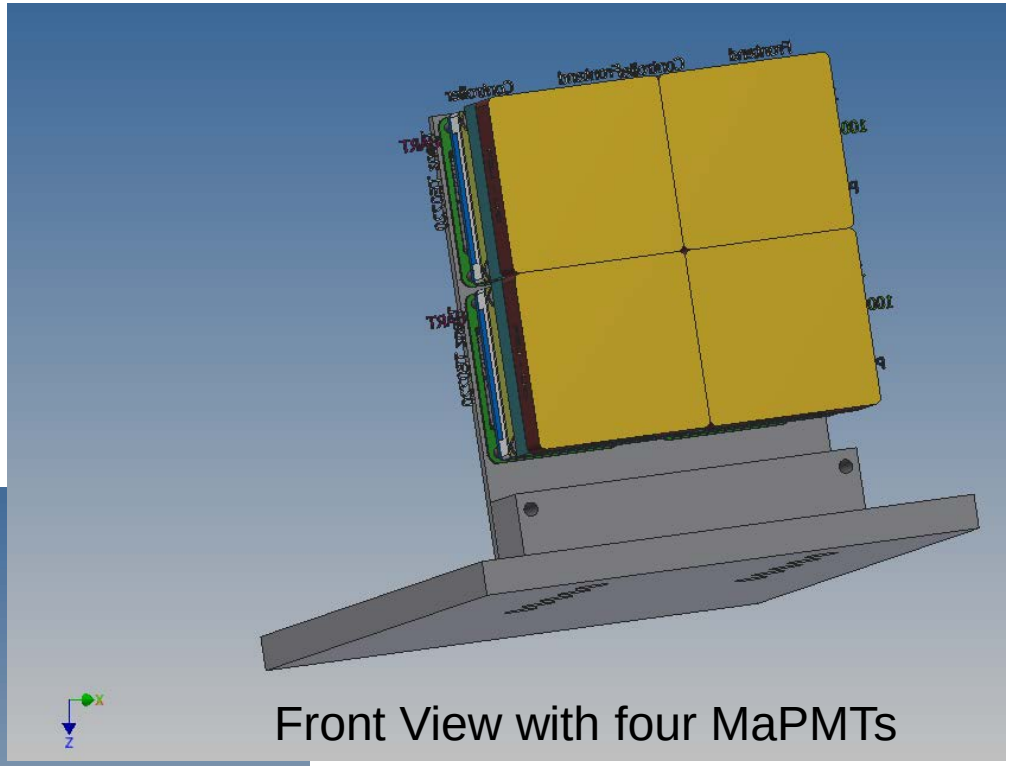

Front View with four MaPMTs

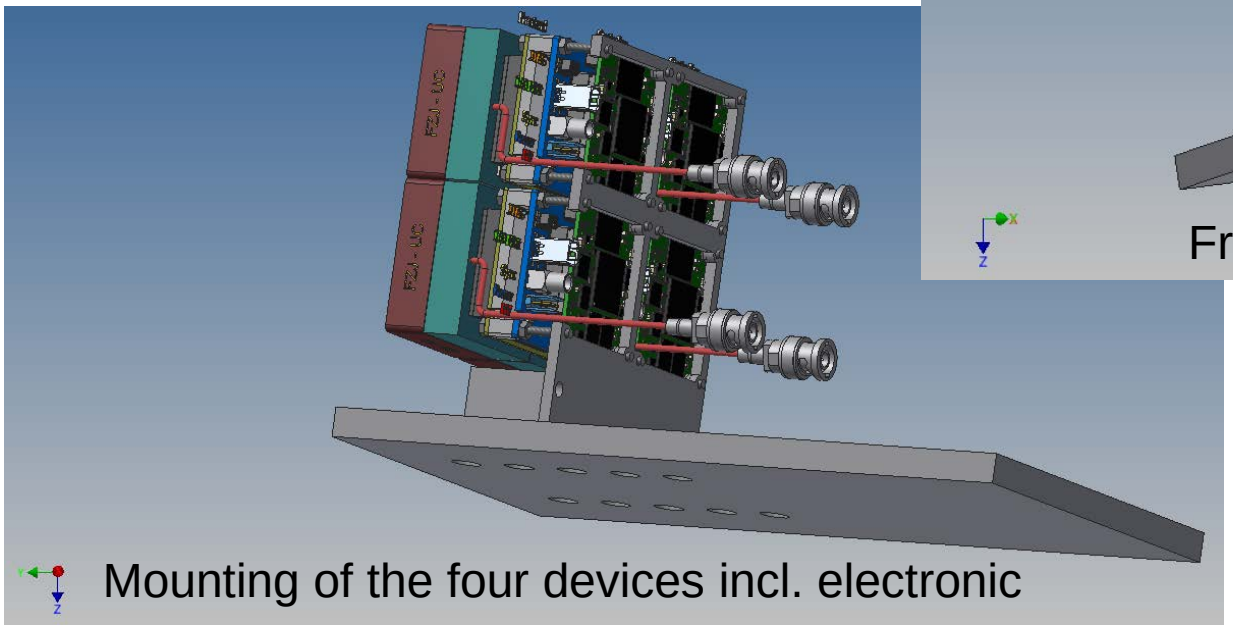

Mounting of the four devices incl. electronic

2x2 Demonstrator Test Setup

Rear View

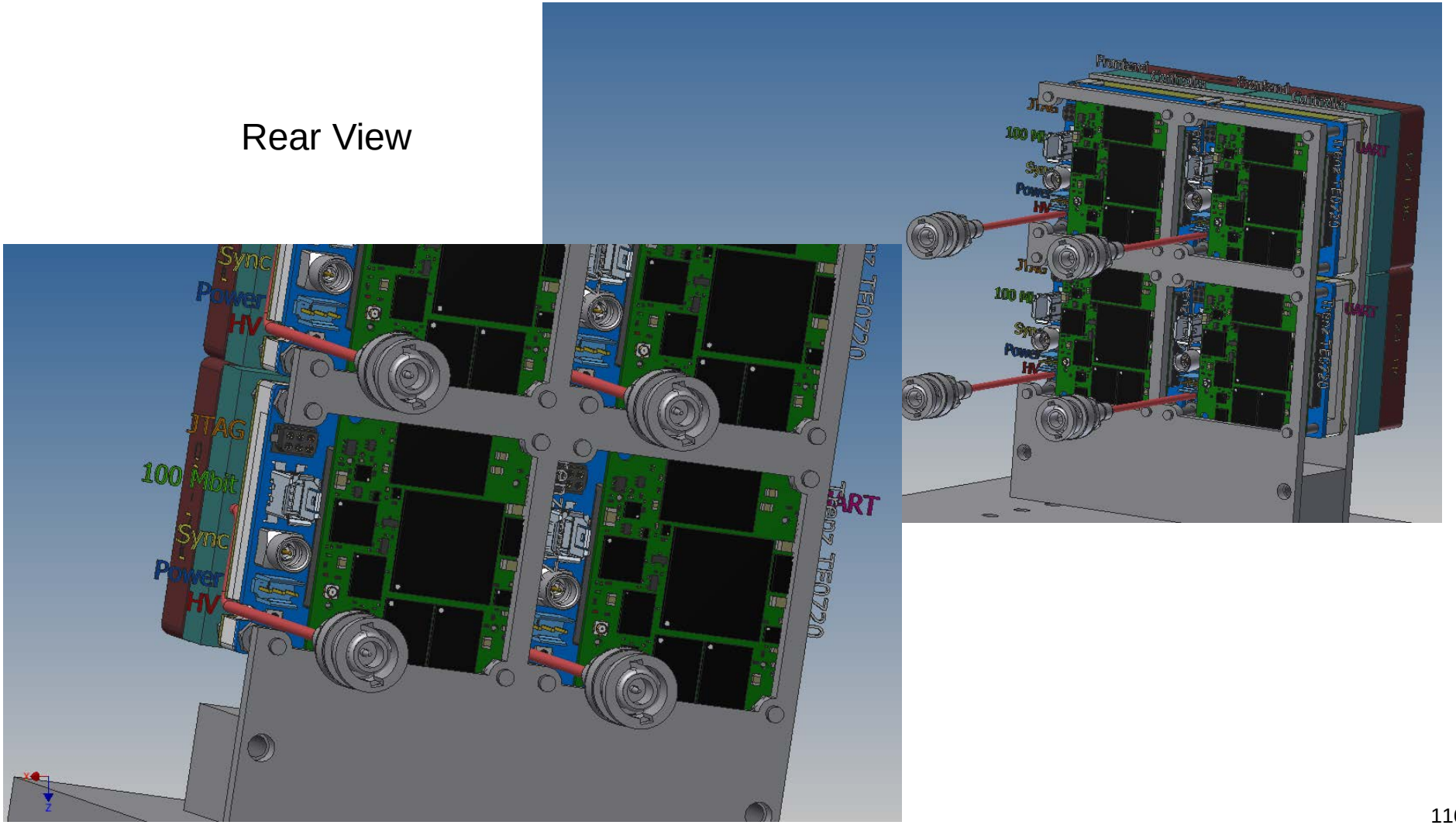

Silicon Drift Detector

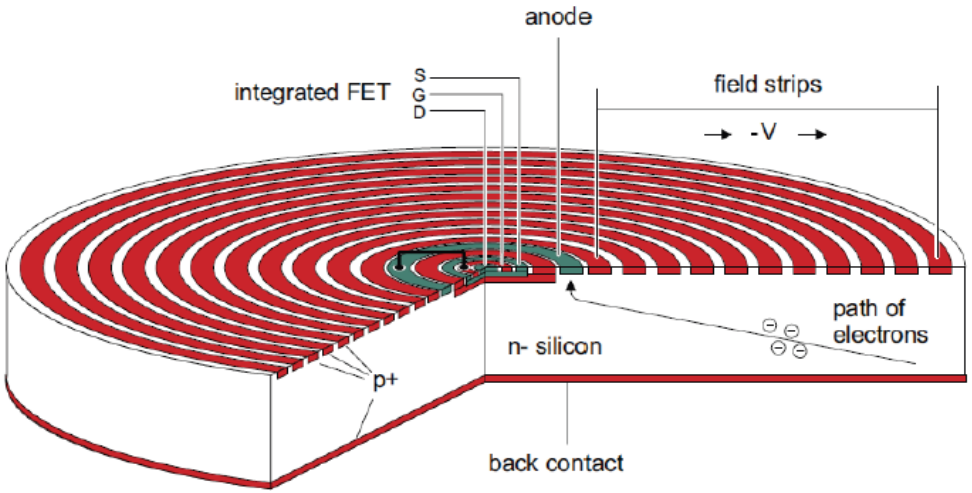

The SDD operating principle is based on the sideward depletion technique that permits the depletion of a large volume of the detector by a small anode, hence the small capacitive noise.

Advantages:

- Compact and robust
- High QE (~80% @ 400nm)
- Broad spectral response (300 to 900 nm)
- Insensitive to magnetic field
- Low excess noise
- Low capacitive noise

Drawbacks:

- Gain = 1
- Required low noise preamplifiers to readout

Si PIN photodiode

- Large dynamic range
- Stable
- Magnetic field insensitive
- Gain = 1
- Small in size (< 5x5 mm^2)

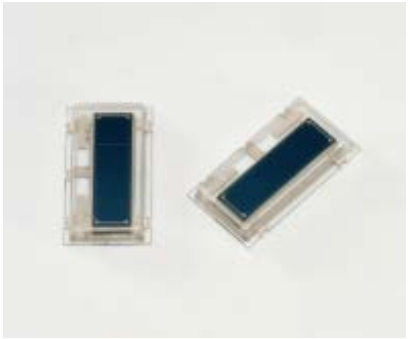

source: Hamamatsu

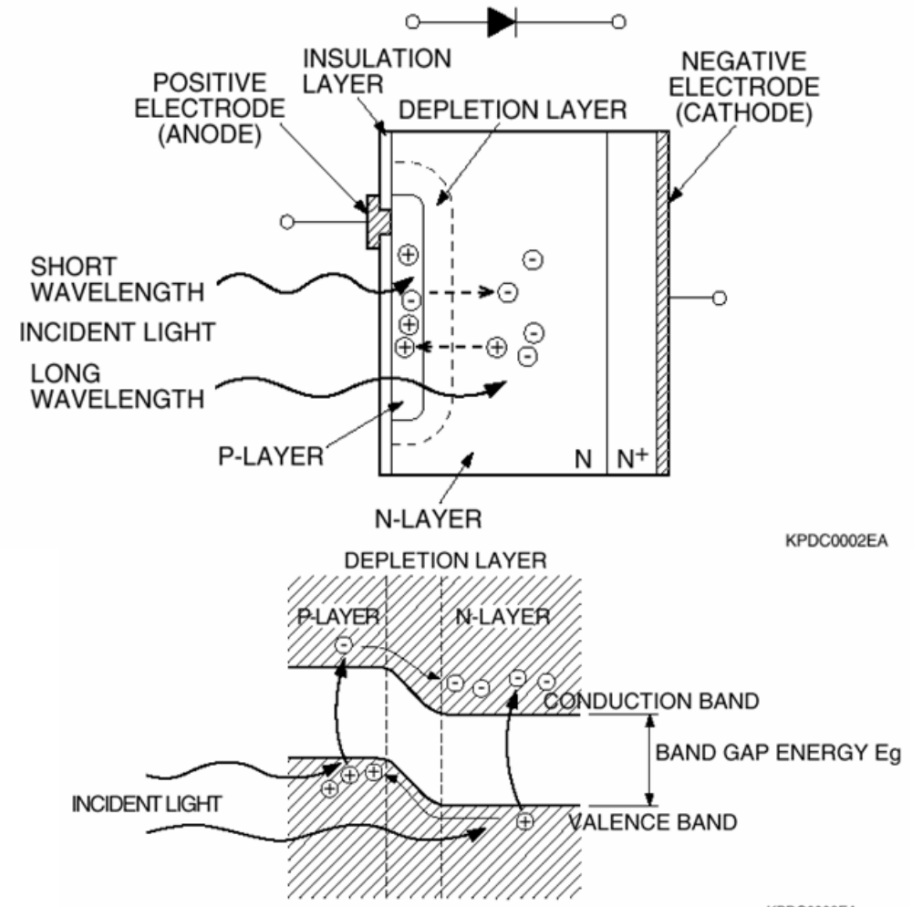

Properties of APD

Advantages :

- Internal Gain (10 – 1000)
- High QE (> 70% for 400 – 600 nm)
- Broad spectral response
- Low bias voltage
- Compact and robust
- Small pixels, individual coupling
- Insensitive to magnetic field

Drawback :

- Gain lower than PMT (~10^2)
- Gain sensitive to temperature and voltage fluctuations
- High excess noise factor

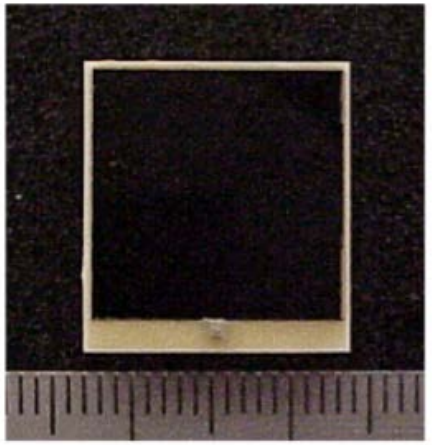

RMD 14x14 mm^2

Single

Hamamatsu S8664-1010
(10x10 mm^2)

Si APD Arrays

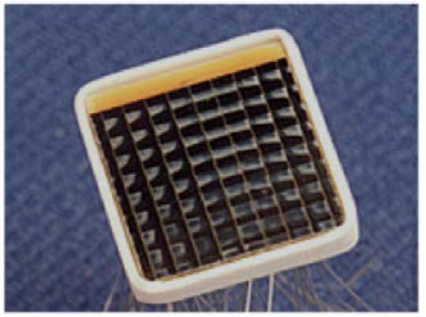

RMD
8x8 APD array

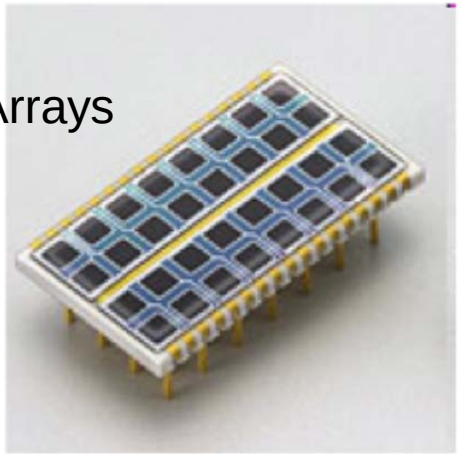

Hamamatsu
4x8 APD array

Silicon Photomultiplier (SiPM)

- Avalanche photodiode operated in Geiger-mode (GM-APD)
  - standard output signal of GM-APD independant from number of photons (binary device)
  - GM-APD does not give information on the light intensity
- Passive Quenching:
  - at diode breakdown, series resistor reduces the voltage across the APD
  - quenches the avalanche

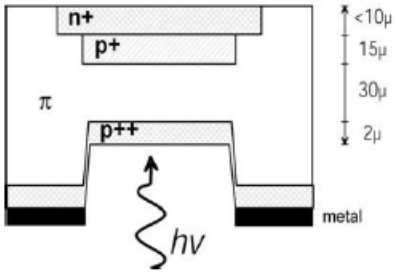

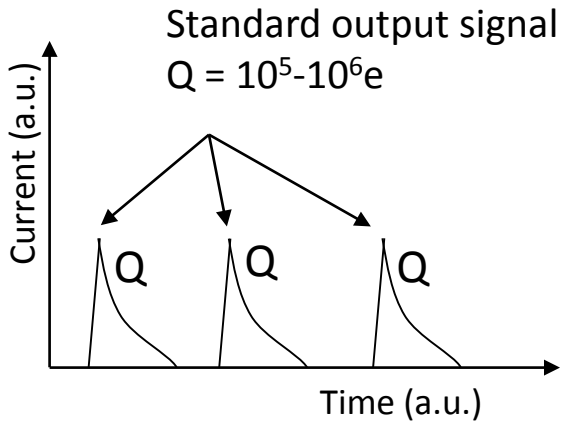

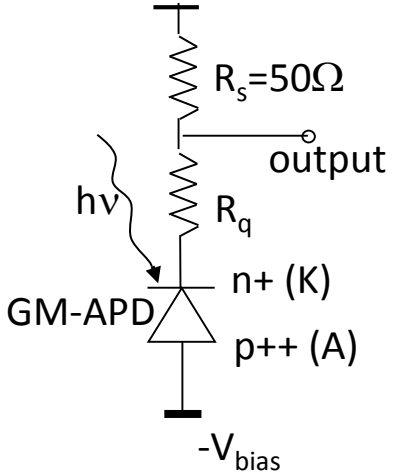

Silicon Photomultiplier (SiPM)

- Silicon photomultiplier contains many GM-APD cells (100…4000 / mm^2)
  - matrix of n pixels connected in parallel on a common Si substrate
  - each pixels = GM-APD in series with R_q
- Quasi analog device:
  - output is the sum of the standard signals: $Q \sim \Sigma Q_i$
  - SiPM gives information on light intensity

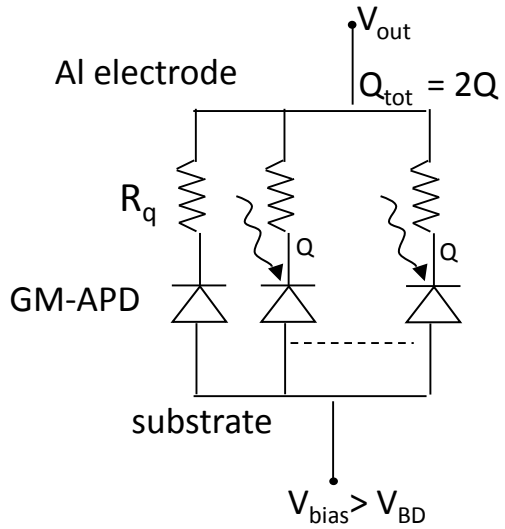

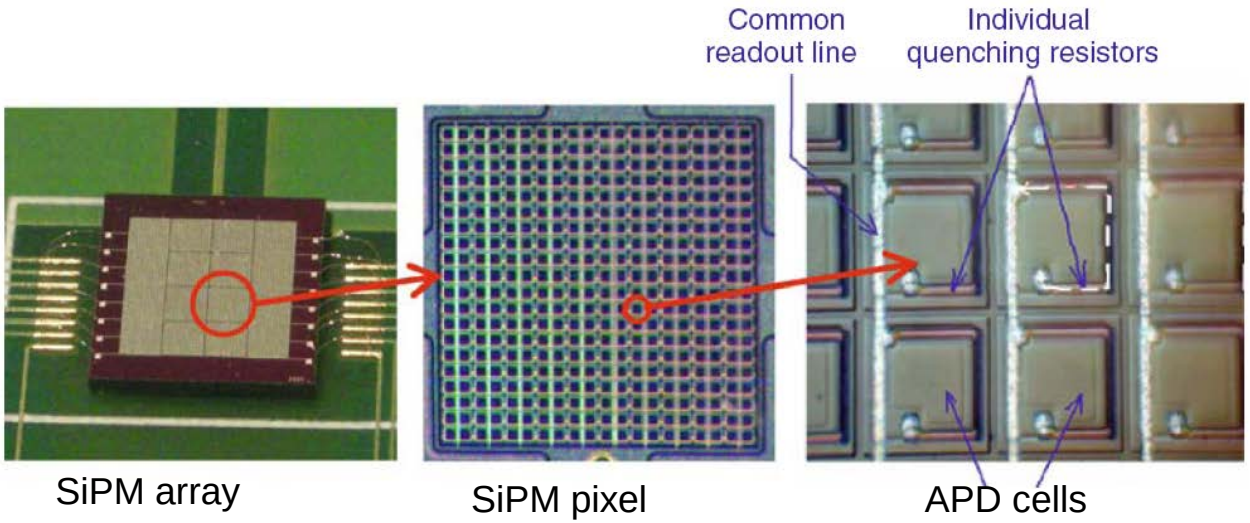

Silicon Photomultiplier (SiPM)

Advantages:

- High gain (10^5-10^6) with low voltage (<100V)
- Low power consumption (<50μW/mm^2)
- Fast (timing resolution ~ 50 ps RMS for single photons)
- Insensitive to magnetic field (tested up to 7 T)
- High photon detection efficiency (30-40% blue-green)

Possible drawbacks

- High dark count rate (DCR) at room temperature
  - 100kHz – 1MHz/mm^2
  - thermal carriers, cross-talk, after-pulses
- Temperature dependence

Different producers give different names: SiPM, MRS-APD, SPM, MPPC…

SiPM Arrays

Sensl 4x4 array of 3x3 mm^2 pixel

Hamamatsu MPPC Arrays

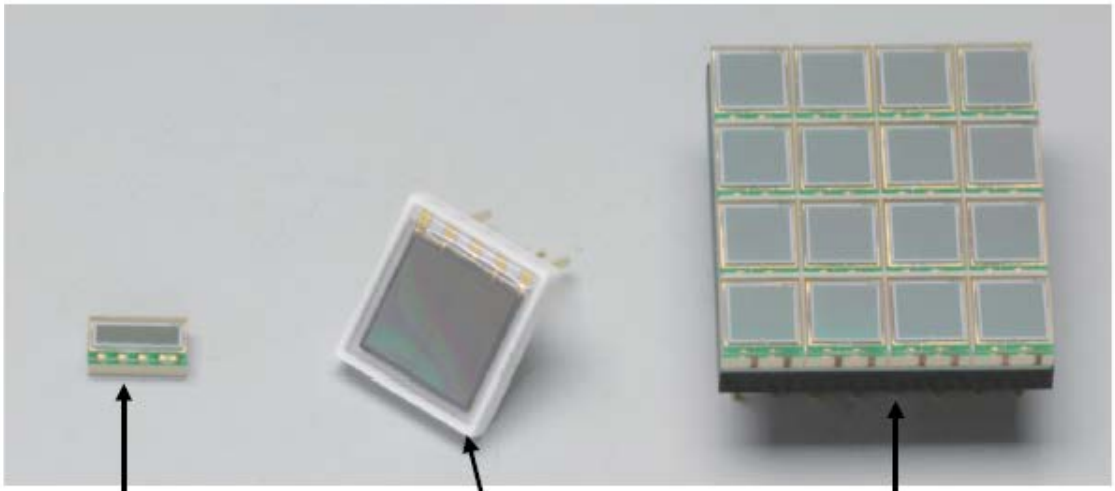

1x4 array of 1x1 mm^2

2x2 monolithic array of 3x3 mm^2

4x4 array of 3x3 mm^2

^{6}Li/ZnS Based Alternatives

- Neutron capture by the ^{6}Li yields α + ^{3}H

- Glass fibers
  - ^{6}Li-enriched lithium silicate glass fibers doped with cerium which fluoresces (Bliss et al. 1995, PNNL)
  - Good efficiency (per unit surface area or neutron module)
  - Gamma-ray sensitive: discrimination with PSD

- Coated wavelength shifting paddles/fibers
  - ZnS scintillator material mixed with ^{6}Li coating
  - Good efficiency (per unit surface
  - area or neutron module)
  - Coating gamma-ray sensitive:
    - Good discrimination with PSD

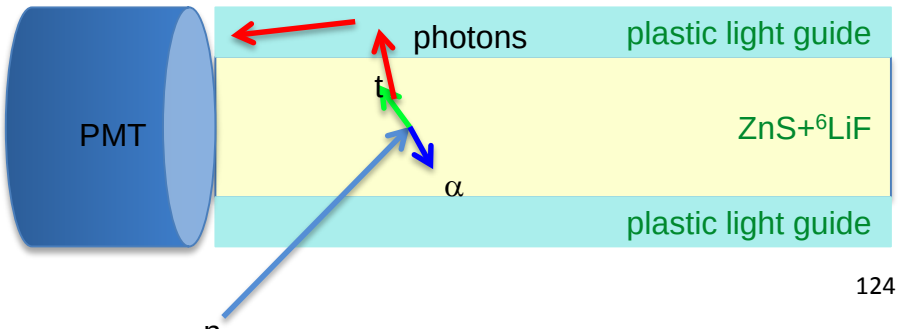

Source : R. Kouzes, PNNL, SORMA 2014

Recent Li-6 Based Developments

- LiCAF and BGO phoswich detectors for simultaneous measurements of atmospheric neutrons and gamma-rays – H. Takahashi et al. (IEEE NSS 2013)

- Lithium alkali halides – V Nagarkar et al. (IEEE NSS 2013)
  - $Li_3Cs_2I_5$ (LCI) and $Li_xNa_{1-x}I$ (LNI)
  - Pulse-shape and pulse-height discrimination

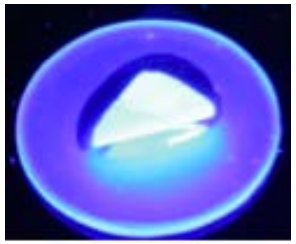

source : R. Kouzes, PNNL, SORMA 2014

Decay time characteristics

Fast component

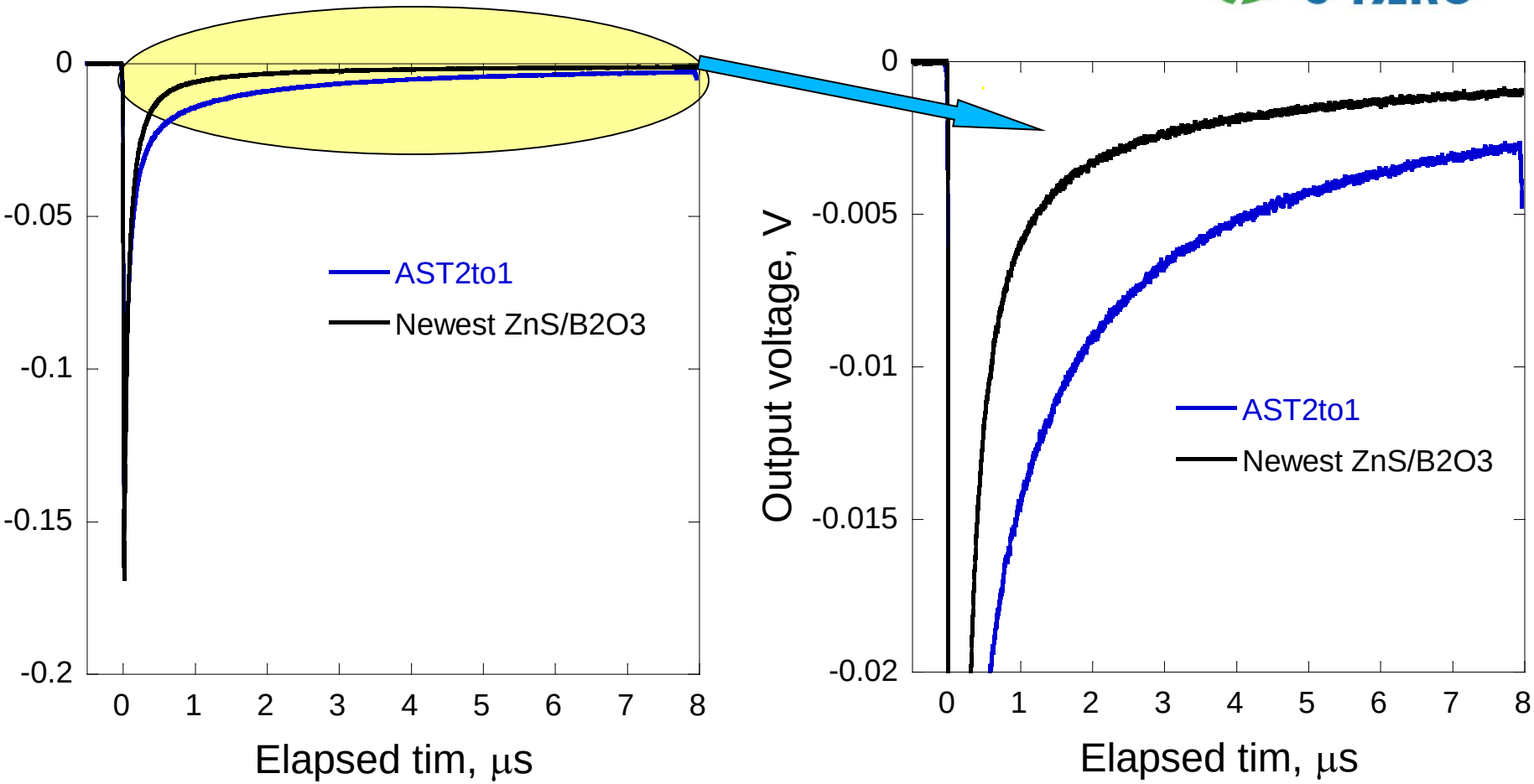

Dramatically, afterglow signal is reduced

source : M. Katagiri, JPARC, PSND 2014

Decay time characteristics

Detection characteristics of developed ZnS/neutron-converter-type scintillators

Scintillator	ZnS	Efficiency at thermal neutron	Integral time:1μs		Integral time:8μs	
			Photons	Decay(μs)	Photons	Decay(μs)
AST 2to1	Comercial	0.325	26766	0.437	57744	2.75
New ZnS/6LiF	New ZnS A	0.405	23539	0.279	33522	1.02
First 10B2O3	Comercial	0.252	21424	0.347	39380	2.24
New 10B2O3	New ZnS B	0.320	20362	0.240	29194	1.10
Organic 10B	New ZnS C	0.284	20016	0.264	29182	1.18

Characteristics of the newest ZnS/^{6}LiF scintillator is excellent to that of the newest $^{10}B_2O_3$ scintillator

Therefore, we will start to use the newest ZnS/^{6}LiF scintillators for our developed neutron image detectors instead of the $^{10}B_2O_3$ scintillator

source : M. Katagiri, JPARC, PSND 2014

neutron detection candidates

Cs_2LiYCl_6

CLYC

$Cs_2LiLaCl_6$

CLLC

$Cs_2LiLaBr_6$

CLLB

- High light yield
  70,000 to 180,000 ph/neutron
- High gamma equivalent
  >= 3 MeV
- High energy resolution
  2-3% at neutron FEP
- Pulse height discrimination
- Pulse shape discrimination
- Cubic structure

∅1 in CLYC

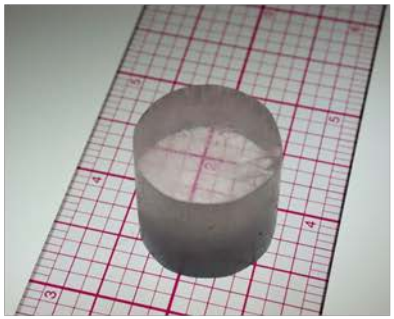

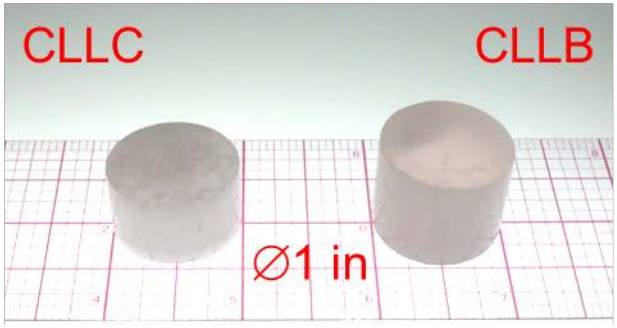

source: Nagarkar, RMD

Other recent developments

- Fast neutron bubble detectors for science (PNNL)

PNNL 130-ml Freon 134a Bubble Chamber, 2” window diameter

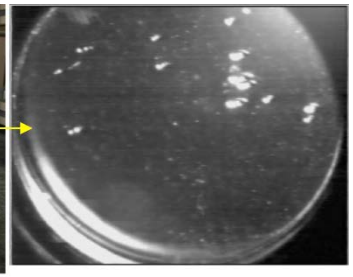

Bubble formation under exposure to AmBe neutron source

- Wavelength shifting fiber detectors for science – Kazuhiko Soyama, JAEA (BES He-3 Workshop)

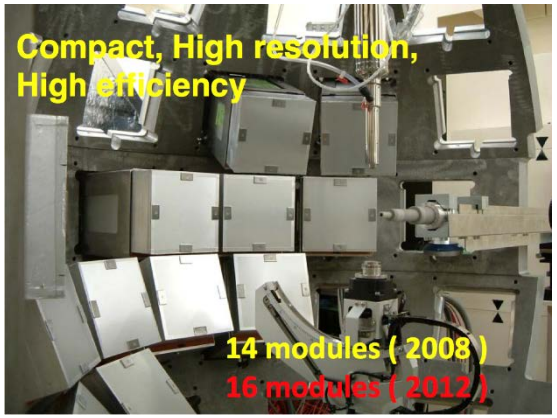

- Liquid scintillator for fast neutrons for IAEA safeguards – A Lavietes et al. (IEEE NSS 2013)

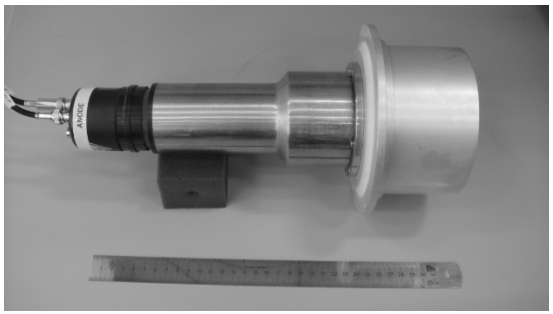

Source : A. Kouzes, PNNL, SORMA 2014

POWGEN instrument @SNS

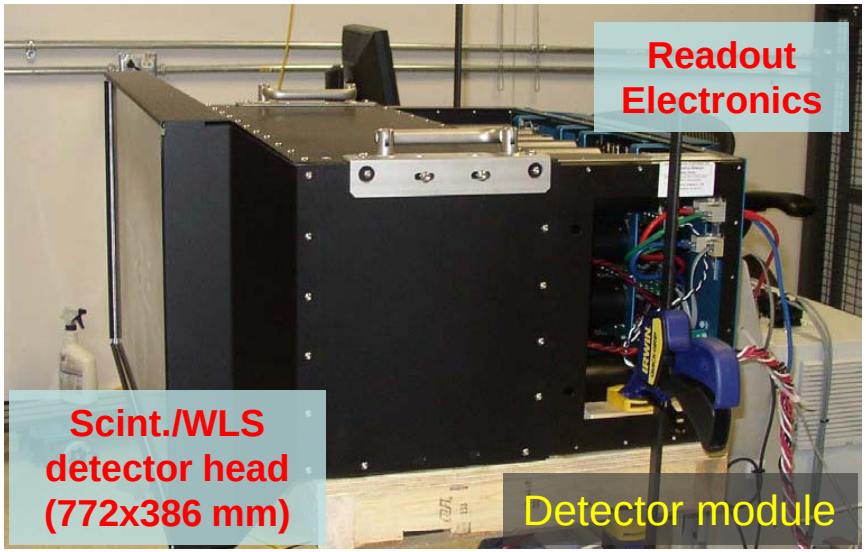

Photos R.Cooper

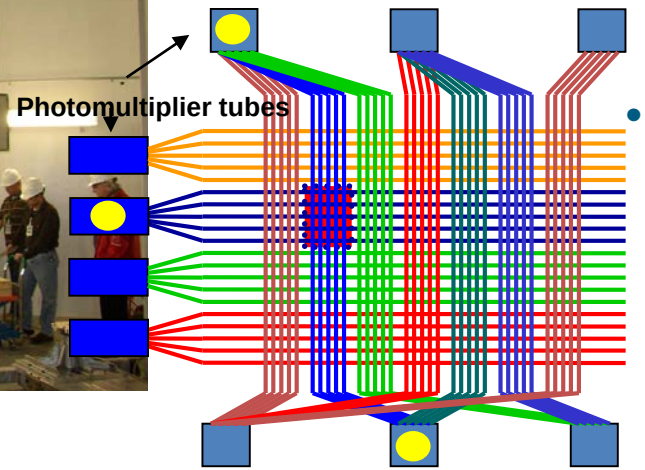

- POWGEN is in service since 2010
  - Detectors manufactured by ParTec
  - 30 Scint./ WLS fibre detectors at SNS
- Specifications:
  - Pixel size 5 x 50 mm
  - V-Shape LiF/ZnS Scintillator
  - Detector efficiency: ~ ^{3}He-tube with 6.6 bar
  - Gamma-Sensitivity: $<10^{-5}$
  - Local count capability ~50k

iBIX instrument @J-PARC

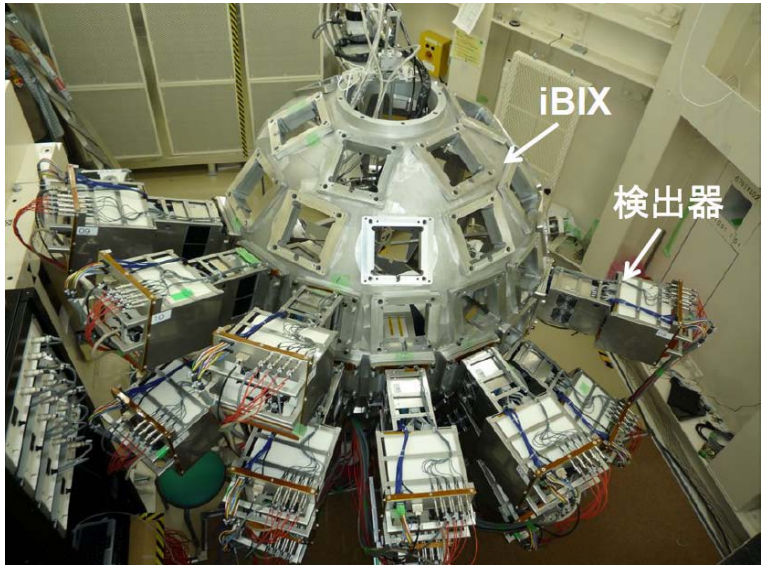

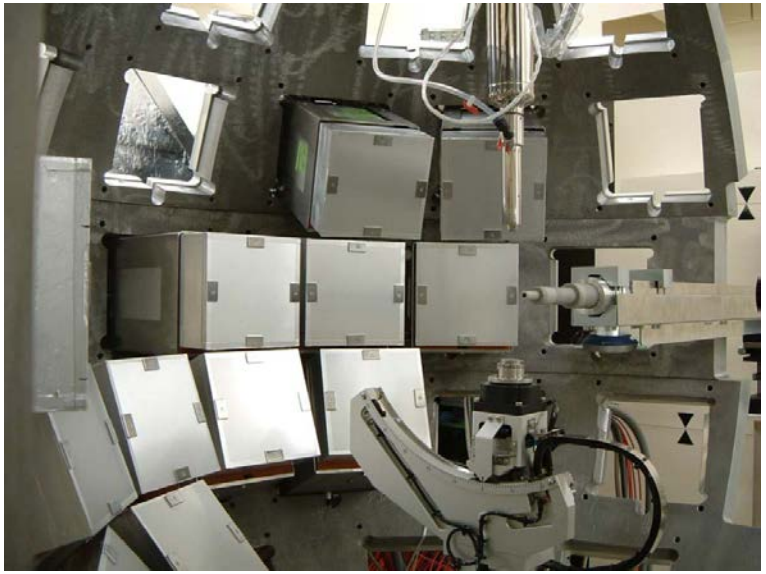

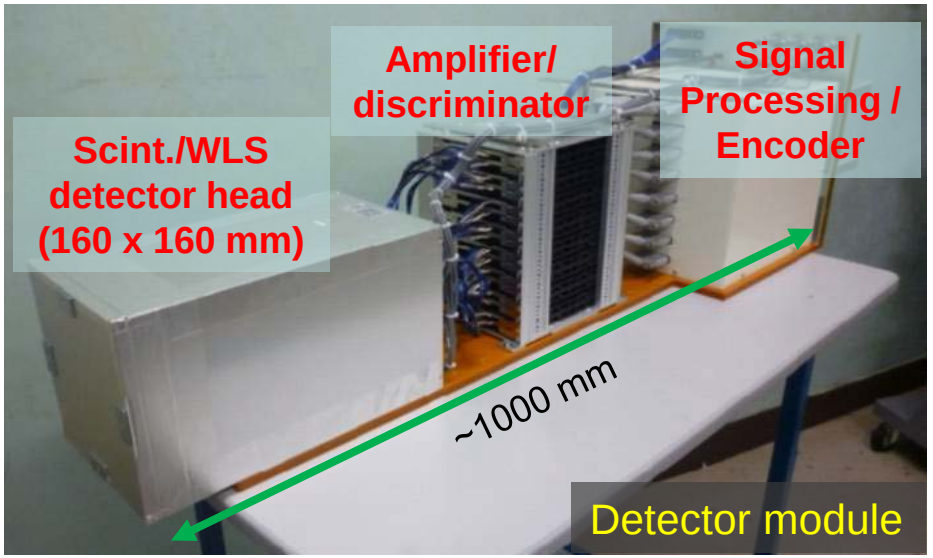

Photos of S.Soyama, T.Nakamura

- iBIX is in service since 2009
  - Detectors developed by JAEA since 2005
  - 14 Scint./ WLS fibre detectors installed
- Specifications:
  - Pixel size: 0.5 x 0.5 mm
  - 2 x $^{10}B_2O_3$/ZnS scintillator in sandwich
  - Detector efficiency 50%@1.8 Å
  - Gamma-Sensitivity: ~10^{-5}
  - Local count capability: ~50k

SENJU Instrument @ J-PARC

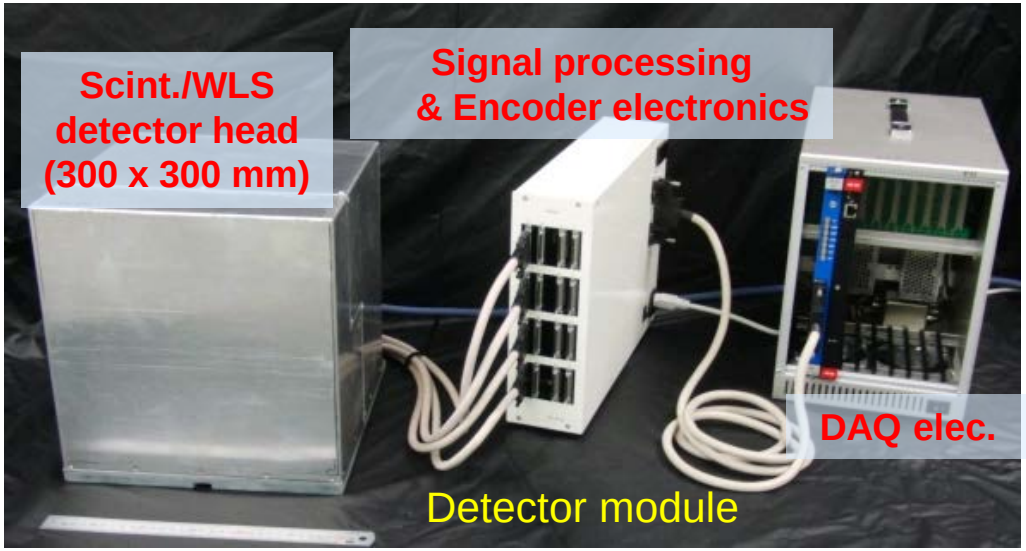

Photos S.Soyama, T.Nakamura

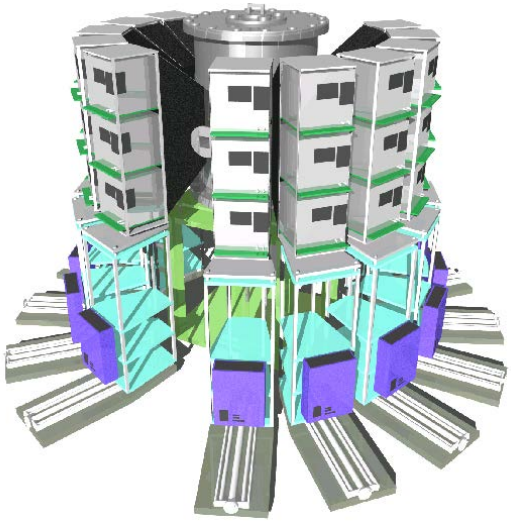

- Specifications:
  - Detector module 300x300 mm
  - Pixel size 4x4 mm
  - 2 x $^{10}B_2O_3$/ZnS scintillator in sandwich
  - Detection efficiency 40%@1.8 Å
  - Gamma-Sensitivity ~10^{-6} at 1.3 MeV
  - Local count capability ~50k
  - Pulse pair resolution < 5μs

GEM Detector @ISIS

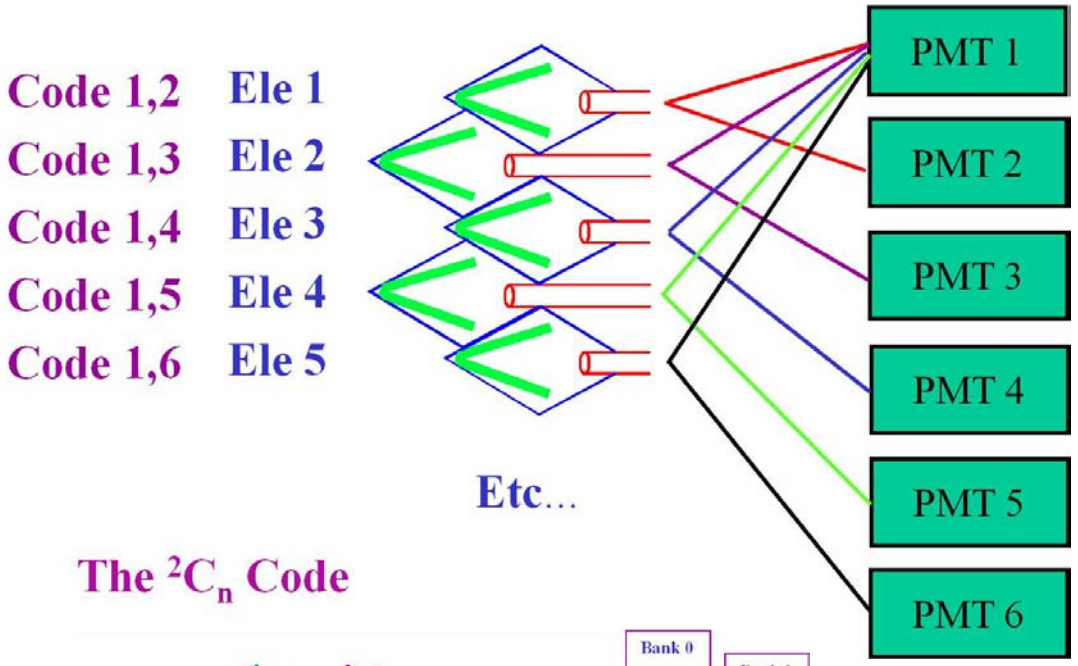

The $^{2}C_{n}$ Code

$$ {}^{x}C_{n} = \frac{!\,n}{!\,(n-x)\cdot !\,n} $$

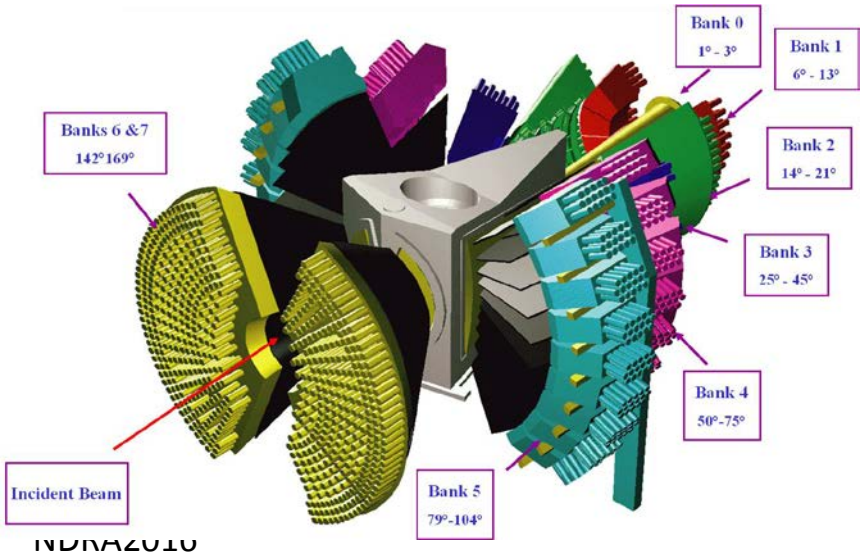

- Specifications of PWOGEN (left):
  - Pixel size 3x3 mm
  - ^{6}LiF/ZnS scintillator in sandwich
  - Detection efficiency 50%@1 Å
  - Gamma-Sensitivity ~10^{-6} at 1.3 MeV

IMAT: The Imaging and MATerials Beam Line @ISIS

- Enabling imaging and diffraction studies on the same beam line.
- Diffraction detectors up to ~18m^2
- Phase 1
- Imaging detectors and
- 90 degree bank 4.5 m2
- First neutrons 2015

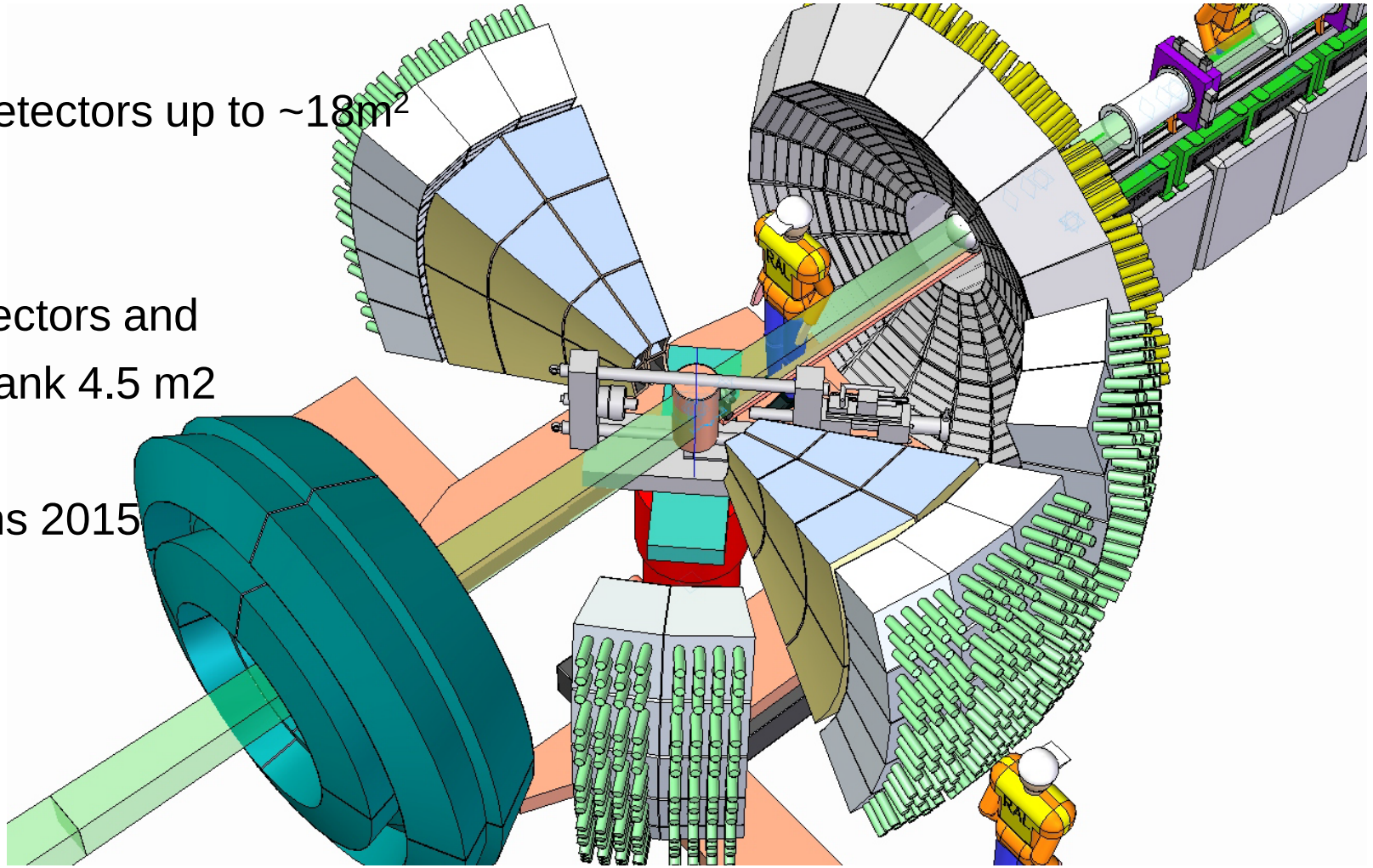

source: Jeff Sykora, ISIS

IMAT Diffraction detector

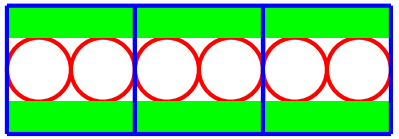

- IMAT 90 degree module
- Initial design based on Megan detector
- Individual elements wrapped in reflector to minimise optical cross talk

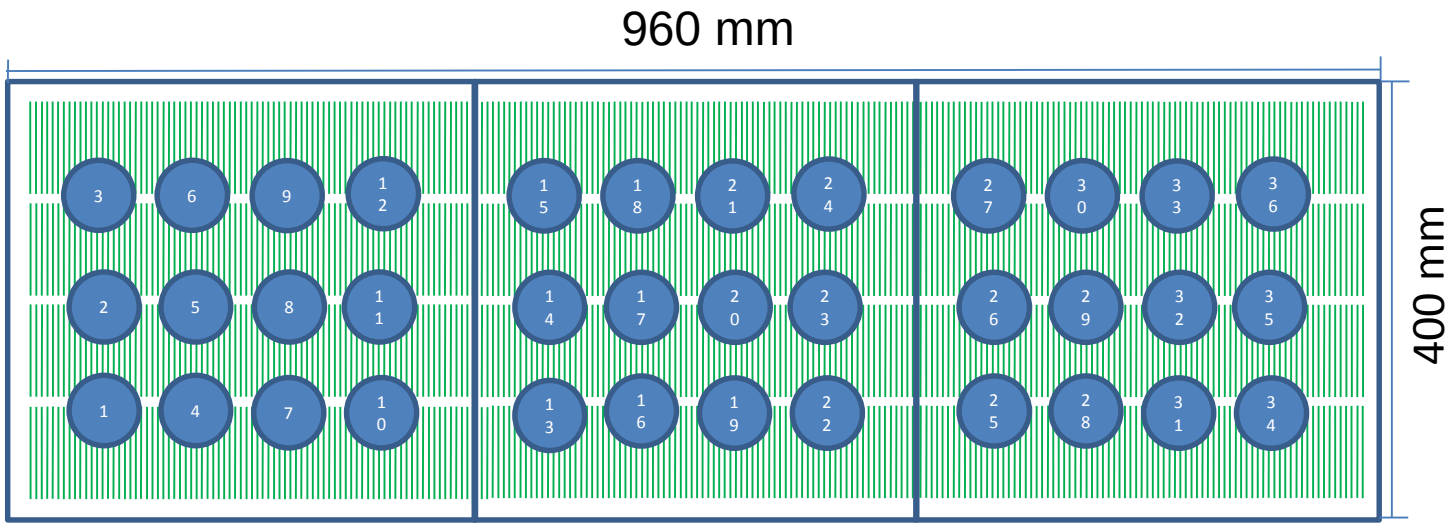

- 920 elements per module divided into three independent segments
- Each element 4 mm wide x 100 mm long
- Quad coincident code
- 3840 fibres read out by 36 PMTs

source : Jeff Sykora, ISIS

IMAT: Trial Detector

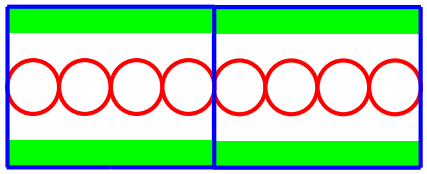

80 element 16 PMTs
0,5 mm spacing
2.0 mm spacing

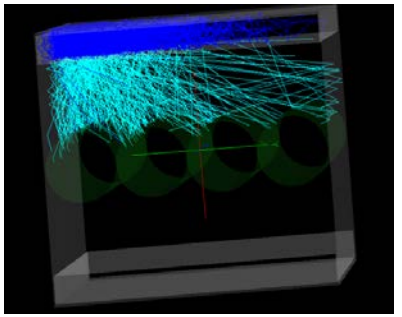

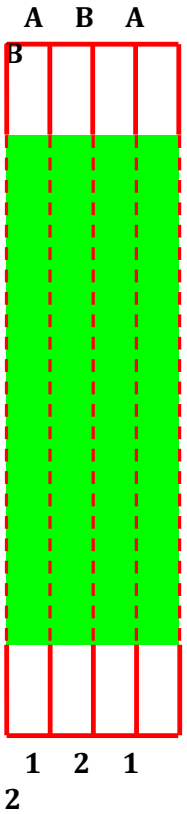

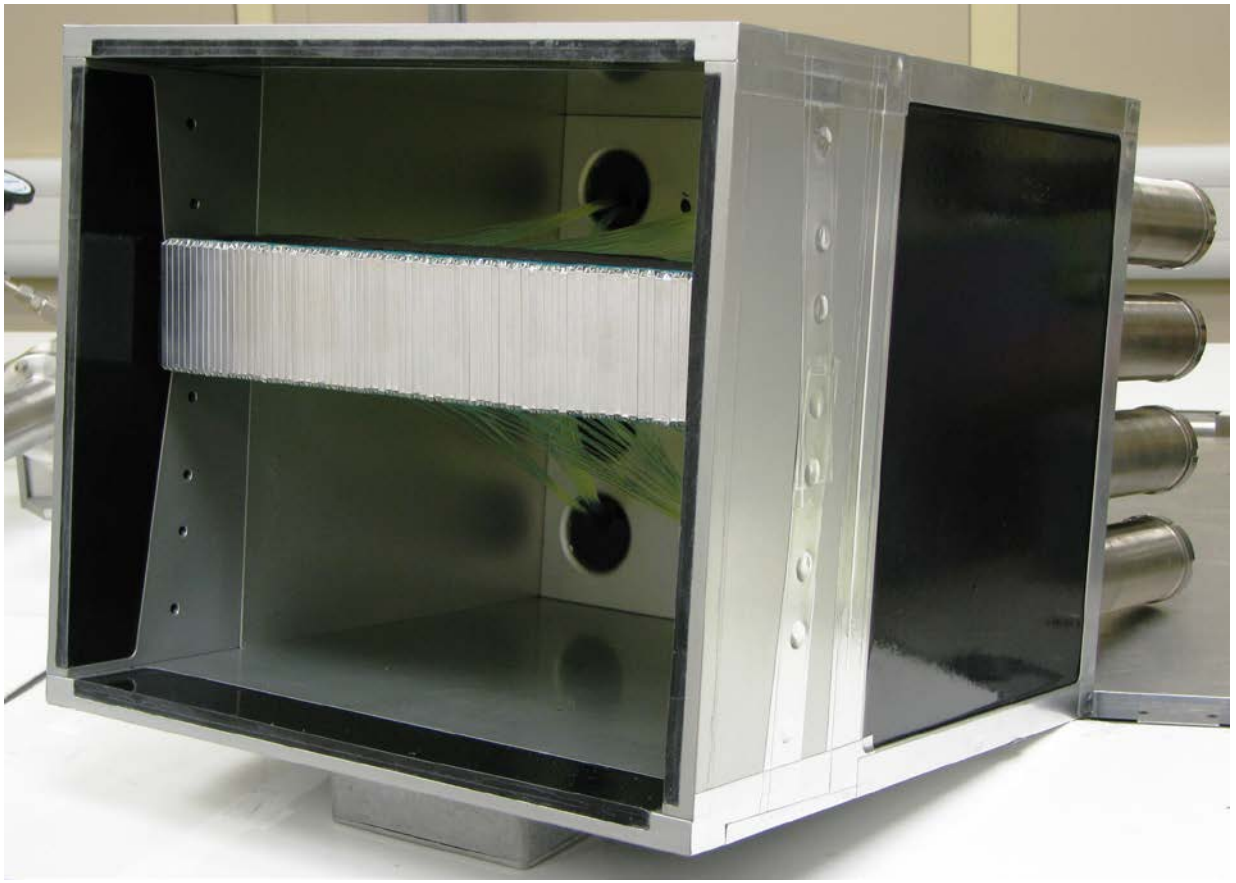

source : Jeff Sykora, ISIS

Summary

- Photodetectors are some of the most widely used devices in particle physics and nuclear medicine for detecting many types of particles (γ, n, e, …)
- Photomultiplier tubes are still the most extensively used despite many of their limiting properties
- New solid state detectors are now achieving the same performance as PMTs in terms of gain and timing, and also work in magnetic fields, but have their own limitations in terms of area coverage, noise, and radiation hardness
- Good overall detector design requires looking at all factors affecting performance (choosing the right photodetector, good light collection and matching, efficiency, and low noise electronics)

Reference Materials

The following materials provide useful information and methods of testing.

- Standards
  - NIM Standard - May 1990 Revision of the NIM standard (formerly TID 20893 (Rev) and NIM/GPIB). DOE/ER-0457T, U.S. NIM committee, May 1990; Standard NIM Instrumentation System, NIST, U.S. Department of Commerce, Springfield, Virginia 22161.
  - IEEE 301-1988, “IEEE Standard Test Procedures for Amplifiers and Preamplifiers used with Detectors of Ionizing Radiation”
  - IEEE 325-1996, IEEE Standard Test Procedures for Germanium Gamma-Ray Detectors”
  - IEEE N42.28-2002, “American National Standard Calibration of Germanium Detectors for In-Situ Gamma-Ray Measurements”

Reference Materials

- IEEE 1160-1993, "IEEE Standard Test Procedures for High-Purity Germanium Crystals for Radiation Detectors"
- IEEE 301-1988, "IEEE Standard Test Procedures for Amplifiers and Preamplifiers used with Detectors of Ionizing Radiation"
- IEEE N42.12-1980, American National Standard Calibration and Usage of Sodium Iodide Detector Systems"
- IEEE N42.14-1978, "American National Standard Calibration and Usage of Germanium Detectors for Measurement of Gamma-Ray Emission of Radionuclides"
- IEC 61151 ed1.0 (1992-09), "Nuclear instrumentation - Amplifiers and preamplifiers used with detectors of ionizing radiation - Test procedures"
- IEC 60412 ed2.0 (2007-06), "Nuclear instrumentation - Scintillation detectors - Nomenclature (identification) - Standard dimensions of scintillators"

Reference Materials

- ISO 11929:2010, “Determination of the characteristic limits (decision threshold, detection limit and limits of the confidence interval) for measurements of ionizing radiation - Fundamentals and application”
- IEC 62327 Ed. 1.0 b:2006, “Radiation protection instrumentation - Hand-held instruments for the detection and identification of radionuclides and for the indication of ambient dose equivalent rate from photon radiation”
- IEC 60462 ed2.0 (2010-07), Nuclear instrumentation - Photomultiplier tubes for scintillation counting - Test procedures”
- IEC 60973 ed1.0 (1989-06), “Test procedures for germanium gamma-ray detectors”
- IEC 61151 ed1.0 (1992-09), “Nuclear instrumentation - Amplifiers and preamplifiers used with detectors of ionizing radiation - Test procedures”

Reference Materials

- IEC 61452 ed1.0 (1995-09), “Nuclear instrumentation - Measurement of gamma-ray emission rates of radionuclides - Calibration and use of germanium spectrometers”

- IEC 61453 ed2.0 (2007-08), “Nuclear instrumentation - Scintillation gamma ray detector systems for the assay of radionuclides - Calibration and routine tests”

- AS 2243.4-1998, “Safety in laboratories - Ionizing radiations”
- Figures do not imply recommendations by Re
- Figure copyright by the respective companies

Reference Materials

- Good practice guides
  - Good practice guides from Duncan.Mcclure@hpa.org.uk
- Text books
  - Knoll, G.F., *Radiation Detection and Measurement*, 4th ed.: John Wiley & Sons, 2010
  - Leo, W.R., *Techniques for Nuclear and Particle Physics Experiments*, 2nd ed.: Springer Verlag, 1994.
  - Tavernier, Stefaan , *Experimental Techniques in Nuclear and Particle Physics*.: Springer-Verlag Berlin Heidelberg, 2010.
  - Hamamatsu, *Photomultiplier Tube Principle to Application*. Hamamatsu Photonics K.K., 1994.
  - Philips Photonics, *Photomultiplier tubes Principles & Applications*. Philips Export B.V, 1994.
  - BURLE INDUSTRIES, INC., *Photomultiplier Handbook*.: Copyright © 1980 by Burle Technologies, INC.

Teamwork !!!